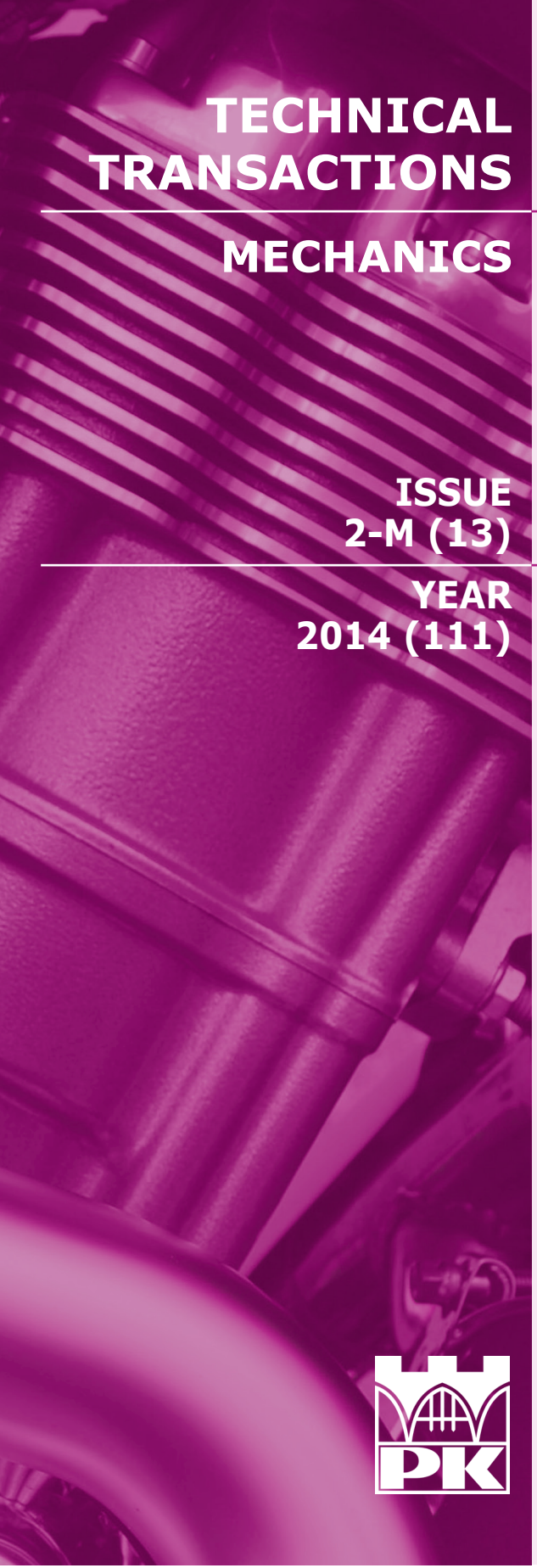

TECHNICAL TRANSACTIONS
CZASOPISMO TECHNICZNE

MECHANICS
MECHANIKA

ISSUE 2-M (13)
ZESZYT 2-M (13)

YEAR 2014 (111)
ROK 2014 (111)

WYDAWNICTWO POLITECHNIKI KRAKOWSKIEJ

TECHNICAL TRANSACTIONS | CZASOPISMO TECHNICZNE

MECHANICS | MECHANIKA

ISSUE 2-M (13) | ZESZYT 1-M (13)
YEAR 2014 (111) | ROK 2014 (111)

Pierwotną wersją każdego Czasopisma Technicznego jest wersja on-line
www.czasopismotechniczne.pl www.technicaltransactions.com

TECHNICAL TRANSACTIONS | CZASOPISMO TECHNICZNE
MECHANICS | MECHANIKA
2-M/2014

MAREK A. KSIĄŻEK*, MARCIN NOWAK**

DESCRIPTION AND ANALYSIS OF THE HUMAN RADIUS BONE

OPIS I ANALIZA KOŚCI PROMIENIOWEJ CZŁOWIEKA

Abstract

The paper shows the modelling process of a 3D digital model of the human radius bone based on its external and internal geometry. The obtained numeral characteristics of the model of the chosen mathematical functions can be used for further static and dynamic analysis of the bone subjected to external forces of different magnitudes.

Keywords: *geometric properties of radius bone, digital modelling of 3D structures, analysis of cross sections of bone*

Streszczenie

Artykuł przedstawia proces modelowania cyfrowego 3D kości promieniowej człowieka na podstawie jego geometrii zewnętrznej i wewnętrznej. Otrzymane charakterystyki liczbowe modelu wybranych funkcji matematycznych mogą być stosowane do dalszej statycznej i dynamicznej analizy kości poddanej różnym obciążeniom zewnętrznym.

Słowa kluczowe: *właściwości geometryczne kości promieniowej, cyfrowe modelowania struktur 3D, analiza przekrojów kości*

* Prof. Ph.D. Eng. Marek A. Książek, Institute of Applied Mechanics, Faculty of Mechanics, Cracow University of Technology.

** M.Sc. Eng. Marcin Nowak, Jagiellonian University, National Synchrotron Radiation Centre.

1. Introduction

Biomechanics is an evolving field that has recently witnessed rapid growth and increase of interest. So far, very few models showing the geometry of the bone have been constructed. This article presents the study of the geometrical properties of one of the arm bones – the radius bone. The aim of this work is to create a digital 3D model of a bone which contains all geometric properties without any simplifications.

The created model shows both, inner and outer geometry. The model was opened in Pro Engineer Wildfire 4.0, a CAD program with a highly developed cross-sections creation. Collected data was used to obtain graphs of functions and thereby, equations describing the examined parameter. In order to exemplify the possible use of the formula, the article presents the calculation of critical force of the radius during buckling.

There are no articles describing the problems included in this work. Bone models are usually simplified, with no internal geometry included. There are bone models obtained from computed tomography, however, the modelling presented in the article gives much more control over the end result.

Geometrical properties of bones haven't been described extensively either. Hence the findings presented in this article concerning this issue hold a great value for other works.

2. The radius

The radius is a long bone located on the thumb side of the forearm. It constitutes to the wrist and elbow joints. The radius consists of a body and two extremities – proximal and distal. The body of the radius has three surfaces – anterior, posterior and medial, and

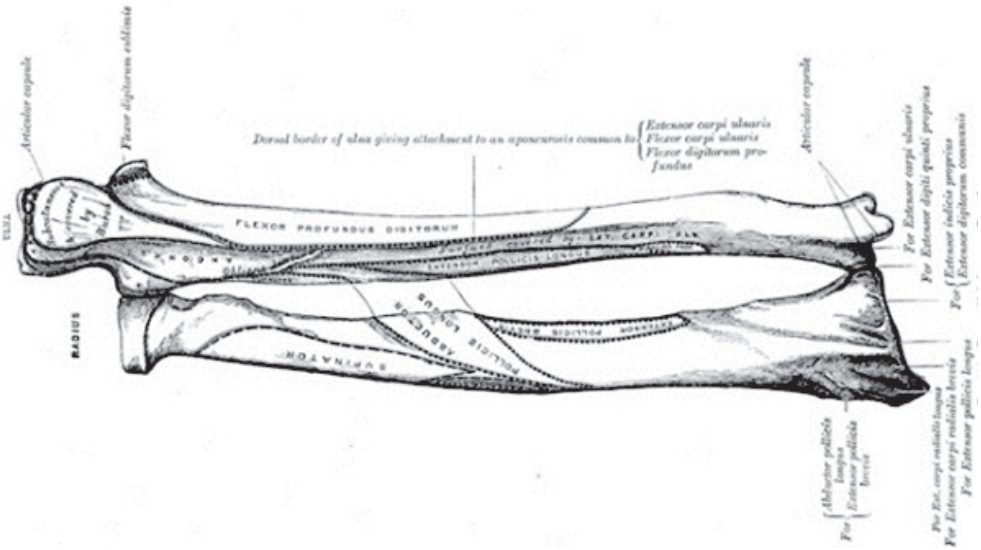

Fig. 1. The bones of the forearm, the ulna (top), the radius (below) [1]

three edges – frontal, external and internal (where the interosseous membrane connects the radius and the ulna). The proximal extremity – the head of the radius – is a surface that articulates with the ulna and the humerus. Around the head runs the circumference of the radial head (the surface which is in contact with the proximal end of the ulna). The head of the radius and the body connect the neck, below which, on the ulna side, is the radial tuberosity. On the distal, medial side of the radial body is the ulna notch (the surface which is in contact with the distal part of the ulna). The dorsal tubercle is located on the external surface of the distal end [1, 8].

3. Construction of the model

The scanned model was moulded out of plastic from the real bone. The bone was scanned with the use of reversed engineering technology thanks to the courtesy of the Coordinate Metrology Laboratory at the Cracow University of Technology. The outcome model of the bone had perfect external geometry parameters. The description of the formation of the model and the technology used can be found in references [2, 5]. In order obtain data necessary to reproduce the internal structure of the bone (the bone marrow cavity), a subject was submitted to a CAT scan at Jagiellonian University Medical College. The subject's right forearm was placed in the anatomical position, while the CT scan made a series of images in planes perpendicular to the axis of the bone adopted. The CT scanning enabled the reconstruction of the marrow cavity shape and its location within the bone. The marrow cavity modelling and its integration with the external geometry of the model was made with the Solid Works 2013 software (Fig. 2). Finally, the position of the coordinate system was set in accordance with the previous model of the scanned arm. The Z axis was taken along the bone and was coinciding with the line connecting the characteristic points on both joint surfaces. The X and Y axes were adopted in order to set the radius in the anatomical position (Fig. 3).

Fig. 2. Digital model of the bone: internal structure (top), external geometry (bottom)

Fig. 3. Location of the coordinate system for the 3D model

4. Cross-section planes analysis

The model prepared in accordance with the procedure presented in the previous chapter was imported into ProEngineer Wildfire 4.0. This program was chosen because of its very extensive module for the analysis section. The first step was to generate a number of planes intersecting the model. The planes were parallel to the XY plane and spaced apart by 1 [mm] each. Subsequently, all planes were tested with a tool for analysing cross-sections. Each cross-section made a base for a separate report. All reports were compiled in Microsoft Office Excel. The last step was to create a chart with all the characteristic properties of the model.

5. Selection of mathematical formulas

There are various programs designed to determine the formula of a function on the basis of its chart data, among those the most popular is Microsoft Office Excel. Excel was chosen for the study because of its trendline option. The graphs below present the changes in the cross-sectional area of the bone and the changes of the moment of inertia of the centre of gravity. Each chart had a trendline with the describing formula generated. The trendline presented was chosen cause of its simplicity (polynomial of the lowest degree possible) in order not to adopt the negative values. This means that the polynomials with lower degrees were taking negative values within the range studied, which is incorrect, since none of the tested properties cannot take those values (Fig. 4–7).

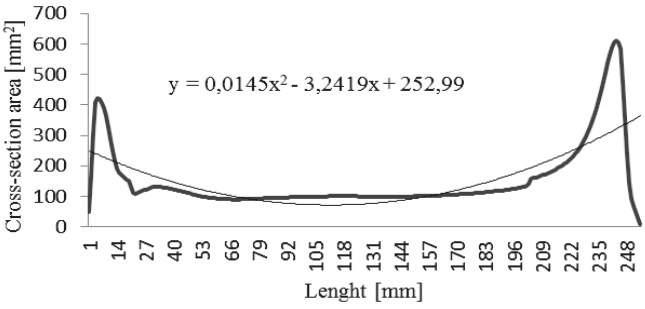

Fig. 4. Changes within the cross-section area

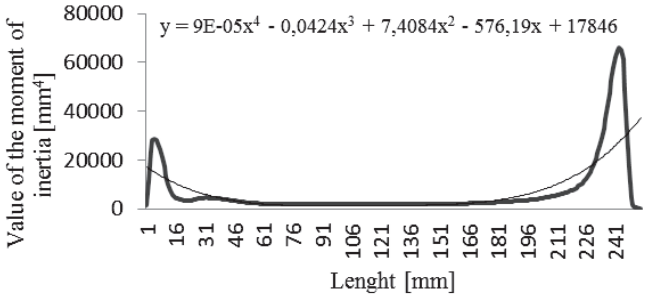

Fig. 5. Changes in the polar moment of inertia related to the centre of gravity

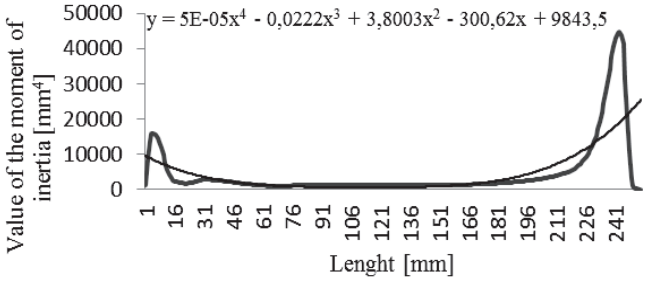

Fig. 6. Changes of the axial moment of inertia relative to the centre of gravity – axis I

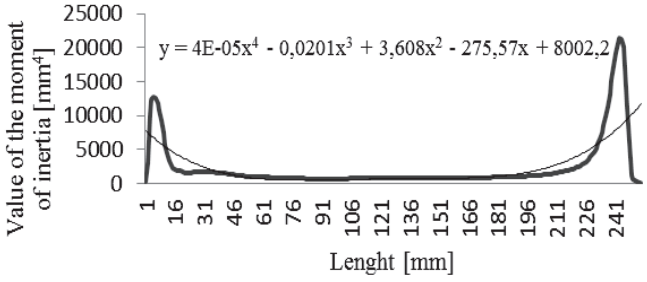

Fig. 7. Changes of the axial moment of inertia relative to the centre of gravity – axis II

6. Application of the formulas

The formulas obtained were used to assess the buckling resistance of the bone. It was determined that the distal joint surface (the wrist joint) occupies most of the surface from the forearm's side, consequently most of the compression load would be transmitted on the radius. Figure 8 presents the buckling model adopted.

Fig. 8. Buckling chart adopted

The bone in the elbow joint, where the radius is in contact with the humerus, best represents the support model of the non-sliding articulated joint. The presence of the distal part of the ulna at the wrist joint can best be described as a sliding joint. The described characteristics are presented in Figure 1.

The energy method was used with this case study. The internal energy of the flexing rod was compared with the compression force being at work at the rod end movement, which resulted in the energy formula for critical force (1).

$$P_{kr} = \frac{\int_0^L EJ\left(y''(x)\right)^2 dx}{\int_0^L \left(y'(x)\right)^2 dx} \tag{1}$$

where:

E – Young modulus,
J – moment of inertia,
L – length of the radius.

Adopted by the approximate form of the function of deflection (2):

$$y(x) = a\left(-\frac{x^4}{12} + \frac{x^3 L}{6} - \frac{L^3 x}{12}\right) \tag{2}$$

where:

L – length of the radius,
a – coefficient = 1.

Young's modulus was adopted on the basis of the available literature concerning the living bones. By applying the formulas describing the function properties to the formula [7] the value of the critical force was obtained.

P1 = 4683.87 [N]
P2 = 1575,52 [N]

7. Conclusions and further research

The study presents the latest techniques that allow the description of extremely complex structures – a level of description which until recently, was impossible to achieve. Extremely accurate waveforms of the characteristic properties of the bone. Moreover, it was possible to present these properties in a graphical form and with mathematical formulas that allowed the most accurate description. One of the most important issues is that received results were adapted to classical theories of mechanics and strength of materials. Further research will be continued in two ways. Firstly, the best model describing the features presented in the study should be chosen, independently from those few that are currently available in the most popular programs. The aim of this study would be to produce a formula describing the function matched as closely as possible to the actual conduct of the property. Secondly a digital model for numerical simulations should be used that could provide a wider view of the behaviour of bones under certain external influences.

References

[1] Grey H., *Grey's Anatomy*, Wyd. 2., Arcturus London 2008.
[2] Karbowski K., *Podstawy rekonstrukcji elementów maszyn i innych obiektów w procesach wytwarzania*, Wydawnictwo Politechniki Krakowskiej, Kraków 2008.
[3] Książek M.A., *Analiza istniejących modeli biomechanicznych układu ręka-ramię pod kątem wibroizolacji drgań pochodzących od narzędzi ręcznych*, Czasopismo techniczne, 2-M/1996, 87-114.
[4] Książek M.A., *Optimal hand-arm system of vibration isolation including human sensitivity to vibration*, mechanics, Vol. 28, No. 2, Kraków 2009, 39-45.
[5] Nowak M., *Procedura przygotowania modelu kości promieniowej, łokciowej i ramiennej człowieka*, Czasopismo Techniczne, 1-M/2011, 167-174.
[6] Ruta P., *Zastosowanie wielomianów Czebyszewa w dynamice dźwigarów o zmiennych parametrach geometrycznych i mechanicznych*, Oficyna Wydawnicza Politechniki Wrocławskiej, Wrocław 2007.
[7] Sobczak A., Kowalski Z., *Materiały hydroksyapatytowe stosowane w implantologii*, Czasopismo Techniczne, 1-Ch/2007, 149-158.
[8] Walocha J., Skawina A., *Kończyna górna kończyna dolna*, Wyd. 1., Wydawnictwo UJ, Kraków 2003.

TECHNICAL TRANSACTIONS | CZASOPISMO TECHNICZNE
MECHANICS | MECHANIKA
2-M/2014

MAREK A. KSIĄŻEK, JANUSZ TARNOWSKI*

CONSTRUCTION OF A NEW STAND FOR INVESTIGATING THE INFLUENCE OF WHOLE BODY VIBRATION ON MAN

BUDOWA NOWEGO STANOWISKA DO BADAŃ WPŁYWU WIBRACJI OGÓLNYCH NA CZŁOWIEKA

Abstract

In this paper, the way of construction, adaptation and testing of a new stand for whole body vibration built on the base of a Heckert electro-hydraulic shaker was presented.

Keywords: *Whole body vibration (WBV), Construction of low frequency vibration stand*

Streszczenie

W artykule zaprezentowano budowę i adaptację stanowiska badawczego do badania wibracji ogólnych zbudowanego nas bazie wzbudnika elektrohydraulicznego Heckert oraz badania testowe prezentowanego stanowiska.

Słowa kluczowe: *wibracje ogólne, konstrukcja stanowiska do badań niskoczęstotliwościowych*

* Prof. Ph.D. Eng. Marek A. Książek, Ph.D. Eng. Janusz Tarnowski, Institute of Applied Mechanics, Faculty of Mechanics, Cracow University of Technology.

1. Introduction

Different approaches exist to assess the effects of whole body vibration (WBV) on men. Research on the influence of vibrations on humans in a standing position requires the employment of a test platform which can be controlled by different low frequency signals. In such tests, powerful and low frequency shakers can be used [1, 2]. Different types of shakers have been described in [3]. Until now, various versions of shakers [4–8] have been used to evaluate vibrations of different sections of the human body and to model and estimate the passage of vibrations through the human body. Electro-hydraulic shakers are suitable for tests where all aforementioned exigencies need to be taken into consideration The Heckert shaker is a good example of such a device, but it must be adapted for standing human operators. Such an adaptation was the aim of the work presented in the paper. The new stand was built and tested in the laboratory at the Department of Dynamics of Material Systems of Cracow University of Technology.

2. Stand construction

The stand was designed as a system composed of a vertical frame and platform joined together by a horizontal axle. The axle supported by bearings was joined with the horizontal beam of the frame placed on the piston of the electro-hydraulic Heckert SHA 140 shaker by two vertical bars. The dimensions of the platform are suitable for vibration investigations of humans in sitting and standing positions. Two versions of the stand (primary and final) are shown in Figures 1a, 1b. In the first version, the platform was constructed as a truss made of welded bars held in place by screws fixed to the rigid, rectangular frame.

a) b)

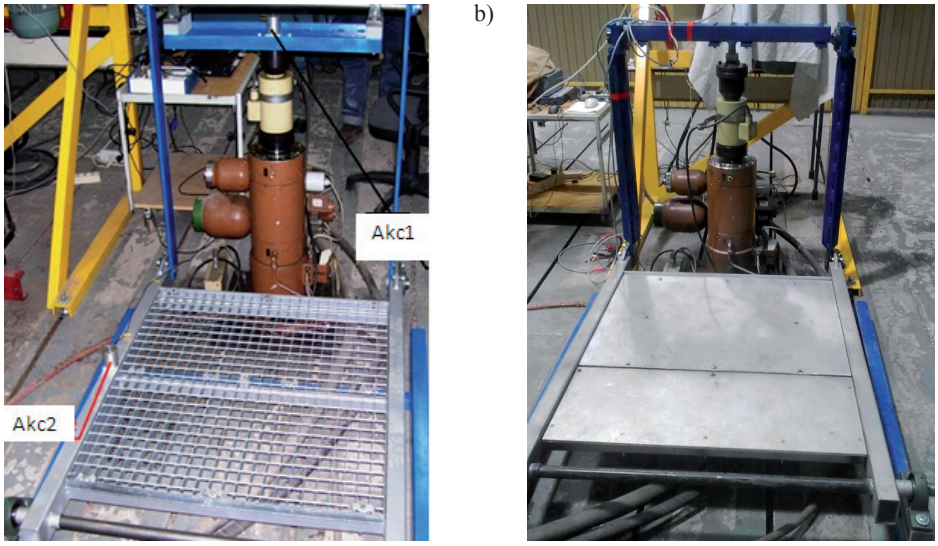

Fig. 1. Primary (a) and final (b) version of the stand

3. Stand tests

The preliminary tests were done using two KB12 accelerometers fixed on the horizontal beam and the frame of the platform as shown in Fig. 1a. The accelerometers, the NI SC 2345 conditioner, and the NI USB 6251 measurement card were linked to a computer. The source input signals used during tests were preprogrammed on the Heckert SHA 140 shaker. The time histories of accelerations measured on the horizontal beam and platform were registered. After the analysis of the registered results, some new modifications of the stand were introduced. The rigid connection between the horizontal beam and the piston of the shaker was substituted with a ball-and-socket joint to eliminate horizontal forces. The plate, made of a non-corrosive lightweight alloy, was fixed to the truss to increase the rigidity of the platform (Fig. 1b). The preliminary tests showed that some modes of vibrations of the platform were at frequencies different from that which is generated by the shaker. These modes were identified by tests with use of the Bruel & Kjaer 8202 impact hammer, the B&K 8200 force sensor and the bi-channel vibration analyzer B&K 2035. The stand and recording arrangement used for taking test measurements is shown in Fig. 2. The application of the impact hammer allowed for the input shock motion of the object to be investigated. Simultaneously, the hammer output signal was recorded and analyzed by the piezoelectric force sensor, the line drive amplifier and the first channel of the analyzer. The transient window of the analyzer allowed for the choice of location and the choice of the length of the window displaying the time history of one full impulse of impact force. The shock duration is dependent upon the shape of the chosen hammer-face. The generated frequencies are dependent upon both the shock duration and upon the shape of the chosen hammer-face. In the presented tests, a steel hammer tip was used. The B&K piezoelectric accelerometer, which was secured at the chosen point, and the second channel of the analyzer were used for concurrent measurements of the stand response. The decay of acceleration was recorded by application of the exponential window. After some preliminary calibrating impacts, the analyzer automatically fixed the gain for both measurement circuits. The following measurements were designed to obtain the estimation of power spectral densities of both channels and their cross-spectral density from the analyzer.

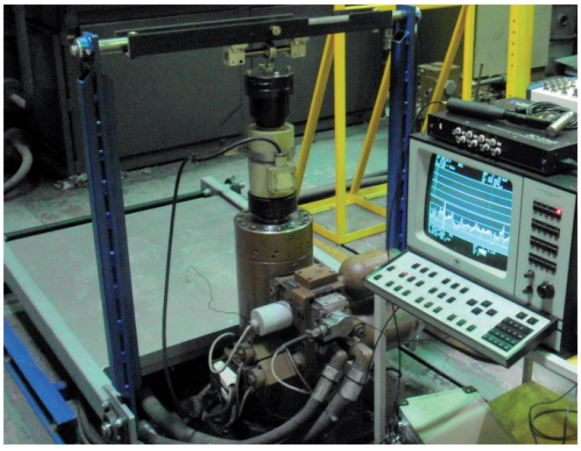

Fig. 2. Stand arrangement during tests

Using the registered signals, the analyzer screened the chosen transfer function calculated according to formula (1):

$$H_1(f) = \frac{G_{xy}(f)}{G_{xx}(f)} \tag{1}$$

where $G_{xx}(f)$ power spectral density of input signal, $G_{xy}(f)$ cross-power spectral density of time input $x(t)$ and time output $y(t)$ signals. The coherence function between random input and output signals given by formula (2) was also calculated and projected on screen. It allowed for the assessment of a linear relationship between $x(t)$ and $y(t)$ at the given frequency where one vibration can be exactly predicted from the other.

$$\gamma_{xy}^2(f) = \frac{\left|G_{xy}(f)\right|^2}{G_{xx}(f)G_{yy}(f)} \tag{2}$$

Configuration of the analyzer's screen is shown in Fig. 3.

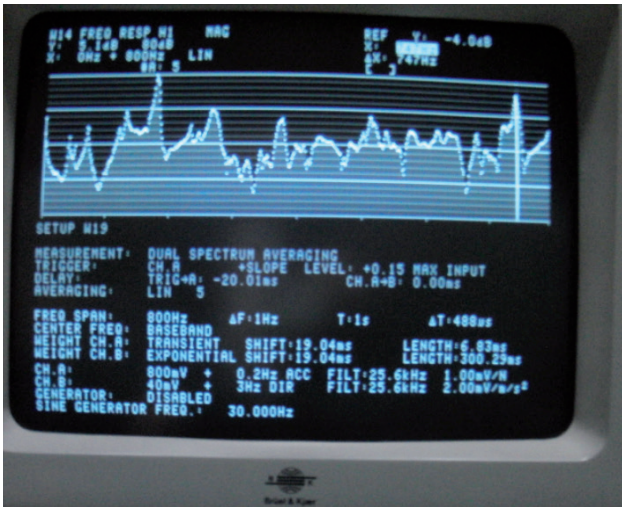

Fig. 3. Analyzer configuration

Downward short-duration impacts of the impact hammer on the structure were applied to the horizontal beam above the point where the ball-and-socket joint was secured (Fig. 4a). The responses of the structure were measured by the accelerometers fixed to the plate and to the frame of the platform (Fig. 4b). The final test results were presented as the mean value of five impacts of the impact hammer for each test. The obtained illustrations allowed for the evaluation of the resonance frequencies of the structure and for the validation of the executed measurements.

a) b)

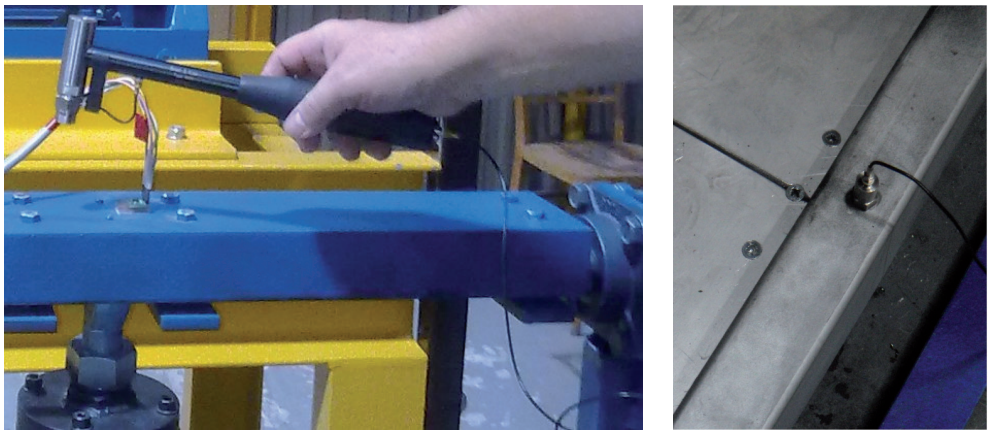

Fig. 4. Impact hammer used as source of excitation (a) and accelerometer used for the respose recording of the system (b)

Some testing with different placements of the accelerometer measuring the output signal were carried out. Figure 5 shows sample results.

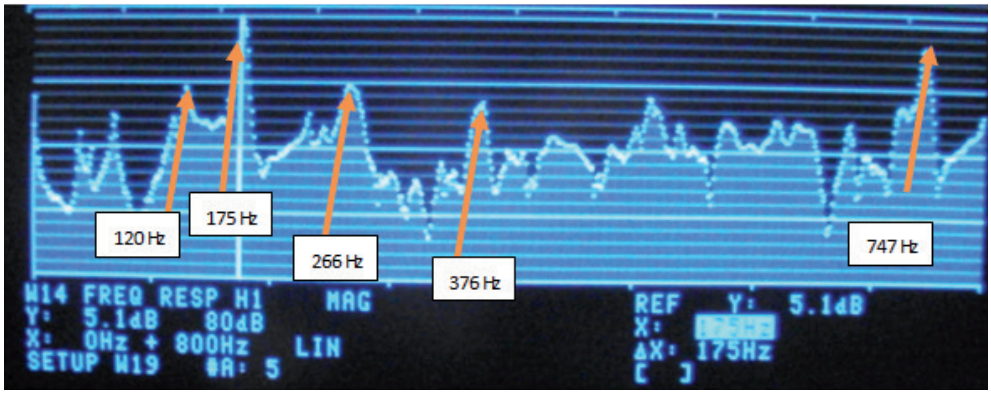

Fig. 5. Exemplary frequency response

In general, the coherence function is bounded at all frequencies by zero and unity, where $\gamma^2_{xy}(f) = 0$ means there is no linear relationship between $x(t)$ and $y(t)$ at frequency f and $\gamma^2_{xy}(f) = 1$ means there is a perfect linear relationship between $x(t)$ and $y(t)$ at frequency f.

The exemplary coherence function from the test is shown in Fig. 6, where at low frequencies, a lack of clear dependencies between signals $x(t)$ and $y(t)$ can be noticed.

Finally, in Fig. 5, only frequencies verified by Fig. 6 were shown. Preliminary testing confirmed the existence of many resonant frequencies of the stand. To eliminate these frequencies, the following upgrades of the stand were carried out:

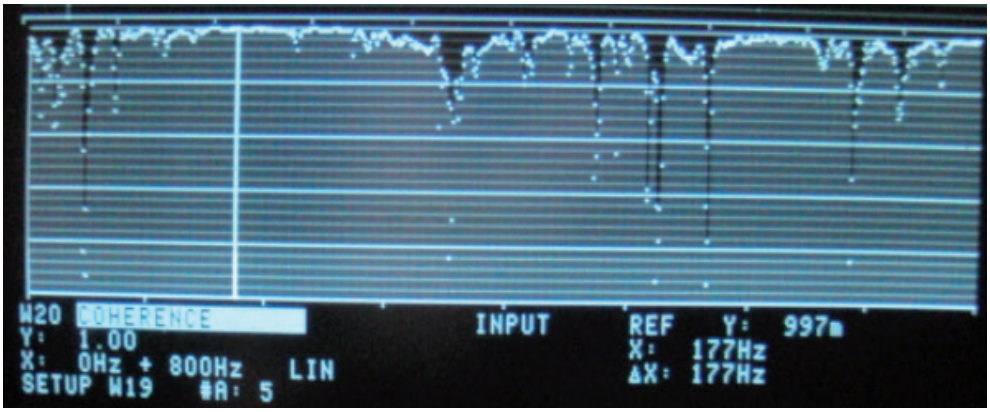

Fig. 6. Exemplary coherence function

1) the platform plate was cut into two sections,
2) the rubber pads were put under each of the sections.

The following summarizes the frequencies identified during the carried out tests:

– The accelerometer placed on the plate of the stand: 120, 175, 266, 376, 747 [Hz].
– The accelerometer placed on the frame of the platform: 120, 177,232, 265, 747 [Hz].
– The accelerometer placed on the loaded plate of the platform: 122, 178, 234, 270, 541, 743 [Hz].
– The accelerometer placed on the half plate with rubber pad: 170, 449, 735 [Hz].
– The accelerometer placed on the frame after platform modification (division and with rubber pad): 118, 170, 443 [Hz].

The aforementioned tests carried out using the impact hammer, accelerometer and analyzer showed that all resonant frequencies of the stand are in a range above 100 [Hz]. This means that the presented direct drive mechanical vibration machine has had all mechanical resonances removed from the operating frequency range shown below in Table 1.

4. Application of stand to WBV measurements

Resonace frequencies of the various body sections submitted to vertical vibration are mainly in a low frequency range as shown in Table 1.

To show these resonances, the excitations developed by the designed test bench must have the adequate range. The used apparatus with piezosensors does not allow for measurements at lower frequencies, thus, in the next stage of the research, other measuring circuits and other excitations were applied. The stand was excited by the electro-hydraulic shaker controlled by its internal signal generator operating in the sine function with adjustable amplitude and frequency. Two laser displacement sensors from Mikro Epsilon were applied to measure the displacement of the shaker and platform. The measuring track uses a National Instruments measurement card (USB 6251) along with LabView Signal Express software. Figure 7 shows the location of the laser sensors.

Table 1

Body sections	Resonace frequency ranges of the various body sections submitted to vertical vibration in [Hz]
Head	4 – 6, 20 – 30 (axial mode)
Chest wall	50 – 100
Chest organs	5 – 9
Jaw	6 – 8
Spinal column (axial mode)	10 – 12
Spinal column (lower part)	4 – 6
Spinal column (upper part)	10 – 14
Eyeballs	20 – 25, 60 – 90
Shoulder girdle	4 – 5
Abdominal mass	3 – 3.5, 4 – 8
Arm	5 – 10
Lower arm	16 – 30
Hand	30 – 50
Knee	20
Legs	2 – 20
Muscles	13 – 20
Bladder	10 – 18
Diaphragm	5 – 8
Pelvis	5 and 9

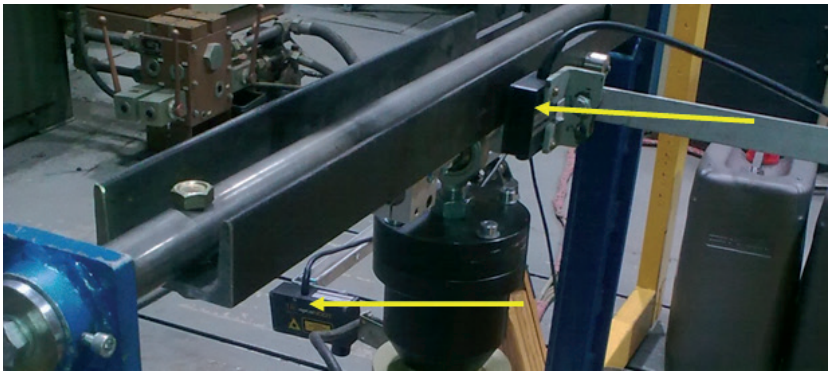

Fig. 7. Location of the laser sensors

Figures 8 and 9 show the time histories of displacements of the shaker and platform for excitation frequency 2 [Hz] and 5 [Hz].

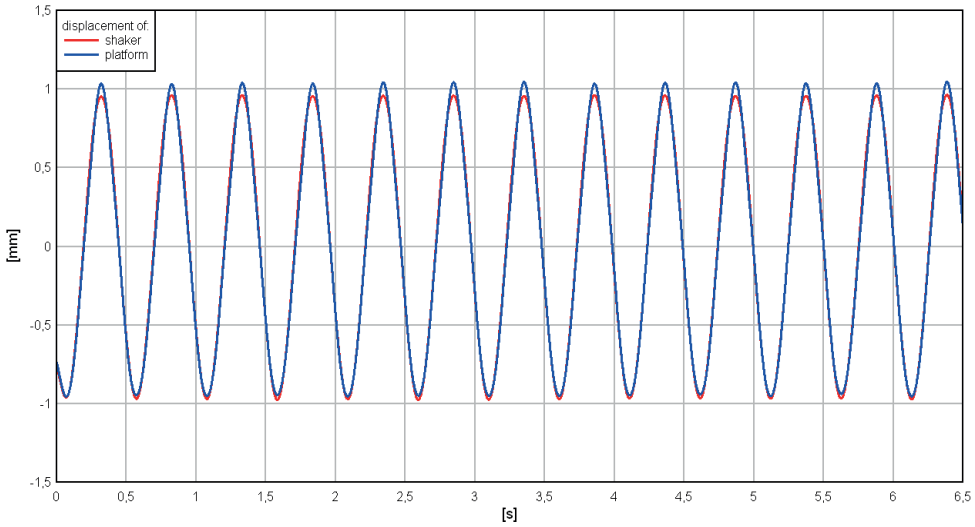

Fig. 8. The time histories of displacements of the shaker and platform for excitation frequency 2 [Hz]

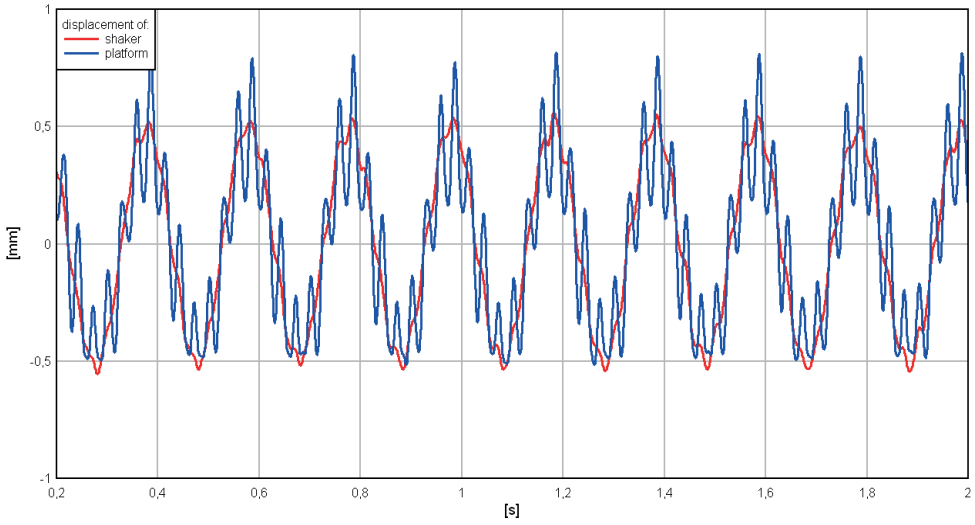

Fig. 9. The time histories of displacements of the shaker and platform for excitation frequency 5 [Hz]

In Fig. 9, one can see additional vibration with higher frequencies that have been set up on the platform. The frequencies of these vibrations are identified by the displacement spectrum in Fig. 10.

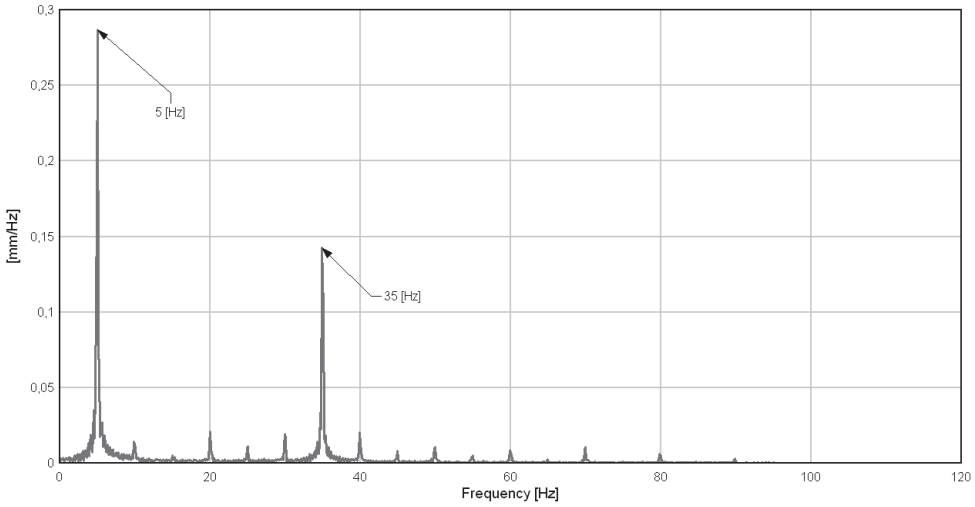

Fig. 10. Spectrum of displacement of the platform for excitation frequency 5 [Hz]

Similarly, for higher frequencies in the displacement spectrum, one can notice vibration with a frequency of 35 [Hz] (see Fig. 11).

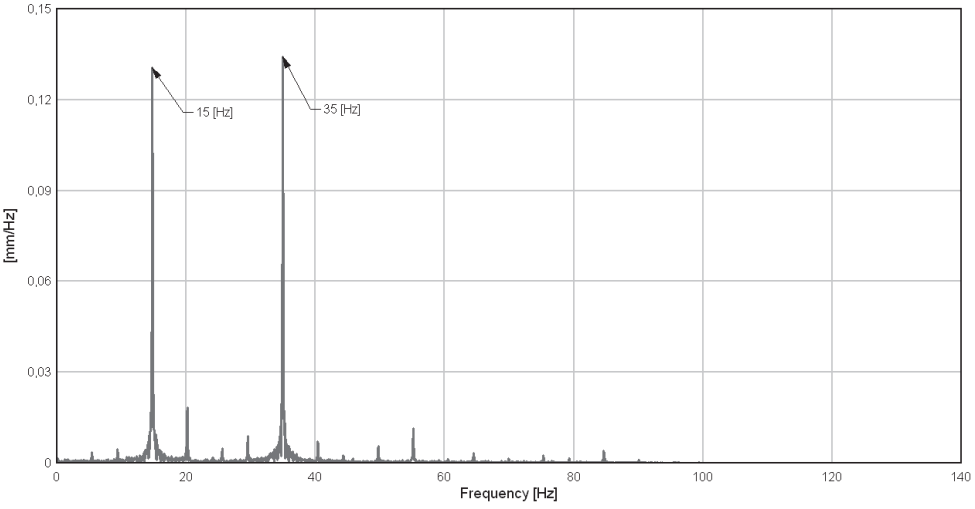

Fig. 11. Spectrum of displacement of the platform for excitation frequency 35 [Hz]

The load on the platform due to a standing man changes the displacement time history of platform vibrations as shown in Figure 12.

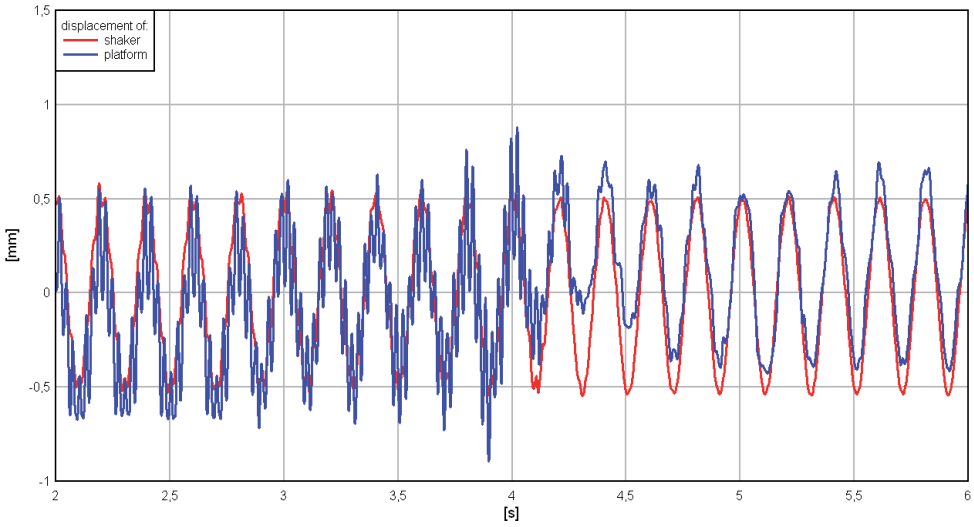

Fig. 12. Influence of the stand load on platform displacement

The presence of a man on the platform largely eliminates pulse-frequency vibrations of 35 [Hz]. During subsequent trials, the platform was loaded with a human operator body in standing position. A lack of components with higher frequencies can be noticed. After the aforementioned tests were completed, the design of the stand platform was changed by loading it with a thick and hard metal plate. This resulted in further elimination of vibration components with higher frequencies in the range important for WBV tests for both sitting and standing positions.

5. Conclusions

The presented laboratory stand allows for the study of vibration acting on a human operator body in both standing and sitting positions. The stand also enables the study of other complex dynamic systems involving higher weights. All of these design and manufacturing solutions that emerged during the implementation of the stand have a unique, leading prototype character. The built stand has been positively tested with an unbiasedly weighted platform and a biasedly weighted platform. Tests showed that the stand should work under load and can be used in scientific research as well as in studies combining whole body and local vibrations acting simultaneously on man.

References

[1] Dynamic Testing & Equipment 8000 Yankee Road, Suite 105 Ottawa Lake, Michigan 49267 USA Ph: 734-847-2681 WWW.DYNAMIC-TESTING.COM EXCITER 3D.

[2] MB Dynamics Inc • 25865 Richmond Rd • Cleveland OH 44146 USA • 216.292.5850.

[3] Piersol A.G., Paez, T.L., *Harris' Shock and Vibration Handbook*, McGraw-Hill, Sixth Edition, Chapter 25 and 27, 2010.

[4] Berthoz A., *Etude biomécanique du systeme homme-siege sur table vibrante*, Le Travail Humain, tom XXX, No. 3–4, 1967, 194-203.

[5] Cho-Chung Liang, Chi-Feng Chiang, *Modeling of a Seated Human Body Exposed to vertical Vibrations in Various Automotive Positions*, Industrial Health, 46, 2008, 125-137.

[6] Subashi G.H.M.J., Matsumoto Y., Griffin M.J., *Modeling resonances of the standing body exposed to vertical whole-body vibration: effects of position*, Journal of Sound and Vibration, 317, (2), 2008, 400-418.

[7] Hinz B., Menzel G., Blüthner R., Seidel H., *Seat-to-head Transfer Function of seated Men – Determination with Single and Three Axis Excitations at Different Magnitudes*, Industrial Health, Vol. 48, 2010, 565-583.

[8] Książek M.A., Tarnowski J., *Estimation of transmission of hand pressure force through human body – experimental investigations*, Mechanics and Control, Vol. 31, No. 1, 2012.

TECHNICAL TRANSACTIONS | CZASOPISMO TECHNICZNE
MECHANICS | MECHANIKA
2-M/2014

MARCIN NOWAK, MARCIN WIKŁACZ*

NUMERICAL MODELING OF THE DYNAMIC IMPACT OF TRANSPORT STRETCHERS ON PATIENTS IN A MOVING AMBULANCE

MODELOWANIE NUMERYCZNE ODDZIAŁYWANIA DYNAMICZNEGO NOSZY TRANSPORTOWYCH NA PACJENTA W PORUSZAJĄCEJ SIĘ KARETCE

Abstract

The paper presents numerical simulation of an ambulance transport system which consists of three elements: the stretcher, the frame which holds the stretcher and a part of the ambulance. The model was designed with the use of SolidWorks 2013 software. The numerical analysis was done with the use of ANSYS Workbench 13 software. During the first stage the natural frequencies and the forms of vibrations of the model were determined. During the second stage the dynamic excitations on the transport system were simulated.

Keywords: *vibrations in the ambulance, natural frequencies medical stretcher*

Streszczenie

Artykuł przedstawia symulacje numeryczną systemu transportowego karetki, w skład którego wchodzą trzy elementy: nosze pacjenta, rama utrzymująca nosze wraz z pacjentem oraz fragment karetki. Model zaprojektowany został w programie SolidWorks 2013, a analiza numeryczna w programie ANSYS Workbench 13. Podczas pierwszego etapu wyznaczono częstotliwości oraz formy drgań własnych modelu. Następnie zasymulowano wymuszenia dynamiczne na system transportowy.

Słowa kluczowe: *drgania w karetce, drgania własne noszy karetki*

* M.Sc. Eng. Marcin Nowak, M.Sc. Eng. Marcin Wikłacz, Institute of Applied Mechanics, Faculty of Mechanics, Cracow University of Technology.

1. Introduction

This article deals with problems concerning the transportation of medical patients by ambulance – it is a problem which has thus far been largely unanalysed. Whilst transporting patients, ambulances will typically travel at relatively high speeds in order to ensure that the time taken to transfer the patient to hospital is kept to a minimum. During the journey, the patient is exposed to the constant vibrations resulting from the movement of the vehicle. These vibrations potentially have serious negative consequences for the patient with regard to an increase in the severity of medical complaints and the deterioration of the patient's health. It should be remembered that with regard to chassis construction, ambulances do not differ in any way from vehicles used for transporting other cargos. With this in mind, it is important to determine the impact that these vibrations have on the patient's wellbeing, and the role which the vibration isolating system can play in improving the patient's comfort.

The primary method of determining the type of vibrations affecting the patient during the transportation is to conduct the test with the use of accelerometer in the ambulance while the vehicle is in motion. Such tests were carried out in the Silesian Center for Heart Diseases in Zabrze and their results will be published in a separate article.

As the modelling of the entire vehicle with all the equipment and the complete crew on board would be extremely complicated, it has been decided to limit the project to constructing a transport system consisting of a stretcher, a steel frame holding the stretcher and some parts of the vehicle. According to the authors of the article, those three elements have the greatest vibration impact on the patient.

The numerical simulation carried out in ANSYS Workbench 13 software determines the natural frequency and the form of vibrations of the transport system. The simulation of the elements' behaviour during the dynamic excitations was carried out with the use of the data received during the measurement of the vibrations in a vehicle moving on the asphalt road.

2. Description of the transport system

As it was noted in the introduction, due to the complexity of the structure of the ambulance, only the so-called transport system was constructed. The transport system simulates the vibrations which have the greatest impact on the transported patient.

The system consists of three elements. The first is a fragment of the ambulance floor to which the force causing the vibrations was applied. This part has the role of substituting the whole chassis of the ambulance. The second element is a steel platform directly bolted to the floor of the vehicle (Fig. 1). It is used to adjust the angle of the patient's position, which helps inserting and removing the stretcher. The maximum angle is 10°. The platform also allows to avoid movement of the stretcher in the ambulance.

The third element of the transport system is the stretcher, located directly on the platform (Fig. 2). It is made mainly from aluminium. Once it is placed in the ambulance, the whole weight is transferred to the four wheels of the stretcher. There is a mattress placed on the stretcher which ensures the patient's comfort.

Fig. 1. Platform in the ambulance

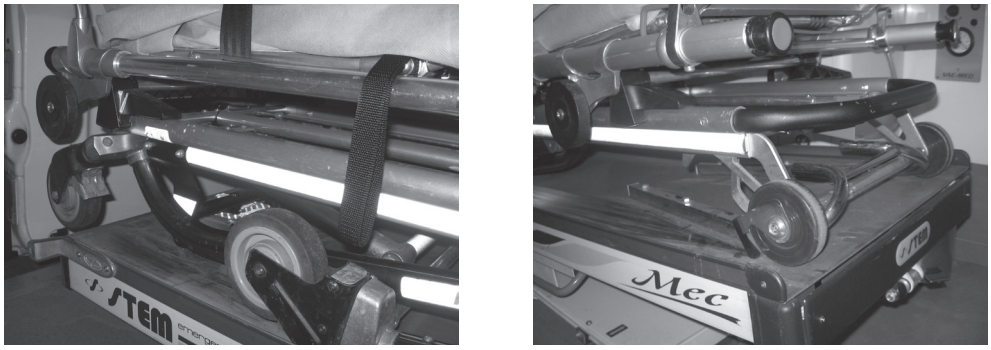

Fig. 2. Transport stretcher

3. Models of the transport system

3.1. Detailed model of the transport system

The model used for analysis has been designed in the Solid Works 2013 software. The authors of the article wanted to reproduce as accurately as possible the relationship between the stretcher and the vehicle. As a result a detailed and realistic model was designed (Fig. 3).

Unfortunately, with such a meticulous designing, a large number of bonds and elements was formed, which hindered considerably the measurement of the natural vibrations of the system. Initially the executive model of a similar stretcher was obtained. The model was simplified and adapted to the accurate parameters of the object. Two additional elements, which are part of the same system, were designed. The first is a mattress which is placed on the stretcher. The second element is a solid plinth which is supposed to represent the stretcher's attachment system in the ambulance and the vehicle itself. All the elements were combined together and transferred to the Ansys Workbench 13 software in order to carry out numerical simulations. After reading the model, it was found out that the number of contacts that the program had read is very large (about 2000), and that some contacts were erroneously adopted. As a result the study could not be continued. Nevertheless, very good parameters of the mesh were obtained (Tab. 1). Considering the significant complication that the detailed model entails, a simplified model was created and used to simulate the vibrations.

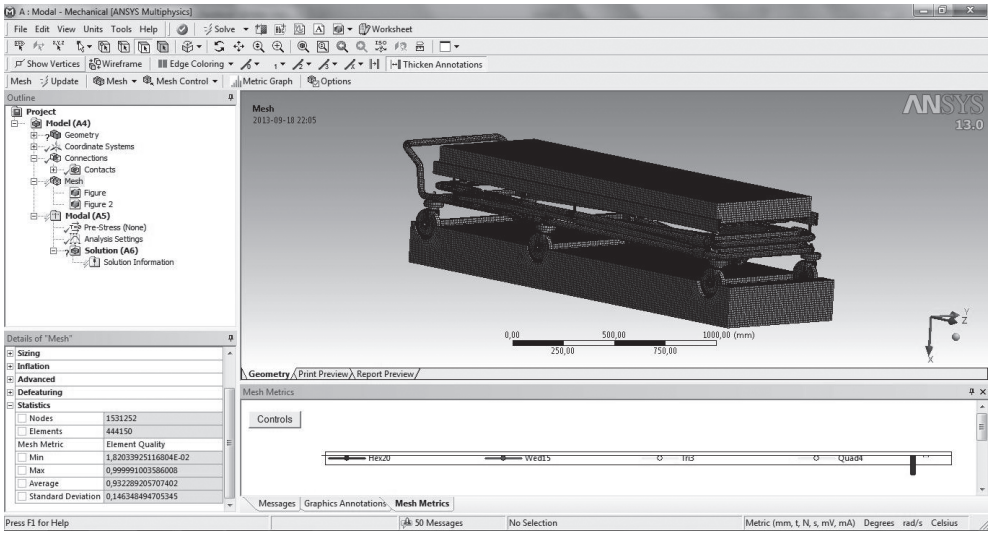

Fig. 3. Detailed model of the transport system

Table 1

Mesh data in detailed model

Bonds	1531252
Elements	444150
Average quality of the item	0,932289

3.2. Simplified model of the transport system

With the support of technical documents and a collection of pictures made by a hospital employee, a simplified model of the stretcher was designed. In terms of the geometry the new model was a good representation of the real object. The elements required for the study were recombined. The result was positive, the number of contacts significantly decreased.

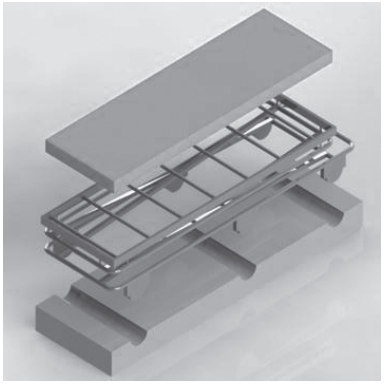

Fig. 4. Simplified model of the transport system

The first two elements of the transport system (the floor fragment and the platform) were represented as one element. One of the reasons for this was the simplification of the model, which in result enabled further analysis. Moreover, it did not affect greatly the results of the study, as the materials of both constructions are very similar, and the combination of these two elements is very rigid. It was assumed that the constructing material would be the structural steel. The final element of the transport system is an aluminium stretcher with a mattress. For the mattress the most similar material available in the program – polyethylene was used (Fig. 4). Selected parameters of the respective structures are shown below (Tab. 2).

Table 2

Selected parameters of simplified model

Parameter	Base	Stretcher	Mattress
Bonds	3495	5889	1722
Elements	2492	16510	1040
Average quality of the item	0.94875	0.59240	0.99935
Material	Steel	Aluminum	Polyethylene
Weight	2300	85	100

4. Determination of the frequencies of natural vibrations

For the simulation all the elements were fixed on all the side walls of the platform, the element located at the bottom of the whole system. The method can be justified by the system clamping the stretcher in the ambulance. It allows to apply the driven force from the lower surface of the model (Fig. 5).

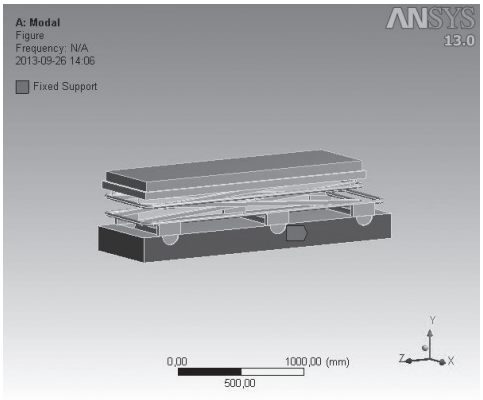

Fig. 5. Fixing of the transport system

Ansys software allows for a modal analysis. After determining the form as value 6, the distribution of the transport system elements' strains for the particular frequencies was obtained (4.56 Hz, 6.5 Hz, 27 Hz, 27.2 Hz, 59 Hz, and 62.7 Hz). The greatest deformations of the mattress can be observed with the low-frequency vibrations (5 Hz). With the increasing frequency the stretcher is becoming more deformed, whereas the deformation of the mattress is minimal (Fig. 6).

4.1. Dynamic excitations on the transport system

The second phase of the simulation was to apply the driven force and to read the values for the top surface of the model. The driven force was applied on the lower surface of the model, on the element substituting the ambulance. The value of the force was set on 10000 [N]. The force had only one directional component exerted along axis Y, adopted at the beginning of the modelling of the coordinate system. The method of fixing for this simulation remained the same as for the study of the natural vibrations frequencies. The result of the simulation is the amplitude-frequency diagram, created for the top surface of the model. The top surface is the upper part of the mattress, where the patient is resting during transport (Fig. 7).

5. Conclusions

The study gives an interesting insight into the behaviour of the relation between ambulance, stretcher, and mattress. Very little research was conducted regarding the impact of transport on the patient's health. The results of this study can be used in many fields, from the designing of the vibration reduction systems for ambulances to medical diagnostics. Further research on the topic is planned to be undertaken. Also the digital model has to be improved in order to achieve the most optimal combination of the model complexity with the quality of numerical calculations. Moreover, it is recommended to carry out laboratory tests and measurements in ambulances.

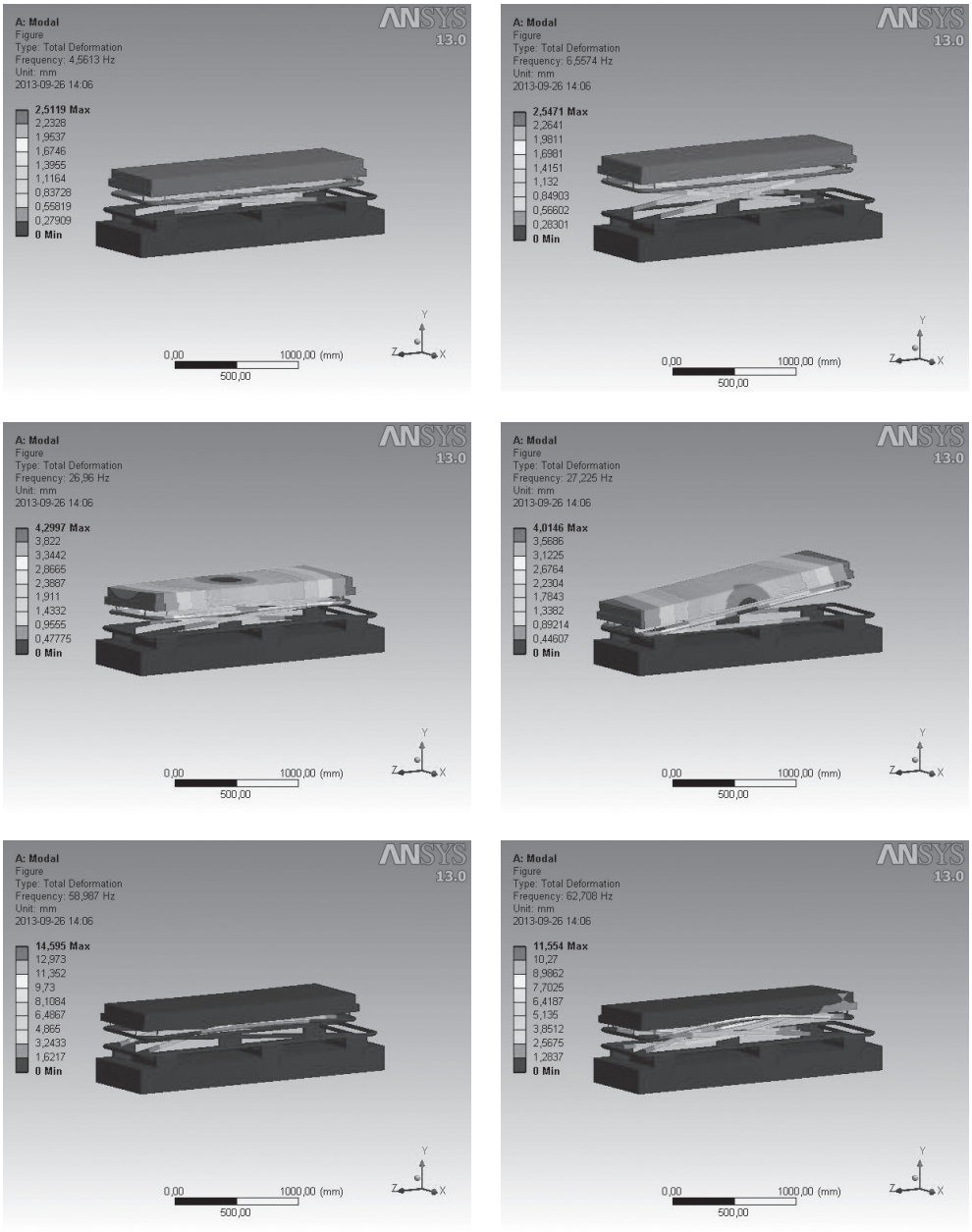

Fig. 6. Degree of elements' deformation depending on the vibrations' frequency

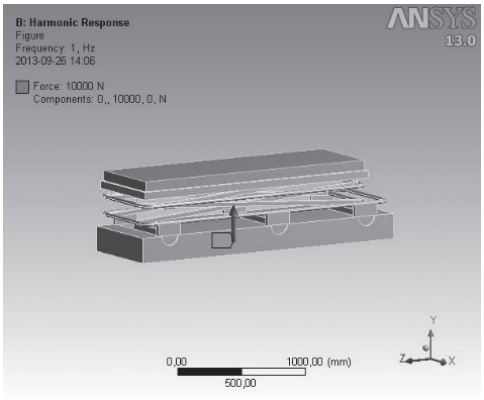

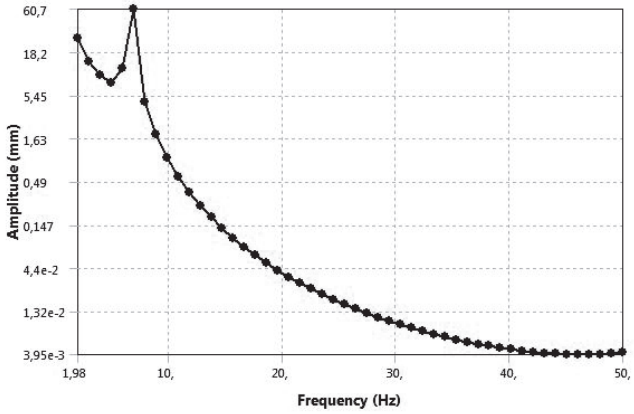

Fig. 7. Dynamic excitations on the transport system

References

[1] Concern: Ferno Group Companies, *Manual Instruction Patient Transport System – Mondial*, United States.

[2] Concern: Stem Emergency System, *Technikal Manual: Hydropneumatic Stretcher Support*, Italy.

[3] Sherwood H.B., Donze A., Giebe J., *Mechanical Vibration in Ambulance Transport*, Journal of Obstetric Gynecologic & Neonatal Nursing, Vol. 23(6), 1994, 457-463.

TECHNICAL TRANSACTIONS | CZASOPISMO TECHNICZNE
MECHANICS | MECHANIKA
2-M/2014

EDWARD PRZYDRÓŻNY, SYLWIA SZCZĘŚNIAK, JULIUSZ WALASZCZYK*

VIBRATION ISOLATION OF VARIABLE FAN SPEED IN HVAC SYSTEMS

WIBROIZOLACJA WENTYLATORÓW ZE ZMIENNĄ PRĘDKOŚCIĄ OBROTOWĄ W SYSTEMACH HVAC

Abstract

This article analyses two samples of existing vibration isolation systems. The first sample applies to rubber absorbers, the second, to spring absorbers. The article presents a method of setting the parameters of a second order differential equation describing oscillation movement. The equation parameters were selected on the basis of amplitude measurement and rotation velocity in two representative points – (i) in the resonance and (ii) at the maximum rotation velocity when the influence of the damping factor for the oscillation amplitude can be ignored. Equations of motion simulations were performed and the results were compared with the actual values of displacement and the velocity vibration platform.

Keywords: *vibration isolation, ventilation, air conditioning, HVAC*

Streszczenie

W artykule przeanalizowano pracę dwóch rzeczywistych układów wibroizolacji. Pierwszy przypadek dotyczył wibroizolatorów gumowych, drugi przypadek amortyzatorów sprężynowych. Przedstawiono metodę wyznaczania parametrów równania różniczkowego drugiego rzędu opisującego ruch drgający. Parametry równania zostały wyznaczone na podstawie pomiaru amplitudy i prędkości obrotowej w dwóch charakterystycznych punktach: (i) w rezonansie oraz (ii) przy maksymalnej prędkości obrotowej, kiedy wpływ współczynnika tłumienia na amplitudy drgań może zostać pominięty. Przeprowadzono symulacje równania ruchu, a wyniki porównano z rzeczywistymi wartościami przemieszczeń i prędkości platformy wibracyjnej.

Słowa kluczowe: *wibroizolacja, wentylacja, klimatyzacja, HVAC*

* Ph.D. Eng. Edward Przydróżny, Ph.D. Eng. Sylwia Szczęśniak, M.Sc. Eng. Juliusz Walaszczyk, Department of Heating and Air Conditioning, Faculty of Environmental Engineering, Wrocław University of Technology.

1. Introduction

Current HVAC (Heating, Ventilation and Air Conditioning) equipment is usually designed for different operational parameters. This applies to variable airflow devices and also to devices with variable hydraulic profiles. In both cases, it can be get through changeable turnovers of the fun rotor. For units with variable airflows, rotation velocity may vary within the range 40% to 100%. For units with significantly changing hydraulic profiles, rotation velocity may vary from 20% to 100% of the maximum rotation velocity. Ventilation and air conditioning units with variable working parameters are used to serve living and technological facilities. Typical applications of this type of equipment are described below:

a) facilities with a high number of rooms where the room occupation factor can change and there is no need to serve non-occupied rooms (i.e. hotels),
b) technological facilities that require a constant airflow and the air need to be purified at few steps of filtration,
c) facilities that require definite pressure difference between particular rooms but are not constantly occupied (i.e. surgical complexes).

For units with a variable rotational speed, we are facing the problem of suitable device fixing and proper vibration damping of the fan and motor.

Properly designed, linear, supercritical vibration isolation can be a cost effective solution ensuring the correct functioning of driving systems. However, in some cases this can lead to the precipitated wear of machine parts. This arises from the fact that the damping system is not dedicated to work in frequencies similar to self-oscillation frequencies. In extraordinary situations, like ground bumps or hammering engine loads, even with properly designed vibration isolation, the unit can get into resonance. To avoid such situations, it's recommended to apply non-linear vibration isolation systems. Such solutions considerably eliminate sudden increases of oscillation amplitude (forces transferred to the ground) that are mostly related to the appearance of resonance. An overview of non-linear systems is presented in reference [1]. By applying passive vibration damping with nonlinear vibration isolation techniques Yang et al. decreased the frequency of normal mode from 11.7 Hz to 2.5 Hz. He achieved this by fitting compressing springs perpendicularly to the direction of oscillation. Compressing springs were reducing the stiffness of the system [2]. A similar solution is presented in reference [3]. The efficiency of a vibration isolation system, including additional, horizontal springs (with regulated parameters), was checked experimentally. As a result, it was affirmed that the usage of a negative stiffness structure (NSS) improves the features of vibration isolation at low force frequencies. This thesis was also confirmed in reference [4]. Xingtian et al. used two deformed Euler beams instead of springs.

Currently, except for passive vibration isolation systems based on springs or other flexible materials, active systems are intensively developed. Hanieh et al. [5] proposed the use of a piezoelectric device to correct the vibration level on the basis of vibrating mass velocity measurements. A slightly more complicated solution based on two spring-joined masses was show in reference [6]. Based on checks of oscillation velocity, a controlling system was generating a positive or negative force to compensate i.a. the displacement. It was proved that active compensation is favourable, but only in some specific cases.

Despite advanced research in the science of active vibration isolation systems, passive linear systems are the most popular in everyday use, as they are simpler and give sufficient

oscillation reduction. The assessment methods of such systems are contemporarily carried out. Michalczyk proposed a new judgement method of maximum oscillation amplitude with few degrees of freedom during temporary resonance [7]. The execution of adequate calculations shouldn't be the final step of the working system assessment. Existing ventilation systems are relatively complicated so the experimental examination of each unit is highly recommended if possible at the site of manufacture (factory acceptance testing FAT), or before start-up of the system at final user facilities [8].

This study describes basic problems related to the carrying dynamic forces of working fans at variable rotational speeds. Displacement and velocity measurements of two existing systems with flexible motor fixing will be presented as well. The first system is equipped with rubber insulators, the second, with spring insulators. This study attempts to create a model of vibration isolation system, based on a commonly used mathematical description. Equation parameters describing oscillating movement were calculated on the basis of displacement and frequency measurements taken at two key working points - in resonance and at four times higher frequency than the resonance frequency. Research confirmed that a two-point check is enough to correctly determine all parameters describing the vibration isolation system.

2. Mathematical description

The flexible motor fitting system is commonly described with a second order differential equation:

$$m\frac{d^2y}{dt^2} + c\frac{dy}{dt} + k_d y = F_0 \sin(\omega t) \tag{1}$$

where:

- F_0 – amplitude of the driving force [N],
- ω – angular frequency [rad/s],
- t – time [s],
- m – vibration isolation loading mass [kg],
- y – displacement [m],
- c – damping coefficient [Ns/m],
- k_d – stiffness coefficient [N/m].

The left side of the equation $F_0\sin(\omega t)$ describes the sinusoidal driving force. This equation can also be presented as follows:

$$\frac{d^2y}{dt^2} + 2\xi\omega_r\frac{dy}{dt} + \omega_r{}^2 y = \frac{F_0}{m}\sin(\omega t) \tag{2}$$

where:

- ξ – dimensionless damping factor,
- ω_r – resonance angular frequency (normal mode) [rad/s].

Joining equation (1) and (2) we get the dependence below:

$$k_d = \omega_r^2 m \tag{3}$$

$$c = 2\xi\omega_r m \tag{4}$$

The above leads to the conclusion that knowing the mass of the system, the frequency of the resonance oscillation and the dimensionless damping factor, we can determine the parameters of the differential equation describing oscillation movement. To make the comparison of the frequency easier, it's recommended to introduce the coefficient μ defined as follows:

$$\mu = \frac{n}{n_r} = \frac{\omega}{\omega_r} \tag{5}$$

where:

n – driving frequency [Hz],
n_r – normal mode frequency (resonant) [Hz].

If $\mu = 1$ it means that vibration protection system operates in resonant area (critical area). If $\mu < 1$ it means that vibration protection system runs in under-critical area and if $\mu > 1$ it runs in over-critical area.

3. Enumeration of differential equation parameters

To calculate the stiffness coefficient, use equation (3), substituting the mass and frequency and the frequency of the normal mode (resonant). To get the value of the damping coefficient (equation 4), it is necessary to know the value of the dimensionless damping coefficient ξ. To know ξ value, it is preferable to use equation (6) and (7) describing dimensionless relative amplitude [9]:

$$\upsilon_0 = \frac{\mu^2}{\sqrt{(1-\mu^2)^2 + (2\xi\mu)^2}} \tag{6}$$

$$\upsilon_0 = \frac{m y_0}{M_w R_m} \tag{7}$$

where:

υ_0 – dimensionless relative amplitude,
y_0 – oscillation amplitude [m],
M_w – rotation mass [kg],
R_m – eccentric radius [m].

In resonant conditions, when $\mu = 1$, equation (6) looks as follows:

$$\upsilon_0 = \frac{1}{2\xi} \tag{8}$$

And after transformation of equation (8) coefficient value ξ can be solve by (9):

$$\xi = \frac{1}{2\upsilon_0} \tag{9}$$

The above equation (9) is correct only for resonant conditions. The dimensionless relative amplitude υ_0 should be calculated from equation (7) after substituting the multiplied rotation mass, eccentric radius and oscillation amplitude (resonant). The oscillation amplitude can be calculated experimentally, and the multiplication of the rotating mass and the eccentric radius can be calculated from joining equations (6) and (7), with the initial assumption that the damping coefficient $\xi = 0$ (equation 10).

$$M_w R_m = m y_1 \frac{\left|1 - \mu^2\right|}{\mu^2} \tag{10}$$

where:

y_1 – oscillation amplitude in the area where the damping factor influence to the conduct of the system can be ignored [m].

Assumption $\xi = 0$ is legitimate, when angular driving frequency significantly differs from angular frequency in normal mode then $\mu \neq 1$ and damping coefficient ξ hasn't got meaningful influence for the dimensionless relative amplitude. This is clearly shown in Figure 1.

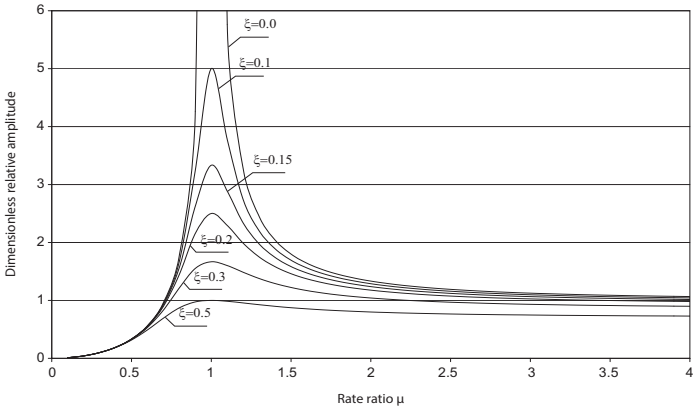

Fig. 1. Relationship between dimensionless amplitude υ_0 and rate ratio μ for different damping coefficients ξ

Example: difference between dimensionless relative amplitudes calculated when $\mu = 4$ with the assumption that $\xi = 0{,}0$ and $\xi = 0{,}1$ equals 2%. The most common values of damping coefficients are below 0.1, so usage of equation (10) to calculate the multiplication of the rotating mass and the eccentric radius at possibly high μ values is justified.

4. Forces in the vibration isolation system

Using equation (11) it is possible to calculate the amplitude of the oscillation driving force.

$$F_0 = M_w R_m \omega^2 \tag{11}$$

Equation (12) can be useful to calculate the coefficient of force transfer (ratio of the force amplitude transferred to the foundation to the driving force amplitude).

$$TR = \frac{P_0}{F_0} = \sqrt{\frac{1 + (2\xi\mu)^2}{\sqrt{(1 - \mu^2)^2 + (2\xi\mu)^2}}} \tag{12}$$

where:

TR – force transfer coefficient,
P_0 – amplitude of the force transferred to the foundation [N].

Knowing the dimensionless damping coefficient ξ and μ, it's easy to calculate the coefficient of force transfer for the particular driving frequency. That can be used to further calculate the amplitude of the force transferred to the foundation. It's important to notice that as the dimensionless damping coefficient gets lower, the force transferred to the foundation gets higher (in resonant area). This phenomenon is presented in diagrams 2 and 3. These diagrams present 4 variants of dynamic force amplitude that are transferred to the foundation at different dimensionless damping coefficients. ξ, different driving frequencies (n) and different frequencies of normal mode (n_r). The amplitude of the driving force was calculated on the basis of a rotating mass equal to 15 kg and the eccentric radius of 0.2 mm. Additionally, the dashed line presents the amplitude of the driving force for the doubled eccentric radius. That shows the rotor unbalance influence for the appearance of the amplitude of dynamic forces. Figures 2 and 3 were developed for driving frequencies of 0-50 Hz and for different maximum μ values. Figure 2 was developed for $\mu = 3$, and figure 3 was developed for $\mu = 5$. The consequences of these assumptions are different resonant frequencies of the units settled on vibration isolators. In the first case, $n_r = 16.67$ Hz, and in the second, $n_r = 10$ Hz.

Presented diagrams show that:

(1) amplitudes of the dynamic forces caused by rotary machines are not dependent on amortization,

(2) applied amortization significantly influence the amplitudes of the dynamic forces transferred by isolators to the ground,

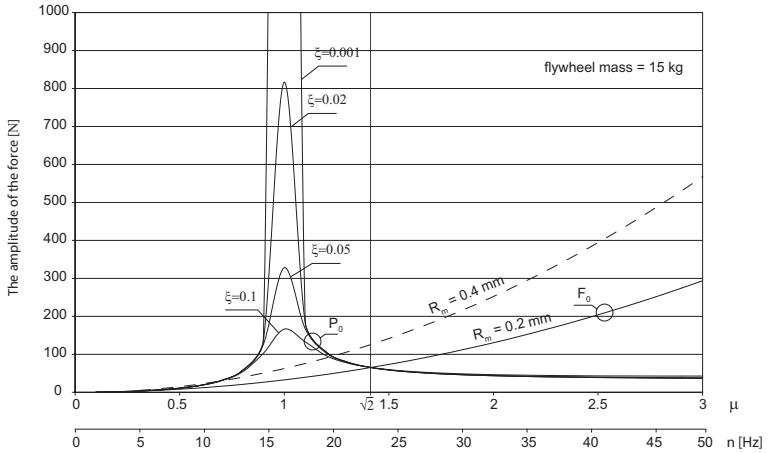

Fig. 2. Amplitudes of dynamic forces in the vibration isolation system at maximum μ = 3 for different damping coefficients ξ and resonant velocity n_r = 17 Hz

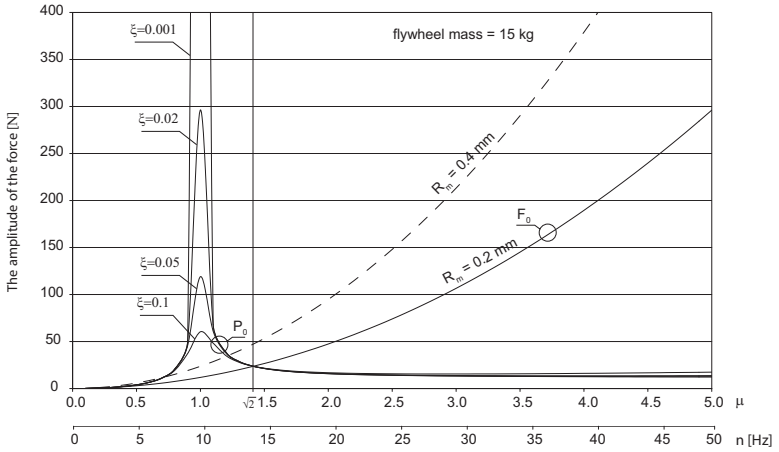

Fig. 3. Amplitude of dynamic forces in vibration isolation system at maximum μ = 5 and different damping coefficients ξ and resonant velocity n_r = 10 Hz

(3) during the machine motion in the resonant area, the amplitudes of dynamic forces can be up to several dozen higher than amplitudes of dynamic forces caused by other machine motion,

(4) along with the increase of the dimensionless damping coefficient ξ, amplitudes of dynamic forces transferred to the ground via isolators are reduced,

(5) dynamic features of the isolators impact the amplitudes of dynamic forces transferred to the ground. Usage of isolators that ensure lower frequencies of normal mode (higher values of maximum μ) effects in decrease of amplitude of dynamic forces. (6) settling the fan on elastic elements and ensuring the value of $\mu \geq 5$ will result in amplitudes of dynamic forces transferred to the ground lower than the amplitude of the force appearing during periods of maximum rotation speed of the moving fan.

5. Measurements of existing object

Parameter measurements were taken for the vibration platform with a mass of 242.4 kg. The platform was located on 4 equally loaded isolators. The examination was carried out in two parts – firstly, with the rubber isolators, secondly, with the spring isolators. Measurements of the vertical displacement of the platform were taken during the experiment. Displacement values were taken in the function of motor rotation speed.

Displacement values were taken in 2 independent series. The first series concerned the frequency range below 10 Hz, and second series, above 10 Hz. Such a division of the frequency range was due to the specification of measuring devices. The employed vibration meter (Lutron VB-8200) operates for frequencies up 10 Hz. Displacements for lower frequencies were measured with a mechanical tactile vibration recorder. The frequency was measured with a stroboscope.

Vibration meter VB-8200 can measure the acceleration (peak) and the velocity (peak), therefore, displacements were obtained indirectly. In order to maintain the reliability of the measurements, frequencies were also obtained in an indirect manner. In this work we used only the results when frequencies measured by the stroboscope were equal to frequencies measured by vibration meter.

Examinated unit had an extra weight added to the shaft to emphasize the unbalance of the unit. Displacement values of the platform settled on the rubber and spring isolators are shown in picture 4.

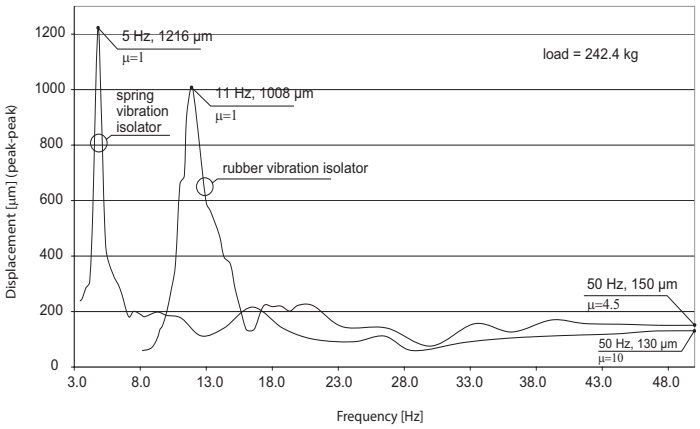

Fig. 4. Displacement (peak-peak) of vibration platform based on a rubber and spring in a function of driving frequency

6. Calculation of the differential equation parameters

The elasticity coefficient in dynamic conditions was calculated with equation (3), after the substitution of normal mode frequency and mass.

The procedure of damping factor *c* calculation was as follows:

a) the calculation of the multiplied rotating mass and eccentric radius from equation (10), after the substitution of system mass, oscillation amplitude (for highest possible μ) and μ itself.
b) calculation of dimensionless relative amplitude for resonant conditions using equation (7) after substituting system mass, multiplied $M_w R_M$ and oscillation amplitude Turing resonance,
c) calculation of the damping coefficient ξ on a basis of equation (9) after substitution of dimensionless relative amplitude in resonance,
d) finally, the calculation of the damping coefficient from equation (4). All acquired data is presented in Table 1.

Table 1

Parameters calculated for vibration isolation system

	n_r	$2y_0$	n_1	$2y_1$	k_d	$M_w R_M$	ξ	c
	Hz	μm	Hz	μm	$10^6 \frac{\text{N}}{\text{m}}$	kg · m		$10^3 \frac{\text{Ns}}{\text{m}}$
Rubber	11	1008	50	150	1.3	0.017	0.07	2.5
Spring	5	1216	50	131	0.2	0.016	0.05	0.8

7. Computer model of the vibration isolation

The calculated parameters of *the* second order differential equation were employed for the development of a computer model of vibration isolation. The transmittance of the vibration platform was calculated using equation (13) and the transmittance of the driving force coming from the motor using equation (14).

$$G(s) = \frac{\frac{1}{m}}{s^2 + \frac{c}{m}s + \frac{k_d}{m}} \tag{13}$$

$$U(s) = \frac{F_0 \omega}{s^2 + \omega^2} \tag{14}$$

Equivalent transfer functions of the motor-vibration platform were calculated afterwards (15) for driving frequencies from 3 to 50 Hz (one transfer function for each one frequency).

$$G_{zn}(s) = G(s)U(s) \qquad n = 3...50 \text{ Hz} \tag{15}$$

Each transfer function from $G_{z3}(s)$ to $G_{z50}(s)$ was explored in simulation in MATLAB. The transfer functions were subjected to Dirac delta $\delta(t)$ using MATLAB command *impulse*. In effect, impulse responses of the objects $G_{zn}(s)$ were explored. A direct result of the simulation was the value of the momentary displacement for the particular driving frequency. Figure 5 presents the peak values of the displacements coming from the simulation with real measured values taken from the existing object.

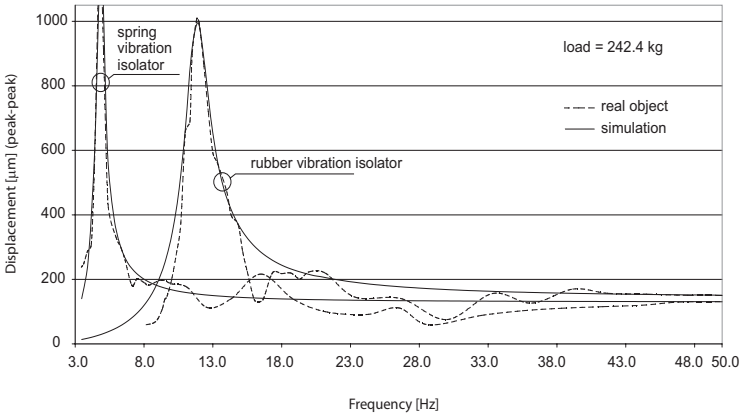

Fig. 5. Real and simulated displacement (peak-peak) of vibration platform depending on driving frequency and the type of applied isolators

By calculating the first derivative from the momentary displacement, momentary oscillation velocity was obtained. The maximum velocity values coming from the simulation and real measures are presented in Figure 6. This diagram additionally shows the maximum allowed velocity level, according to the ISO 2372 (10816) [10].

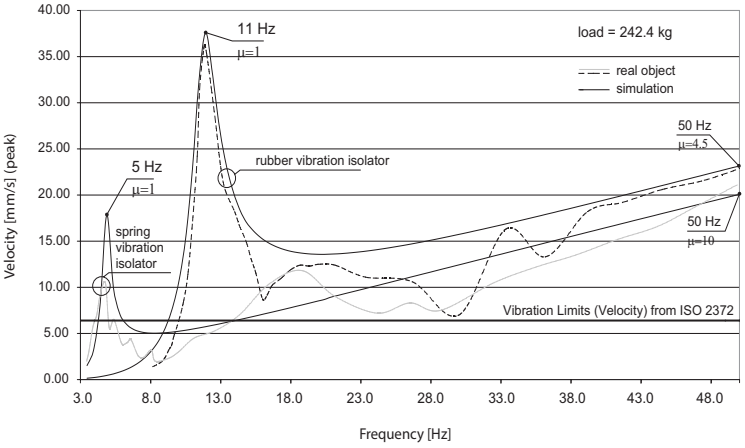

Fig. 6. Real and simulated velocity (peak) of the vibration platform as a function of driving frequency and the type of applied isolators

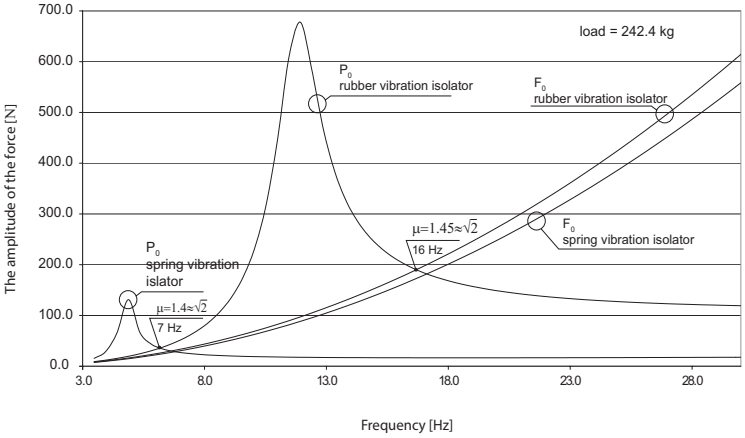

Fig. 7. Amplitudes of dynamic forces appearing in considered systems as a function of driving frequencies

Based on the simulation results, we developed the graphs showing the amplitudes of the dynamic forces in the examined system. The results are shown in Figure 7.

8. Model results analysis

Displacement graphs confirm that the isolators with lower dimensionless damping coefficient (for spring isolator) are more efficient in displacement reduction but this applies only to the situations when the vibration isolation works in overcritical area

In the resonant area, oscillation amplitude exceeds oscillation amplitude of the vibrating platforms placed on the rubber elements. Additionally, increase of the oscillation amplitude for the spring isolators takes place at significantly lower driving force. According to this, reduction of the damping coefficient may lead to excessive vibrations in the resonant area, for instance, in situations with a long accelerating drive when the unit gets through resonance area to achieve nominal rotation speed.

At $\mu > \sqrt{2}$, the force transferred to the foundation is lower than the driving force, this confirms the accuracy of the simulation results.

In Figure 7, two lines appear illustrating the amplitude of driving force $F_{0.}$ This is a result that the product of $M_w R_M$ calculated according to equation (10) for the spring isolators configuration is different to the rubber isolators configuration and the results are as follows:

$(M_w R_M)^{sprongs} = 0.016$ kg/m,

$(M_w R_M)^{rubbers} = 0.017$ kg/m.

The motor shaft located at the platform had an extraordinary imbalance weight to increase the dynamic forces during the experiments. This had an negative impact for the working conditions. The examined unit in wide scope of work was exceeding allowed vibration amplitudes according to the ISO 2372 According to this norm, the maximum allowed momentary velocity for machines below 15 kW equals 6.36 mm/s.

Experiments related to vibration isolation become an effective tool in the rotary machine assessment process. Comprehensive mathematical tooling and it's availability results in simplified creation of the mathematical models for real vibrating units. The obtained results can be used for the current evaluation of operating machinery, this can lead to potential failure detection (Fault Diagnostic and Detection FDD). Simulation can be also useful in estimating the effectiveness of the applied vibration isolation system in different conditions, i.e. at different rotation velocity or different weight mass.

The developed tests of the isolators prove the necessity of checks for newly implemented isolators as their real parameters may be different to their design and manufacturing features. The reasons for the above may be different – i.e. additional friction or rubber features that weren't taken into account during the design phase.

9. General tips for amortization systems selection

In HVAC systems, we always consider two-part rotating machinery. The work of the pump, the fan or the compressor is always related to the work of the powering motor. We can feature three main types of couplings between the motor and the rotary machine:

a) direct system, where the rotation velocity of the fan and motor are the same,

b) clutching systems, where the rotation velocities on the motor and fan are usually similar,

c) belt driven systems, where the rotation velocities of the motor and fan can be different as a function of driving wheels.

For the systems where the rotation velocity is the same on both elements, driving velocity is obvious. The value of rotation velocity is extremely important for the selection of amortization systems with belt driven units. Generally, in HVAC systems, isolators should be selected to let the unit work in conditions distant from the resonance at the frequency ratio $\mu \geq 3$.

For the calculation of the frequency ratio μ, it is recommended to apply the rule of selecting the minimum rotation speed $n^{\min}(n_w, n_s)$. When for lower rotation velocity, the vibration isolation condition is met, it is also met for higher rotation velocities. Following this, we can say that for higher rotation velocities, the value of the ground transferred reduced force will be much smaller than for lower rotation velocities. At the same time, let's not forget that correctly selected isolators should have small enough ξ so that the limitation of the force should be as high as possible. The value of the ξ should also be big enough to let the machine go through the resonance phase without damaging the foundation as a result of too high amplitude of the force transferred to the foundation. Considering the design of reinforced supporting frames, the basis for the calculations should be maximum driving velocities.

10. Vibration isolation of the fans with variable airflows

Considering for calculations the frequencies ratio $\mu \geq 3$ referred to minimum driving velocity leads to a major reduction of dynamic forces transferred to the ground by isolators.

The achievement of low normal mode frequencies (i.e. 2 Hz) requires special isolator constructions and specific fitting systems to the ground and mounting frame. Considering variable rotation speed fans working in the range of 50–100% of maximum speed, the assumption of frequency ratio $\mu = 5$ allows us to ensure the satisfactory working parameters of the motor/fan at minimum speeds. When fans are designed to work in the range 20–100% of maximum speed, the assumption of frequency ratio of $\mu = 5$ for maximum speed will result in resonance of the fan/motor. In those cases, systems located on the isolators should be calculated with $\mu = 8$ for maximum speeds. At a minimum speed around of 20% of the maximum speed, values of the dynamic forces transferred to the ground would be lower than the amplitudes of created forces.

11. Conclusions

During the design phase of vibration isolation of variable speed fans, it is essential to consider the minimum and maximum rotation speeds. It is recommended to keep the vibration isolation in the overcritical area along with the full range of the designed rotation speeds and keep the minimum value of μ at least at a level of 1.6. Dimensionless damping coefficients should be as low as possible. In cases when the maximum rotation speeds of the motor/fan are not exceeding 20 Hz and the minimum are not exceeding 4 Hz, achievement of overcritical isolation can be difficult. To remedy this, it is worth thinking about the possibility of resonant work at minimum rotation speeds and applying isolators with dimensionless damping coefficients $\xi > 0.05 \div 0.1$. Amplitudes of dynamic forces transferred to the ground via isolators during resonant work will be much lower than the dynamic forces created at maximum speeds. To reduce the amplitudes of fan/motor oscillation, it's advised to use **lean limiters**, similar to the ones used in marine vibration isolation. In this case, implementation of under critical vibration isolation will cause that amplitudes of dynamic forces transferred to the ground will be higher than the amplitudes created as a result of working. It is true for the full range of fun work.

References

[1] Ibrahim R.A., *Recent advances in nonlinear passive vibration isolators*, Journal of Sound and Vibration 314, 2008, 371-452.
[2] Yang C., Yuan X., Wu J., Yang B., *The research of passive vibration isolation system with broad frequency field*, Journal of Vibration and Control 19(9), 2012, 1348-1356.
[3] Le T.D., Ahn K.K., *Experimental investigation of a vibration isolation system using negative stiffness structure*, International Journal of Mechanical Sciences 70, 2013, 99-112.
[4] Liu X., Huang X., Hua H., *On the characteristics of a quasi-zero stiffness isolator using Euler buckled beam as negative stiffness corrector*, Journal of Sound and Vibration 332, 2013, 3359-3376.
[5] Hanieh A.A., Preumont A., *Multi-axis vibration isolation using different active techniques of frequency reduction*, Journal of Vibration and Control 17(5), 2010, 759-768.

[6] Alujević N., Wolf H., Gardenio P., Tomac I., *Stability and performance limits for active vibration isolation using blended velocity feedback*, Journal of Sound and Vibration 330, 2011, 4981-4997.
[7] Michalczyk J., *Transient resonance of machines and devices in general motion*, Journal of Theoretical and Applied Mechanics, 50, 2, Warsaw 2012, 577-587.
[8] DiGiovanni M., Thomas R., Spearman P.E., *Fan Vibration Specifications*, ASHRAE Journal, February 2008.
[9] Goliński J.A., *Wibroizolacja maszyn i urządzeń*, WNT, Warszawa 1979.
[10] ISO 10816-1 Annex B, Mechanical vibration – Evaluation of machine vibration by measurements on non-rotating parts, 2003.

TECHNICAL TRANSACTIONS | CZASOPISMO TECHNICZNE
MECHANICS | MECHANIKA
2-M/2014

BOGDAN SAPIŃSKI*, ZBIGNIEW SZYDŁO**

PROTOTYPE CONSTRUCTIONS OF MAGNETORHEOLOGICAL DAMPERS WITH ENERGY HARVESTING CAPABILITY

PROTOTYPOWE KONSTRUKCJE TŁUMIKÓW MAGNETOREOLOGICZNYCH Z ODZYSKIEM ENERGII

A b s t r a c t

The paper briefly summarises the design structure of a prototype linear and rotary magnetorheological (MR) damper with energy recovery capability, engineered by the authors, and provides selected characteristics of those devices based on laboratory testing.

Keywords: *damper, electromechanical transducer, signal conditioning and processing system, energy harvesting*

S t r e s z c z e n i e

W artykule opisano budowę zaprojektowanych i wykonanych przez autorów prototypowych konstrukcji liniowego i obrotowego tłumika magnetoreologicznego (MR) z odzyskiem energii. Przedstawiono również wybrane charakterystyki tych urządzeń wyznaczone na podstawie badań laboratoryjnych.

Słowa kluczowe: *tłumik MR, przetwornik elektromechaniczny, układ kondycjonująco-przetwarzający odzyskiwanie energii*

* Prof. Ph.D. Eng. Bogdan Sapiński, Department of Process Control, AGH University of Science and Technology.

** Ph.D. Eng. Zbigniew Szydło, Department of Machine Design and Technology, AGH University of Science and Technology.

1. Introduction

The recovery of energy involved in mechanical vibration has received a great deal of attention in the field of harvesting energy from the surroundings. There are three basic methods of mechanical to electric energy conversion: electromagnetic methods; electrostatic methods; the use of smart materials. Thus, the recovered energy can then be utilised to power other devices. The solutions with which recovered energy is used to power piezoelectric sensors in wireless monitoring systems are now well known. These solutions are applicable as long as the vibration frequency is in the order of several hundred Hertz, the amplitudes are in the order of micrometers and the energy sources have power ratings of several micro or milliwatts.

This paper introduces newly designed, prototype constructions of MR dampers, power-supplied with energy recovered from mechanical vibrations of frequency ranging from several to about 20 Hz and with amplitudes in the order of ten millimetres. Reports on these types of linear MR dampers can be found works [1–4, 17, 18], although information about rotary dampers is rather scarce. The available literature on the subject includes just the patent [16], which may be the associated with the lack of relevant applications and the need to fabricate the appropriate control system.

The MR devices presented in this paper were designed and fabricated by the authors as a part of their research program. The underlying assumptions are included in patent applications [9−12]. These devices incorporate an electromechanical vibration transducer (generator), so the electric energy required to activate the MR damper is recovered from a vibrating object [1−2, 6−8]. The transducer, operating in accordance with Faraday's law of magnetic induction, converts the mechanical energy into electrical energy (the velocity of the vibrating object is 'converted' into voltage induced on the converter coil). This voltage gives rise to a variation of current in the MR damper control coil (receiver), and of the force generated by the damper. Typically, MR dampers are not directly activated by output voltage from the converter, but the voltage signal is first conditioned in the signal conditioning and processing system.

A block diagram of the MR dampers considered in this study is shown Fig. 1.

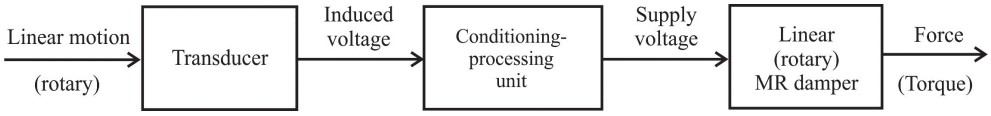

Fig. 1. Schematic diagram of energy harvesting in the MR damper

2. Structure design

The structure of the linear MR damper with energy harvesting capability is shown in Fig. 2. The device consists of a linear MR damper (1–7) connected to a linear electromechanical transducer (9–15) via a connecting lid (8). The MR damper incorporates a piston (4, 5) housing a control coil (6) and powered via a signal conditioning and processing unit (13). A magnetic field in the damper, induced by current flowing through the control coil, causes

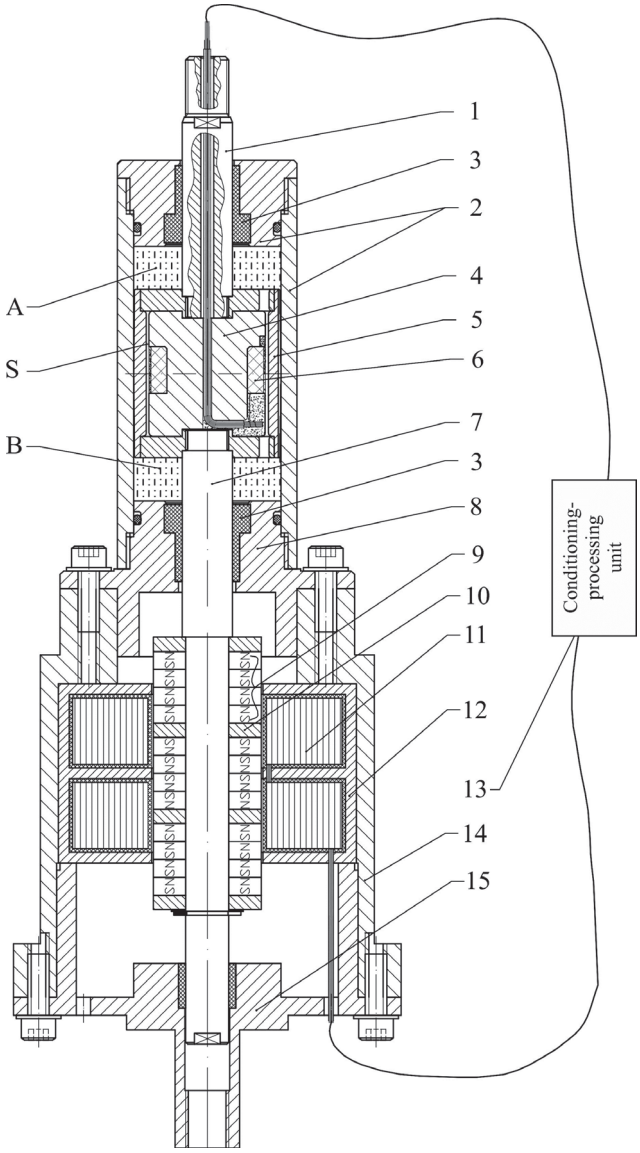

Fig. 2. Structure of a linear MR damper with energy harvesting capability: 1 – piston rod; 2 – damper housing; 3 – sleeve; 4 – piston core; 5 – piston ring; 6 – damper coil; 7 – transducer stem; 8 – connecting lid; 9 – permanent magnets; 10 – pole pieces; 11 – transducer coil; 12 – transducer coil housing; 13 – signal conditioning-processing system; 14 – transducer frame; 15 – transducer cover; S – slit, A, B – space filled with MR fluid

the MR fluid viscosity in the slit (S) to change, thus enabling the control of the MR fluid flow rate from the chamber (A) to (B) and in the opposite direction. There are piston rods on both ends of the piston and the rod (7) acts as the transducer stem supporting the

permanent magnet systems (9), separated by pole pieces (10). The movement of the stem with the magnets inside the transducer coil (11) induces the electromotive force (emf) in the coil.

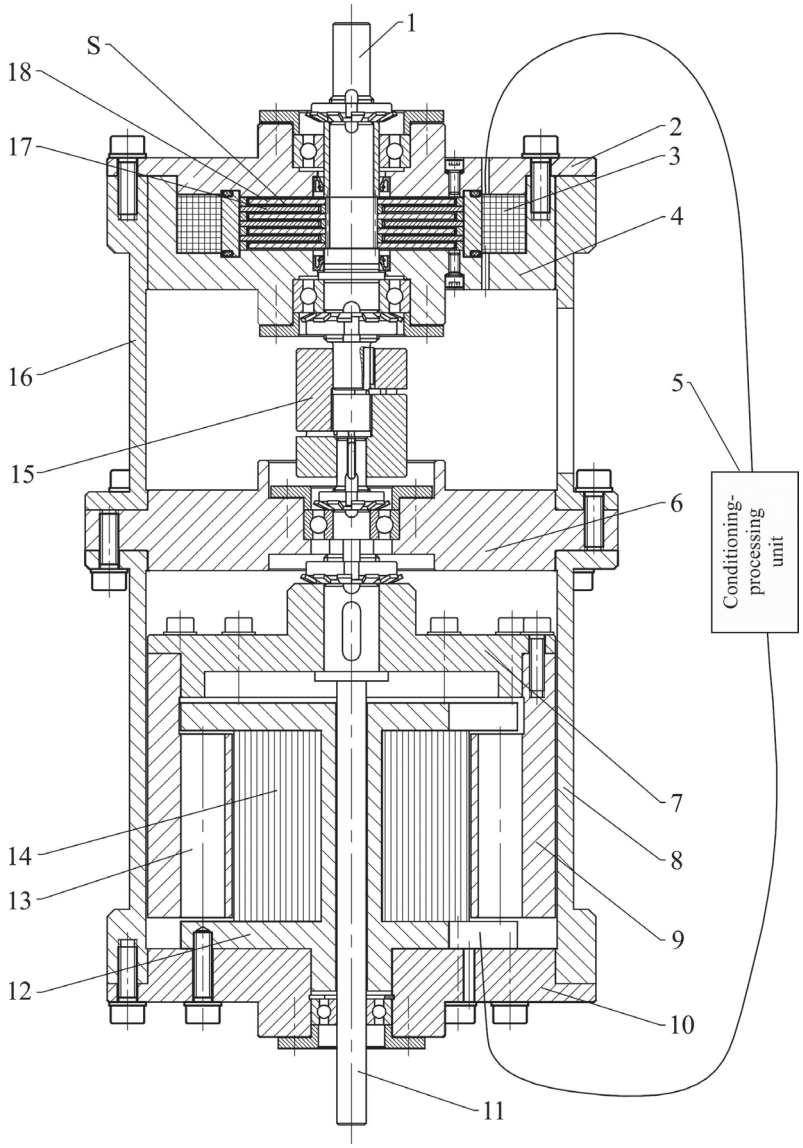

Fig. 3. Structure of a rotary MR damper with energy harvesting capability: 1 – shaft; 2 – damper lid; 3 – damper coil; 4 – frame; 5 – signal conditioning-processing system; 6 – plate; 7 – rotary frame; 8 – housing; 9 – sleeve; 10 – transducer cover; 11 – shaft in the transducer coil; 12 – pole pieces; 13 – permanent magnets; 14 – transducer frame; 15 – coupling; 16 – sleeve; 17 – immobile disc; 18 – rotating disc; S – slit

The design structure of the rotary MR damper with energy harvesting capability is shown in Fig. 3. The device consists of a rotary MR damper (1–4, 17, 18) connected to an electromechanical rotary transducer (6–14) via a sleeve (16). There is a set of rotating discs (18) supported on the shaft (1), a set of immobile discs (17) placed in the frame housing the control coil (3) and it is powered via a conditioning system (5). The magnetic field generated by current flowing through the coil causes the MR fluid viscosity in the slit S to change, thus enabling the control of the rotating discs' movement with respect to the immobile discs. The shaft in the damper is connected to the shaft in the transducer coil (11) via a coupling (15) and it supports the rotating frame (7) with the sleeve (9) on which the permanent magnets are arranged. There is a coil (14) in the notches on an immobile pole section (12) with radial incisions. When the magnets rotate, an electromotive (emf) force is induced in the transducer coil (14).

The engineered devices are shown in Fig. 4 and Fig. 5.

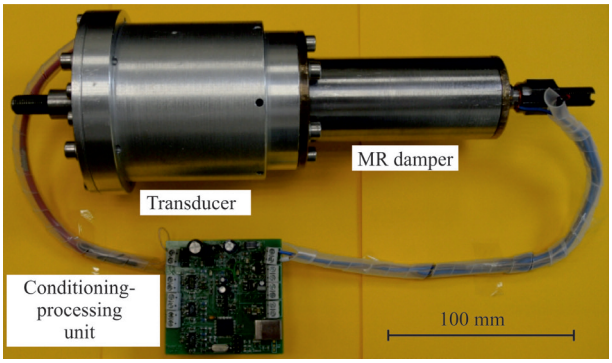

Fig. 4. Linear MR damper with energy harvesting capability – general view

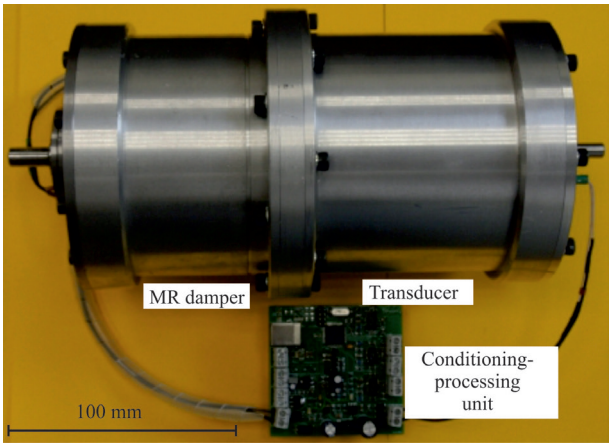

Fig. 5. Rotary MR damper with energy harvesting capability – general view

3. Characteristics

The engineered MR dampers were then subjected to tests in laboratory conditions to determine their basic operational characteristics.

The linear MR damper was tested on a testing machine under the applied sine excitations (displacement) of the piston. Tests were performed under an idle run when the coils in the transducer and the damper were not connected (1) or under load - in one case, the coils in the transducer and the damper were connected directly (2), in the other case, they were connected via the signal conditioning and processing system (3). The selected characteristics obtained under those operating conditions are shown in Fig. 6, giving the dependence between the force generated by the device on piston velocity and displacement under the applied excitations of amplitude 10 mm and frequency 3 Hz. These characteristics differ from that of a typical MR damper, the main reason being the cogging force appearing in the transducer [14]. The plots reveal that under loading condition 2, the maximal force generated by the device approaches 900 N, which can be related to 700 N (state 3) and about 500 N (state 1). The main reason for the force registered in state 3 being less than in state 2 is the voltage drop in the signal conditioning and processing unit [5].

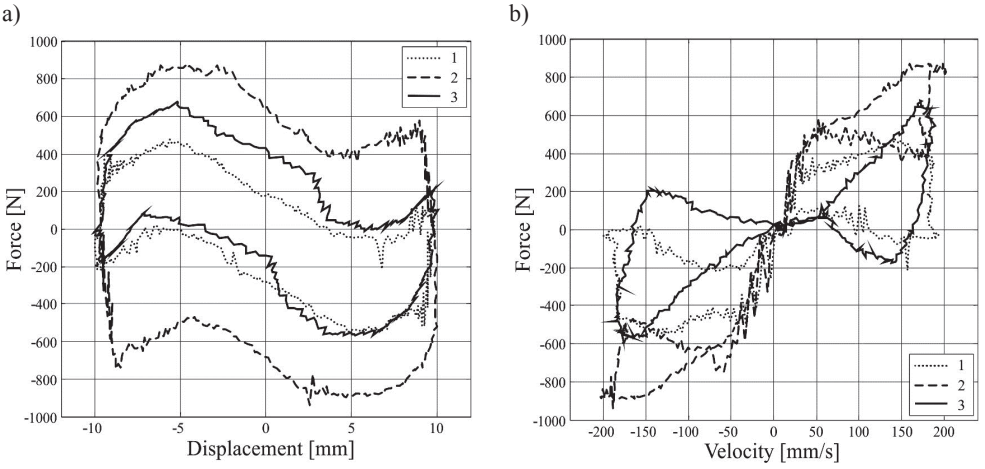

Fig. 6. Characteristic of a linear MR damper with energy harvesting capability: a) force vs displacement, b) force vs velocity

The rotary MR damper was subjected to laboratory tests on the test facility engineered specifically for the purpose of the research program [13]. The damper was tested in the direct powering mode only, at a rotational speed in the range 0–250 rpm. Selected characteristics of the MR device are shown in Fig. 7, giving the plots of voltage U, current I in the MR damper control coil and the torque T generated by the damper in the function of rotational speed. Of particular interest are changes in the torque generated by the damper, the contribution of the clogging moment being far from minor [15] and its decreasing with increasing rotational speed.

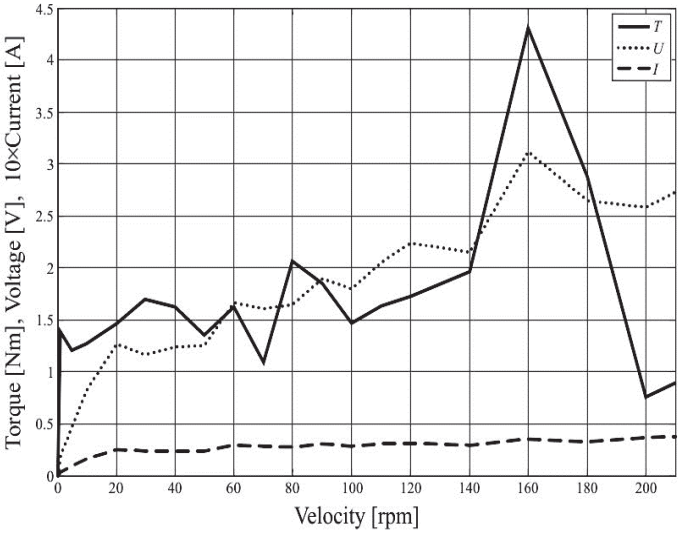

Fig. 7. Characteristic of a rotary MR damper with energy harvesting capability: voltage, current and torque vs velocity

4. Conclusions

The prototype designs of MR dampers with energy harvesting capability are described based on data provided in patent applications. Laboratory tests have revealed the need for further improvement of the devices and further research work has been now undertaken.

As regards the vibration transducers, their capacity will be enhanced, their size reduced and the cogging force/cogging moment will also be reduced. The signal conditioning system will be modified, which will involve an output voltage increase and reduction of the size of the device, as the transducer is planned to be integrated with the MR damper within a single housing.

The results of testing done on a rotary MR damper with energy recovery capability have revealed the need to change the structure design of the rotary generator such that the position of permanent magnets and that of the coil assembly should be reversed, the permanents magnets should be placed inside immobile coil assembly.

This research is supported by the National Centre for Research and Development under grant No. NR 03 0046-10.

References

[1] Chen C., Liao W.H., *A self-sensing magnetorheological damper with power generation*, Smart Materials and Structures, 21, 2012, 02501.

[2] Choi Y.T., Werely N.M., *Self-powered magnetorheological dampers*, Journal of Vibration Acoustics, 131, 2009, 44-50.

[3] Li Z., Zhuo L., Kuang J., Luhrs G., *Energy-Harvesting Shock Absorber with a Mechanical Motion Rectifier*, Smart Materials and Structures, 22, 2013, 028008.

[4] Liao W.H., Chen C., *Self-powered and self-sensing magnetorheological dampers*, International Application Published under the Patent Cooperation Treaty, WO 2012/016488 A1, 09.02.2012.

[5] Rosół M., Sapiński B., Jasiński J., *Układ kondycjonująco-przetwarzający elektromechanicznego przetwornika drgań*, Modelowanie w Mechanice, Vol. 47, No. 16, 2013, 1661-71.

[6] Sapiński B., *Vibration power generator for a linear MR damper*, Smart Materials and Structures, 19, 2010, 1050-1062.

[7] Sapiński B., *Experimental study of self-powered and sensing MR damper-based vibration control system*, Smart Materials and Structures, 19, 2010, 1050-1062.

[8] Sapiński B., Krupa S., *Efficiency improvement in a vibration power generator for a linear MR damper: numerical study*, Smart Materials and Structures, 22, 045011 (15 p.), 2013.

[9] Sapiński B., Krupa S., *Przetwornik energii mechanicznej nawrotnego ruchu liniowego na energię elektryczną*, Wniosek o udzielenie patentu, nr P-395 786 z dnia 28.07.2011.

[10] Sapiński B., Krupa S., *Przetwornik energii mechanicznej ruchu obrotowego na energię elektryczną*, Wniosek o udzielenie patentu, nr P-395 787 z dnia 28.07.2011.

[11] Sapiński B., Szydło Z., *Wibroizolator magnetoreologiczny z elektromagnetycznym przetwornikiem drgań*, Wniosek o udzielenie patentu, nr P-399 320 z dnia 28.05.2012.

[12] Sapiński B., Szydło Z., *Magnetoreologiczny tłumik drgań skrętnych z elektromagnetycznym przetwornikiem ruchu obrotowego*, Wniosek o udzielenie patentu, nr P-403 371 z dnia 29.03.2013.

[13] Sapiński B., Węgrzynowski M., *Experimental setup for testing rotary MR dampers with energy harvesting capabilities*, Acta Mechanica Automatica Vol. 7, No. 4, 2013, 241-244.

[14] Sapiński B., Krupa S., Matras A., *Siła zaczepowa w elektromechanicznym przetworniku drgań o ruchu liniowym*, Przegląd Elektrotechniczny, ISSN 0033-2097, R. 88, NR 12a/2012, 83-87.

[15] Sapiński B., Krupa S., Matras A., *Moment zaczepowy w obrotowym przetworniku elektromechanicznym*, Przegląd Elektrotechniczny, R. 89 NR 4/2013, 19-24.

[16] Liao W.H., Guo H, *Magnetorheological actuators*, United States Patent Application Publication, US2010/231069 A1.

[17] Wang Z., Chen Z., Spencer B.F. Jr., *Self-powered and sensing control system based on MR damper: presentation and application*, *Proc. SPIE Smart Structures/NDE*, 2009.

[18] Zhu X., Jing X., Cheng Li., *Magnetorhelogical fluid dampers, A review on structure design and analysis*, Journal of Intelligent Material Systems and Structures 23(8), 2013, 839-873.

TECHNICAL TRANSACTIONS | CZASOPISMO TECHNICZNE
MECHANICS | MECHANIKA
2-M/2014

JACEK SNAMINA, BOGDAN SAPIŃSKI*

ANALYSIS OF AN AUTOMOTIVE VEHICLE ENGINE MOUNT BASED ON A SQUEEZE-MODE MAGNETORHEOLOGICAL DAMPER

ANALIZA SEMIAKTYWNEGO ZAWIESZENIA SILNIKA SAMOCHODOWEGO Z WIBROIZOLATORAMI MAGNETOREOLOGICZNYMI

Abstract

Methods are outlined that can be employed to reduce the dynamic components of interaction forces between the vehicle engine and the car body, taking into account the main sources of vibration in the engine. The transmitted forces arising due to the reciprocating motion of the pistons in a two-cylinder engine are calculated. The amplitude and frequency characteristics are used to develop a method for controlling the engine mount stiffness and damping depending on the angular velocity of the crank shaft motion. The study explores the feasibility of damping control in the mount through the use of magnetorheological (MR) dampers operated in the squeeze mode.

Keywords: *vibration, engine mount system, MR damper, control*

Streszczenie

W artykule omówiono metody obniżenia wartości składowych dynamicznych sił oddziaływania silników spalinowych na karoserie samochodów biorąc pod uwagę podstawowe źródła drgań silników. Przeprowadzono obliczenia przenoszenia sił powstających w wyniku ruchu posuwisto-zwrotnego układu tłoków dla prostego silnika spalinowego. Na podstawie analizy otrzymanych charakterystyk amplitudowo-częstotliwościowych zaproponowano ogólną metodę sterowania sztywnością i tłumieniem zawieszenia silnika w zależności od prędkości obrotowej wału korbowego. Przedstawiono możliwości sterowania sztywnością i tłumieniem zawieszenia przy zastosowaniu specjalnie skonstruowanych tłumików magnetoreologicznych (MR).

Słowa kluczowe: *drgania silników spalinowych, zawieszenie silnika spalinowego, charakterystyka tłumika MR*

* Prof. Ph.D. Eng. Jacek Snamina, Prof. Ph.D. Eng. Bogdan Sapiński, Department of Process Control, Faculty of Mechanical Engineering and Robotics, AGH University of Science and Technology.

1. Introduction

An automotive vehicle engine is a rigid body with a complex geometry. It is fixed to the car body on supports whose placements and parameters are derived from calculations of the static and dynamic behaviour of the entire driving system. The static calculations involve the displacements of the main sub-assemblies and deformation of the applied supports under static equilibrium conditions. The dynamics calculations are much more complex. They take into account the fundamental reasons for the drive unit vibrations such as inertia forces produced by the motions of unbalanced elements of the crank shaft system, the periodically fluctuating torque transmitted via the engine to subsequent components of the driving system in the vehicle and some random forces. A vibrating engine is one of the sources of vibrations of the car body. These vibrations are induced by forces transmitted via the engine mount elements onto the frame. The minimisation of the dynamic components of these forces is a major problem in vibration control. As the reasons of engine vibrations cannot be wholly eliminated, it is of particular importance that the structural design of the engine mount is such that the engine position should be stabilised and the dynamic components of forces between the engine and the car body should be minimised.

Elastic mounts of the automotive vehicle driving systems date back to the 1930s [10]. The first mount systems would be made of relatively small and cheap rubber elements. In the 1960s, the mount system was introduced in which the engine was fixed with hydraulic elements. In the following years, these elements were modified and improved. Currently, research efforts are focused on semi-active and active engine mount systems, enabling more effective reduction of undesired interaction forces between the engine and the vehicle body.

This study presents the results of the calculations of forces acting upon the car body as a result of the reciprocating piston motion. The model of a two-cylinder engine was used in calculations. Based on the obtained frequency response functions, a method is developed for controlling the engine mount vibrations (stiffness and damping control) depending upon the angular velocity of the crank shaft motion. The potentials of using dedicated MR dampers for mount damping and stiffness control are explored.

2. Design structure of key components of the vehicle engine mount systems

The reason why the selection of the engine mounts has received such a great deal of attention from design engineers is the current trend in vehicle development to fabricate lighter front-wheel drive vehicles having light engines with low idle speeds. The most stringent requirements could be satisfied only by mounts with controllable stiffness and damping characteristics. The first components developed in consideration of this requirement were hydraulic elements patented in 1962 [10]. When vehicle mounts are fitted with such components, the amplitudes of car body vibrations during the motion are decidedly lower in comparison to when using mounts with rubber components. The cross-section of a typical hydraulic element is shown in Fig. 1.

The top housing (3) connected to the engine via the fixing system (5), is made of rubber. It closes the top chamber (1) containing oil. Oil flows from the top to the bottom chamber

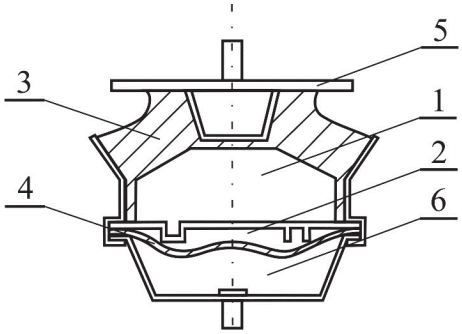

Fig. 1. Cross-section of a hydraulic pressure element [10]

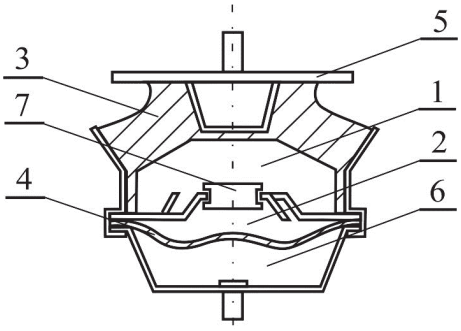

Fig. 2. Cross-section of a hydraulic pressure element with the de-coupler system [10]

(2) via an orifice or through a conduit with a precisely controlled diameter. The bottom chamber is limited from below by a rubber housing (4), which can expand due to the liquid pressure increase. It expands to the inside of the restricted volume (6) where the atmospheric pressure will prevail. The rubber housing deformed under the weight of the engine will generate pressure in both chambers. Dynamic displacement components give rise to further deformations of the upper housing (made of rubber), causing the oil flow through an orifice or a calibrated pipe. Mount stiffness and damping can thus be effectively controlled over a wide range of movement.

The most advanced version of hydraulic elements is shown in Fig. 2. Here, the solution incorporates an inertial system for decoupling the flow between the chambers (7). The aim of this system is to make the damping amplitude-dependent and frequency-dependent. The system controls the liquid flow between the chambers, such that the orifice should be bypassed at precisely selected amplitudes – thus, damping control is provided. In relation to the engine vibration parameters the mount characteristics can be better fitted to the engine performance. The operating principles of hydraulic elements employed in engine mounts are investigated, based on linear and nonlinear models [1, 3, 7]. The model parameters can be determined using simulation data or calculation procedures based on optimisation methods, alternatively, they can be determined experimentally.

Hydraulic mounts are tunable under the applied sine variable inputs of precisely controlled frequency. In the case of more complex inputs with a wide frequency range, the mount is no longer effective, this is a feature of passive mounts. Improved mount performance in one frequency range often leads to its deterioration in other frequency ranges. Therefore, the selection of model parameters will always involve a certain trade-off.

Optimal mount performance in the entire frequency range can be achieved with semi-active or active mounts, where the adequate control algorithm is applied [2, 4]. The literature on the subject abounds in reports on mounts in which MR and electrorheological (ER) fluids are employed. The property of these fluids is utilized – their apparent viscosity changes significantly under the influence of a variable electric field. The design structure of semi-active elements used in mounts is similar to that of hydraulic components. Around the flow path from the top to the bottom chamber, there are electrodes generating the electric

field acting upon the ER fluid. Thus, the mount damping can be controlled and the optimal damping can be ensured in any frequency range. An integral part of any semi-active mount is a control system to implement the control algorithm.

3. Engine – frame interactions

To determine the interactions between the engine and the frame in the car body, the forces are calculated that appear in the engine mount due to the reciprocating motion of pistons in a two-cylinder four-stroke combustion engine. The schematic diagram of the engine is shown in Fig. 3.

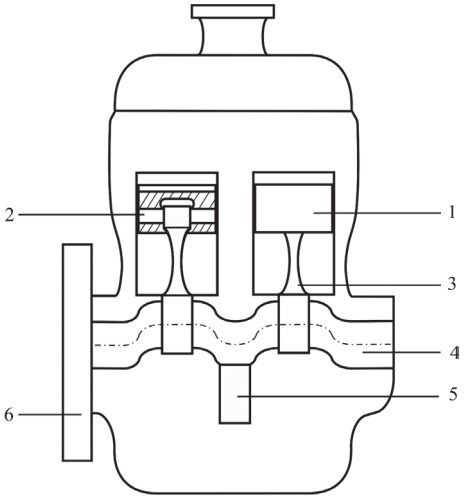

Fig. 3. Cross-section of the engine

Two pistons (1) are in concurrent operation. During the upward motion, the compression stroke is implemented in one cylinder and the exhaust stroke in the other. During the downward motion, the respective power stroke and intake stroke are performed. On account of the pistons' concurrent operation, a counterweight (5) is provided on the crank shaft (4) to partially balance the first harmonic of the inertia force associated with the pistons' reciprocating motion and the inertia force of the crankshaft web. The diagram also illustrates the flywheel (6), connecting rods (3) and the bolt (2) fixing the piston on the connecting rod.

It is assumed that the calculation procedure should involve only the engine motion in a vertical direction in the plane perpendicular to the crank shaft, passing through the crank centre of gravity. The simplified diagram of the crank shaft and piston mechanism in the engine block is shown schematically in Fig. 4.

This diagram indicates all masses taken into account in the calculation procedure. The mass of the connecting rod is reduced to two points: point A,

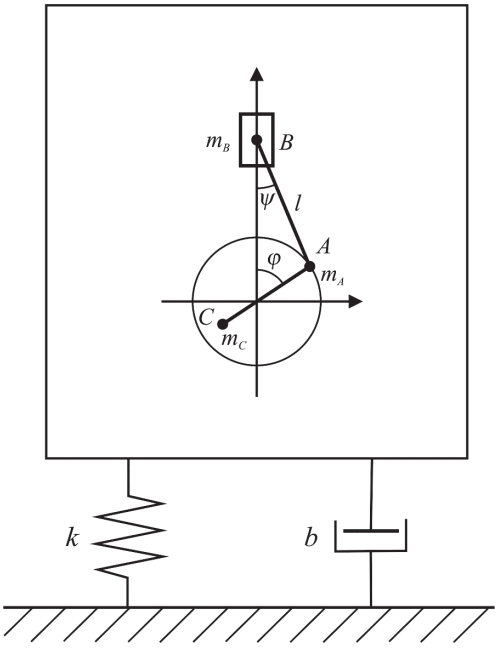

Fig. 4. Schematic diagram of a crank shaft and piston system inside the engine block

representing the connection of the rod and crank shaft and point B, representing the piston-rod connection. This is a widely employed method of reducing the mass of the connecting rod. Finally, m_A stands for the sum of the reduced crankshaft web mass and the reduced mass of the bottom part of the connecting rod, m_C is the mass of the counterweight, reduced to its centre of gravity.

The frame to which the engine is attached is assumed to be fixed and the engine mounting system is modeled by a spring and a viscous damper connected in parallel. During the steady-state operation of the engine, the angle φ is linearly dependent on time (φ = ω*t*, where ω − angular speed of the shaft rotation). The equation of engine vibration is given as:

$$M\ddot{y} + b\dot{y} + ky = \frac{1}{2} m_B r_A \omega^2 \cos(\omega t) + \\ + m_B r_A \omega^2 \left[\left(\lambda + \frac{1}{4}\lambda^3 + \ldots \right) \cos(2\omega t) - \left(\frac{1}{4}\lambda^3 + \ldots \right) \cos(4\omega t) + \ldots \right] \tag{1}$$

M stands for the engine mass, its components m_A, m_B, m_C are indicated in Fig 4. The coefficient *k* expresses the mount stiffness and *b* is the equivalent mount damping coefficient. The coordinate *y* represents the engine frame displacement with respect to its static equilibrium position. The assumption of model linearity allows the vibration equation to be separated from that governing the static equilibrium: $ky_{eq} = Mg$. The right-hand side of Eq (1) contains the term expressing the fundamental harmonic and the subsequent two harmonics of the piston inertia forces. The remaining harmonic components are neglected. The fundamental harmonic of the inertia forces is partly balanced by providing a counterweight. The most popular solution has been adopted here, whereby half of the first harmonic of the piston inertia force is balanced in such a way that the first harmonic of the resultant inertia force of the whole crankshaft-piston mechanism should become a vector with a constant modulus and rotating at the angular speed ω in the direction opposite to the crank shaft rotation [5, 6]. In such a configuration, the higher harmonic components of the inertia force will not be balanced. The coefficient λ is expressed as the quotient of the crank web length and the length of the connecting rod. Since the value of λ is always less than one, it is a widely adopted parameter used when expanding the inertia forces into the power series.

When analysing the vibration transmission from the engine onto the car body, the amplitude of the force of the mount-frame interaction is of particular importance. This interaction force can be derived as the resultant force of the force in the spring and the force in the damper:

$$S = b\frac{dy}{dt} + ky \tag{2}$$

Since Eq (1) and (2) are linear, the force $S(t)$ has the component $S_1(t)$ with the frequency ω associated with the first harmonic inertia force of the crankshaft-piston mechanism and the higher order components $S_2(t)$, $S_3(t)$ associated with higher harmonics of the inertia force. The amplitudes of all force components are functions of the angular speed of the crank. The amplitudes of the first and second harmonics can be derived from the formulae:

$$S_{10} = \frac{1}{2}\frac{m_B}{M} r_A k\tilde{\omega}^2 \sqrt{\frac{1+4\zeta^2\tilde{\omega}^2}{\left(1-\tilde{\omega}^2\right)^2+4\zeta^2\tilde{\omega}^2}}$$
$$S_{20} = \frac{m_B}{M} r_A k\tilde{\omega}^2 \left(\lambda+\frac{1}{4}\lambda^3+\frac{15}{128}\lambda^5+....\right)\sqrt{\frac{1+4\zeta^2\left(2\tilde{\omega}\right)^2}{\left(1-\left(2\tilde{\omega}\right)^2\right)^2+4\zeta^2\left(2\tilde{\omega}\right)^2}} \tag{3}$$

where $\tilde{\omega}$ is the dimensionless angular speed of the crank shaft and ζ is a dimensionless engine mount damping coefficient. These quantities are defined by the formulas:

$$\tilde{\omega}^2 = \omega^2 \frac{M}{k}$$
$$\zeta = \frac{b}{2\sqrt{kM}} \tag{4}$$

The relationship between the first and second harmonic amplitudes of the engine – car body interaction force and angular speed is shown in Fig. 5. Dimensionless amplitudes are computed by dividing the force amplitudes in Eq (3) by the expression $m_B r_A k/M$. The values of the dimensionless damping coefficient ζ used when plotting the graphs are 0.01, 0.205, 0.305, and 0.8.

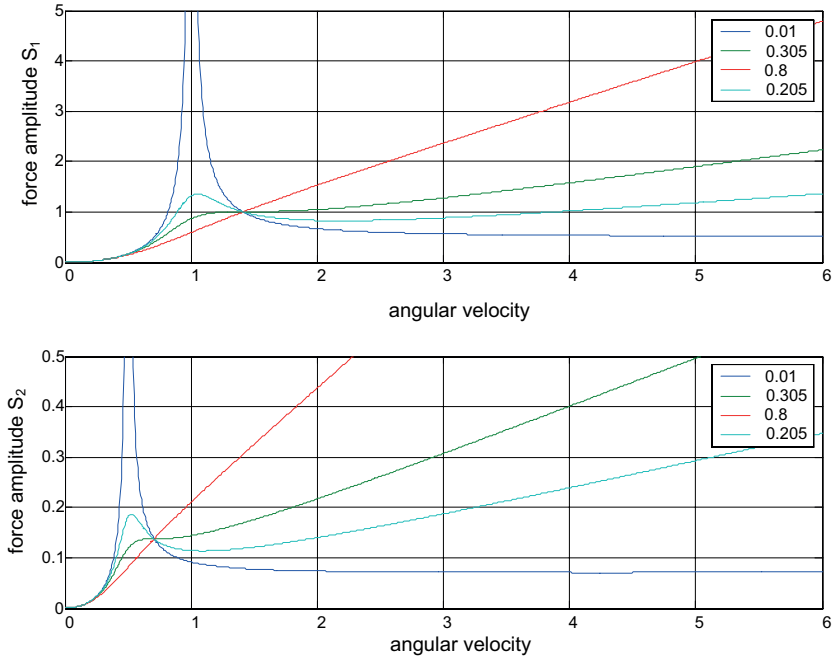

Fig. 5. Dimensionless amplitudes of the first S_1 and second S_2 harmonics of the engine-frame interaction force as functions of dimensionless angular velocity of the crank shaft motion

The function expressing the amplitude of the first harmonic becomes zero for zero frequency and tends to infinity when the angular velocity of the shaft is tending to infinity. There are two points where all graphs of the functions will intersect, regardless of the actual value of ζ. The coordinates of these two points are: (0; 0), ($\sqrt{2}$; 1).

The function governing the amplitude of the second harmonic follows a similar pattern, yet its values are significantly smaller. Resonance vibrations of the engine body cannot be observed due to the action of the second harmonic, since the maximum of the analysed function is placed for the angular velocity less than the idle speed.

4. Engine mount vibration control

The formula (3) defining the fundamental harmonic amplitude and graphs shown in Fig. 5 are utilised to develop the algorithms for engine mount stiffness and damping control. It is readily seen that:

- for the dimensionless angular velocity equal to $\sqrt{2}$, the value of the force's first harmonic becomes $m_B r_A k/M$, no matter what the actual value of the dimensionless damping coefficient,
- the force reaches its maximum for the dimensionless angular velocity being slightly more than 1 and less than $\sqrt{2}$,
- for the dimensionless angular velocity tending to zero, the force will also tend to zero,
- when the dimensionless damping coefficient is more than zero, then for the dimensionless angular velocity tending to infinity, all harmonic components of force will also tend to infinity, increasing at the rate 20 dB/decade,
- when the dimensionless damping coefficient is equal to zero, then for the dimensionless angular velocity tending to infinity, the amplitude of the force's first harmonic will approach 0.5 $m_B r_A k/M$, which is a finite value and greater than zero,
- for a dimensionless angular velocity smaller than $\sqrt{2}$, further increasing the dimensionless damping coefficient will cause the force value to be reduced, whereas for a dimensionless angular velocity greater than $\sqrt{2}$, an increase of the dimensionless damping factor will cause to the force value to increase,
- the force value goes up when the stiffness coefficient is increased and decreases when the stiffness coefficient decreases,
- the larger the ratio m_B/M, the larger the force value.

4.1. Damping control

The impacts of damping vary with the changed angular velocity of the shaft, this is why damping control algorithms have to utilise the instantaneous velocity value. This does not present any major difficulty as the angular velocity of the shaft is measured with sensors installed in the dedicated control systems provided in modern combustion engines. A damping control algorithm need not take into account the static analysis, since damping does not affect the static equilibrium position of the engine. Assuming that damping in the mount system is exclusively the result of providing an actuator placed parallel to the mount spring, the equation of vibration can be rewritten as:

$$M\,\ddot{y} + F_{con}(t) + ky = F_{ind}(t) \tag{5}$$

where $F_{ind}(t)$ is the inertia force inducing the vibration and $F_{con}(t)$ stands for the interaction force of the actuator in the control system.

The research investigation indicates that the simplest damping control algorithm is that switching between a large value of damping coefficient for angular velocities of the shaft less than the characteristic value (a product of $\sqrt{2}$ and natural frequency of the engine vibration) and a smaller value of the damping coefficient after a characteristic value of angular velocity is exceeded. It is worthwhile mentioning that the smallest angular velocity that can be maintained in the steady-state is the idle speed. It is slightly higher than the natural frequency. According to the control algorithm, the damping coefficient should assume a large value in the interval of crank shaft speed, starting from the idle speed to the characteristic value (being the product of $\sqrt{2}$ and natural frequency of the engine vibration).

Such an algorithm can be implemented by installing a spring and an MR damper connected in parallel in an engine mount. The spring should maintain the engine in static equilibrium and ensure the adequate natural frequency, slightly below the idle speed of the shaft. The design structure of the MR damper should be such that its stiffness is low and the damping ratio is easily switched between a very large and very small value.

4.2. Stiffness control

Stiffness reduction results in a decrease of the amplitudes of particular harmonics. However, when the total stiffness is reduced, the static equilibrium position of the engine will be changed which is unacceptable in the context of the drive system performance. Variation of the dynamic stiffness (i.e. the change of the stiffness coefficient in the vibration equation only, without changing the coefficient in the static equilibrium equation) can be accomplished by an indirect method, by connecting an actuator of the control system, parallel to the spring. Accordingly, the vibration equation will be rewritten as:

$$M\,\ddot{y} + b\dot{y} + ky = F_{ind}(t) + F_{con}(t) \tag{6}$$

In order that the control algorithm should lead to a change in the mount's dynamic stiffness, the actuator interaction force has to be dependent on the coordinate y, representing the engine vibration with respect to the static equilibrium position and be expressed by the formula: $F_{con} = \alpha\, y$. The vibration equation will be rewritten as:

$$M\,\ddot{y} + b\dot{y} + (k - \alpha)\, y = F_{ind}(t) \tag{7}$$

Accordingly, the effective stiffness coefficient being the difference of $(k - \alpha)$ will decrease in comparison to a stiff spring as long as the gain factor α in the control system is positive. This means that a system is required with positive feedback from the coordinate of displacement with respect to the static equilibrium position. This algorithm can only be easily implemented in active systems.

5. Application of squeeze-mode MR damper to engine vibration control

Further considerations are focused on applications of dampers filled with MR fluid and operated in squeeze mode when the damper is to be used as an actuator in a semi-active vibration control system for a combustion engine. The conceptual design of a MR damper operated in the squeeze mode is outlined in [8, 9]. In this operation mode of the MR fluid in the damper, its characteristic will differ from that of commonly employed MR dampers operating in shearing mode. The family of MR damper characteristics obtained for various current levels in the control coil inducing the magnetic field is shown in Fig. 6.

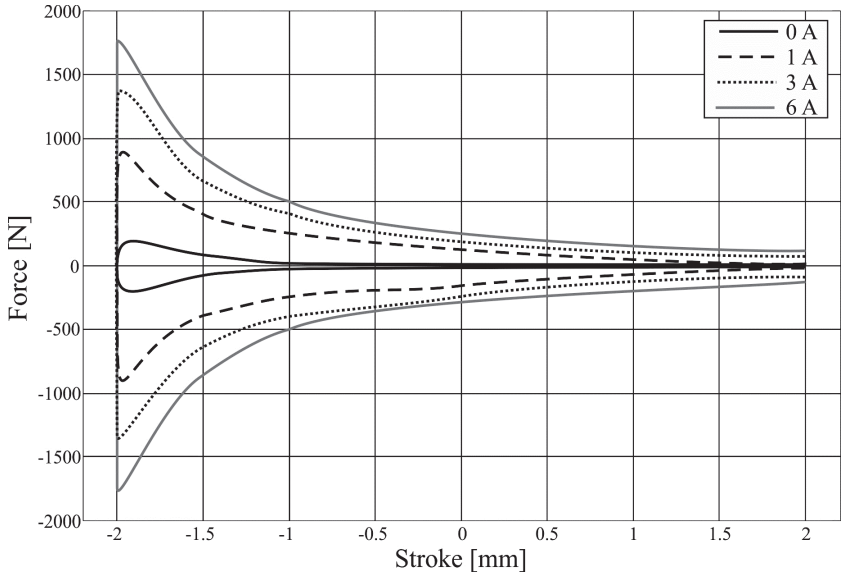

Fig. 6. Characteristics of an MR damper in the squeeze mode

Characteristics plotted in Fig. 6 show the damping force during the preset piston movement with respect to the housing under the applied sine displacement input with an amplitude of 2 mm and a frequency of 50 Hz. The selected input is similar to that experienced during steady-state damper operation in engine mounts. It is apparent that the MR damper is an energy-dissipating element and does not exhibit elastic properties. The distinctive feature is a major asymmetry of the damper performance pattern under compression and tension. This is a most undesirable feature in the context of the projected damper's performance in vibration control systems. The application of an asymmetric spring or damper causes that the vibrating system oscillates around the position shifted with respect to the static equilibrium point To avoid this effect, the mount design has to be modified such that it incorporates two dampers connected in parallel and operated in such a way that the piston motion towards the inside of the first damper should coincide with the piston motion in the opposite direction in the second damper, and vice versa. Such operation of dampers is possible when dampers are

located in opposite sites of the vibrating element. As a result, the characteristic for the pair of dampers will be symmetrical (Fig. 7).

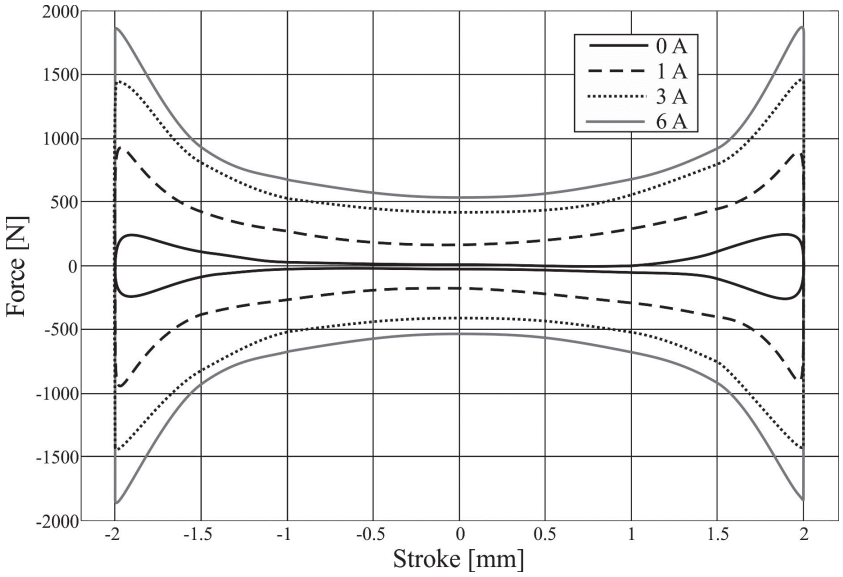

Fig 7. Resultant characteristics of two dampers connected in parallel

The characteristics shown in Fig. 7 are used for estimating the feasibility of damping control in the engine mount with the use of the two-damper system. Equivalent, dimensionless damping coefficients were calculated for the following current levels: 0, 1, 3, 6 A. The equivalent dimensionless coefficients were determined through comparing energy dissipated by an MR damper within one period of vibration with energy dissipated by a viscous damper operating under the same conditions. The calculations were performed for a two-cylinder engine with a mass of $M = 65$ kg. The stiffness coefficient of the mount was $k = 4 \times 10^5$ N/m. The natural frequency was slightly lower than the angular idle speed. The application of the viscous dampers whose characteristics are shown in Fig. 7 yields the equivalent dimensionless damping coefficients in the range 0.1 to 1.2. Graphs in Fig. 5 suggest that such dimensionless damping coefficients enable an effective damping control in accordance with the objectives of the control algorithms mentioned in earlier sections.

6. Conclusions

Research investigations summarised in this study underpin the feasibility analysis of using MR dampers in engine mounts. The calculations were restricted in the case where the engine vibrations were induced by inertia forces of the crankshaft-piston mechanism. Based on the results, in particular the formulas expressing the amplitudes of engine-car body interaction

force, the principle of vibration control is formulated. Damping control can be successfully effected with the use of MR dampers. However, the quality of control depends on the damper design structure. It appears that effective control requires an angular velocity signal from the crank shaft in the engine. This signal is measured with sensors in the engine control system and can be effectively used in the MR damper control system. This first analysis of MR damper characteristics obtained for the squeeze mode and in the given configuration reveals their adequacy for use in the semi-active vibration isolation of the engine. The application of semi-active elements to mount stiffness control is a more complex task and active systems seem to be the recommended solutions. However, they might not prove cost-effective due to the high power demand of actuator systems while implementing the positive feedback control algorithms.

This study is supported through the research grant No PBS 1/A6/3/2012.

References

[1] Flower W.C., *Understanding hydraulic mounts for improved vehicle noise, vibration and ride qualities*, SAE Paper # 952666, 1995.
[2] Graf P.L., Shoureshi R., *Modeling and implementation of semi-active hydraulic engine mounts*, J. Dynamic Systems, Measurement Control 110, 1988.
[3] Helber R., Doncker F., Bung R., *Vibration attenuation by passive stiffness switching mounts*, J. Sound Vib. 138 (1), 1990, 47-57.
[4] Ivers D.E., Dol K., *Semi-active suspension technology: An evolutionary view*, ASME DE, Vol. 40, Advanced Automotive Technologies, Book, No. H00719, 1991, 1-18.
[5] Jędrzejowski J., *Mechanika układów korbowych silników samochodowych*, WKŁ, Warszawa 1986.
[6] Kamiński E., Pokorski J., *Dynamika zawieszeń i układów napędowych pojazdów samochodowych*, WKŁ, Warszawa 1983.
[7] Singh R., Kim G., Ravindra P.V., *Linear analysis of automotive hydro-mechanical mount with emphasis on decoupler characteristics*, J. Sound Vib. 158 (2), 1992, 219-243.
[8] Sapiński B., „Wibroizolator z cieczą magnetoreologiczną", Zgłoszenie wynalazku do Urzędu Patentowego Rzeczypospolitej Polskiej z dnia 01.02.2012.
[9] Sapiński B., „Wibroizolator z cieczą magnetoreologiczną", Zgłoszenie wynalazku do Urzędu Patentowego Rzeczypospolitej Polskiej z dnia 27.06.2013.
[10] Yunhe Yu, Nagi G. Naganathan, Rao V. Dukkipati, *A literature review of automotive vehicle engine mounting systems*, Mechanism and Machine Theory 36, 2001, 123-142.

TECHNICAL TRANSACTIONS | CZASOPISMO TECHNICZNE
MECHANICS | MECHANIKA
2-M/2014

KAMILA TOMCZAK-HORYŃ, RYSZARD KNOSALA*

EVALUATION OF EMPLOYEE CREATIVITY IN THE CONTEXT OF A PRODUCTION ACCOUNTING SYSTEM

OCENA KREATYWNOŚCI PRACOWNIKÓW PRODUKCYJNYCH W ASPEKCIE SYSTEMU ROZLICZANIA PRODUKCJI

Abstract

The main goal of the modern enterprise in employee evaluation should be creativity. This article provides guidance on the criteria of creativity, which is part of the production accounting system. The paper shows the concept of measuring the creativity of employees of higher and lower levels. Also proposed a tool for measuring creativity of employees.

Keywords: *evaluation, creativity, innovation, production workers*, *notification management system*

Streszczenie

W nowoczesnym przedsiębiorstwie głównym założeniem w ocenie pracowniczej powinno być kryterium kreatywności. W artykule przedstawiono wytyczne odnośnie kryterium kreatywności, będącego jednym z wielu kryteriów systemu rozliczania produkcji. Przedstawiono koncepcję pomiaru kreatywności pracowników wyższego oraz niższego szczebla. Zaproponowano również narzędzie wspomagające ocenę pracowników w świetle kryterium kreatywności.

Słowa kluczowe: *ocena, kreatywność, innowacyjność, pracownicy produkcyjni, system zarządzania zgłoszeniami*

* M.Sc. Eng. Kamila Tomczak-Horyń, Prof. Ryszard Knosala, Institute of Processes and Products Innovation, Opole University of Technology.

1. Introduction

Creativity becomes essential attribute of a company. Characterized by original look at problem and new opportunities for change. Appeared issues in management and production often require innovative solutions. Finding them requires creative approach to the problem [8].

Creating innovative attitudes in a enterprise it's important to support development of creativity among employees and appropriate selection of managers. Creative managers have positive relation to creative efforts of their co-workers [1]. The creative manager responds to problems and refers successful especially in taking on new challenges. These in turn require innovative and unconventional solutions. The Creative manager, is able to inspire others [8].

In evaluating employees, except criteria measurable, are also important immeasurable [4]. This group includes the criterion of creativity. It is one of many criteria for a production evaluating [5].

2. Creativity and innovation

Concepts of creativity and innovation are closely linked. In the literature there are many definitions of these concepts. Word a "Innovation" understood as the ability to stimulate innovation (organizational and technical) is the next step and a result of a creative process [3].

Before appeared the innovations in a company, is a number of important stages in which creativity plays a decisive role. It combines the two stages of the creative process: the step to generate ideas and their implementation. Generated solutions are designed to implement the innovation. This means that creativity contributes to their formation. [1].

Creativity is ability to create and a inventiveness [9]. Creativity characterized by a production new and valuable ideas. Creativity also connects cognitive process and individual characteristics of the person. In view of a goal, creativity is divided to [1]:

– "conceptual creativity" – essential during the development of new methods, products, concepts,
– "operational creativity" – essential when choosing and implementing a results "conceptual creativity" into a practice.

These two concepts of creativity are a combination of "soft" and "hard" elements of the process model of creativity.

The combination of creativity and innovation is an important feature of the transfer of the enterprise, from creativity to innovation. The first stage of this cycle it's creativity, which has the huge importance. In this step, the process is initiated in response to the need for innovative changes. They are born in the creative minds and imagination. With imagination are formed ideas. Through the creativity conceptual and organizational appears a new concepts organizational improvements or technical. They form a group of ideas. Then they are checked whether they can be used. The last step is the implementation process of innovation.

Figure 1 presents a simple model of the transfer from creativity to innovation. It's a form of geometric figures. They create a space where creativity and innovation are in one cycle time. Occur in these various a phenomenon. Their goal is to transition from a creative activity to innovation in the enterprise [1].

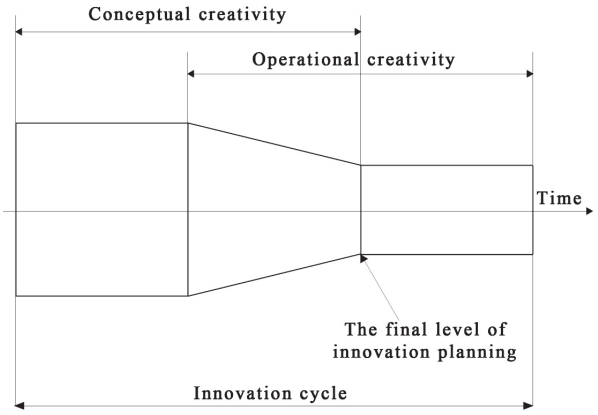

Fig. 1. Model from creativity to innovation in the enterprise [1]

3. The process of evaluating employee creativity

Creative thinking involves the exploration of new ideas and the use of the accumulated knowledge and experience [11]. Employee creativity consists of three components [7] (Fig. 2):

1. Knowledge – knowledge of procedures, technical knowledge, intellectual qualifications.
2. The ability of creative thinking – approach to the problem, the ability to solve them.
3. Motivation – a kind of motivator that stimulates the employee to act. Motivation may be from outside (bonuses, promotions) and from inside (driven by an internal passion or interest).

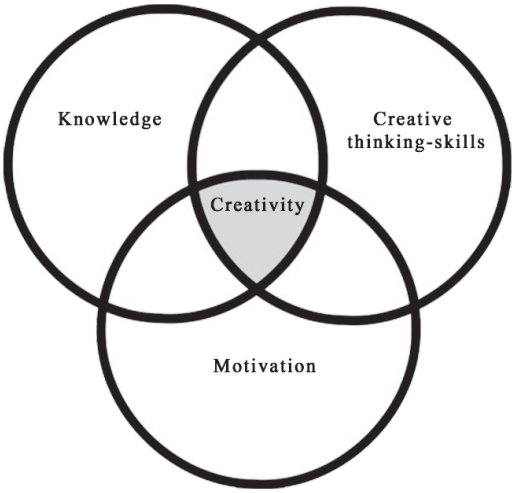

Fig. 2. Components of creativity [7]

An important feature of creative thinking is easy to see stuff that is invisible to others. Creative employee sees the problem and notify on the innovative enterprise improvements or his workplace. That's micro solution [8].

The first step in the evaluate process (Fig. 3) is to determine the characteristics of a creative worker. In this step, you should collect a team of experts who will designate the requirements to be fulfill by a creative worker. The next step is gather and selection data about of employees from the viewpoint of creativity. In this step specify the method and tool for collecting and selecting data. Next is evaluation of the data. In this step, you should select the method and tool to assess creative solutions employees. There are many methods of rating. Stands out the method of absolute, consisting in comparing the results achieved by the employee with pre-established standards (e.g., rating scale, descriptive assessment) and the relative method, involving a comparison of workers among themselves (e.g., ranking, comparing pairs). For the instruments used during the evaluation of employees include: checklists and assessment sheets [6]. The next step in the evaluation process is to analyze the results and provide their presentation to employees. At this stage, you can use two-way closed model, which is based on a dialogue between the person conducting the assessment and evaluation person. Both sides wonder together for to learn about what is best to take steps to achieve their goal [12]. Next the results of the evaluation are transformed to the type of reward that employee.

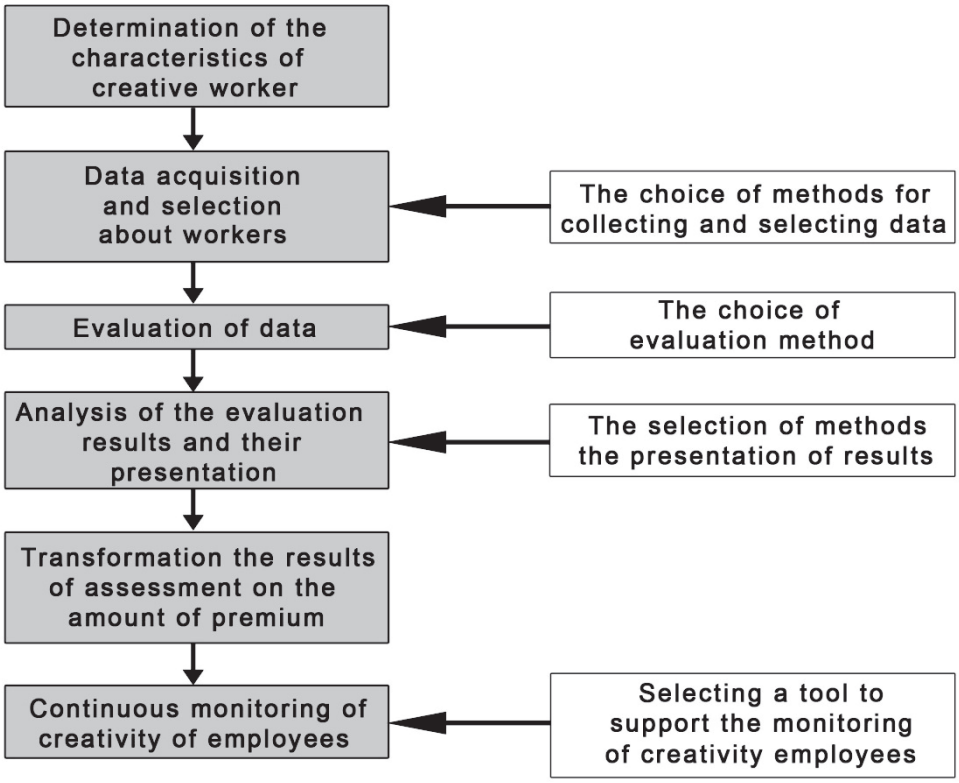

Fig. 3. The process of evaluating employee creativity

Gets this could be, for example, an additional premium to the base salary. The evaluation process of employees should be repeated in a certain period of time to monitor their creativity and motivate for her development.

4. The conception of evaluate workers in the criterion of creativity for a practical example

Supporting tool for monitoring and evaluation of creativity of production workers was developed on the example of enterprise specializing in the manufacture and distribution of gutter systems.

Evaluation of employee, with respect to the criterion of creativity will be fair if will be reduced a subjective nature of this criterion. The measurement of creativity is not an easy task. Due to the fact that creativity has its own unique perspective on the problem and on the new possibilities of changes in the enterprise, it was proposed a systematic approach to this issue.

The basis of the developed system will be a relational database, created in MySQL. It is the world's most popular database application. It is available under open source license, anyone can install it and use it without paying any costs. MySQL is "neutral technology" can be used in any technology. The software package includes: MySQL database server, applications and a number of utilities [2].

In the studied company the employee evaluation is carried out according to the following criteria: absenteeism, punctuality, productivity and creativity. Outcome of the assessment effects the amount of the premium that receives an employee. The enterprise does not have a tool that will monitor creativity of the employee. In the enterprise is assumed that the creativity employee:

– improving his working place,
– inform the employer about the emerging the problems and proposing their solution,
– wants continually improve themselves.

5. Tool for supporting the evaluation of employees under the criterion of creativity

In order to facilitate monitoring of employee creativity, was proposed the notifications management system called "Electronic box of the problems / solutions".

The electronic box has a three groups of users: administrators, senior staff (line managers) and lower-level employees (production workers). Each group will have a different level of access to information.

The first group of users with the highest privileges are administrators. Their task will be, among other things: adding new information and correcting errors. This group also includes immediate supervisor, who will have access to management at all levels. His tasks include inter alia, evaluate the creativity of line managers.

The second group of users, with limited access, is the senior staff. The main function of this group will be introducing applications of production workers and their evaluation.

Line managers will have permissions to management and evaluation of staff only from their department. Rest of the results will be available only for inspection. These solutions will be introduced by the senior staff. At any time, they will have the opportunity to submit their innovative ideas, without access to their evaluation.

The last group, with the lowest privileges are lower-level employees. Members of this group will have only access to information. They will not have the permissions to edit them or delete them.

Content manage system of employees will be built with the graphical template and parts of the workspace. The system will be designed so that access to the information they had only users who have an account with the appropriate permissions. After passage to a website will appear the login panel (Fig. 4). If the person is not a user of the system, will show the message about incorrect username and password. Each user, after passing through the login process will be transferred to the appropriate panel.

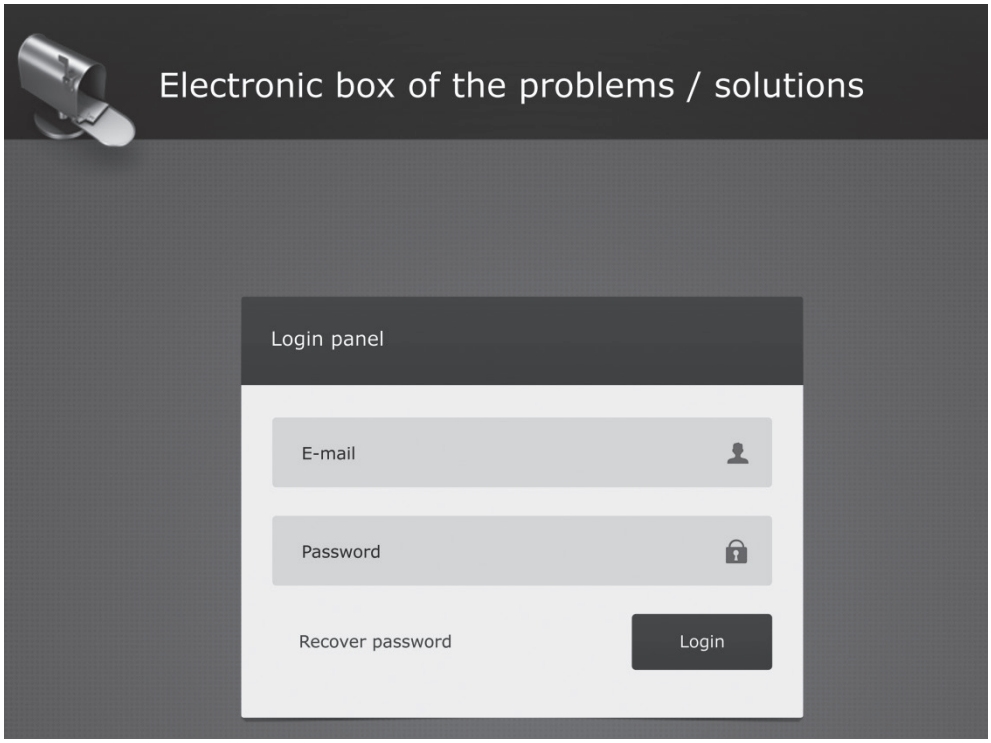

Fig. 4. Graphic design of the login panel

For example, in the panel menu of higher-level employees, can be manage (Fig. 5):

- Notifications – adding, viewing notifications;
- employees – adding, deleting, evaluation of employees, monitoring their creativity;
- statement of results – the ranking of employees, the number of applications in a given time interval, the number of applications / department.

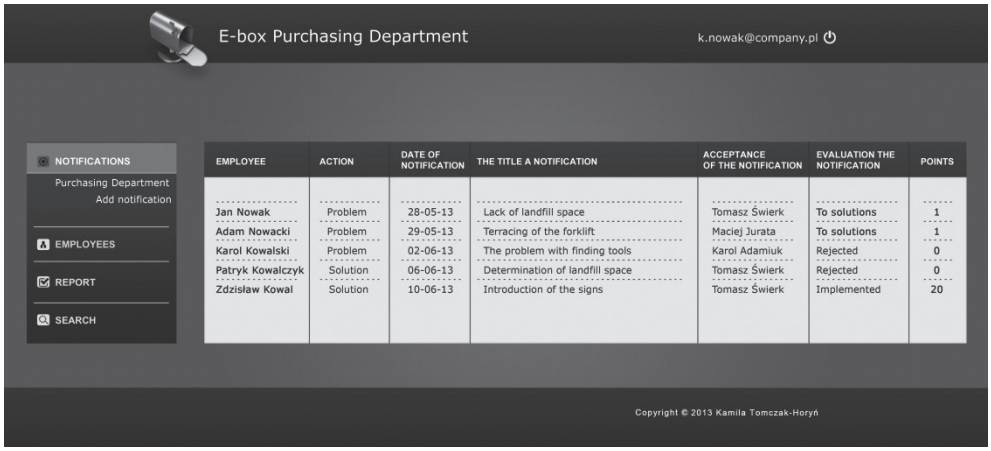

Fig. 5. The graphic design of workers high-level panel – notification management

The panel will also have the option to search an employee or department and the problems. In the preview of applications will be listed information such, as (Fig. 5):

– name and surname employee's the declarant a problem / solution. When you click in the employees will be displayed full information about it (for example, a department name, where you work, work job name, date of commencement of work);
– action – type a application (the problem or the solution problem);
– time the notification about problem / solution;
– title of the report (by clicking on the title of the notification will displayed his full description);
– name and surname a person who save a notifications;
– evaluation a notification (for example, whether the solution will be realized, or will be rejected);
– the number of points obtained for reporting.

In the "view employees" will be listed information such as (Fig. 6):

– name and surname employee who the notification problem / solutions,
– the number of accepted problems to solve,
– number of rejected problems,
– number of implemented solutions,
– the number of rejected solutions,
– sum of points awarded for all notifications in a given time interval.

User will be able to choose the time interval in which the results will be shown for the selected employee.

Final evaluation of the employee in the criterion of creativity, will be the sum of points obtained during the evaluation of all notifications. In case when the reported problem or the solution is rejected, workers receive 0 points. If the reported problem will be considered the worker received 1 point. For reporting the solution to the problem, which will be enforced, workers will receive 20 points (Tab. 1). It is important to reward employees for creative solutions. Only reporting the issue is not as important as the notification solution that will be

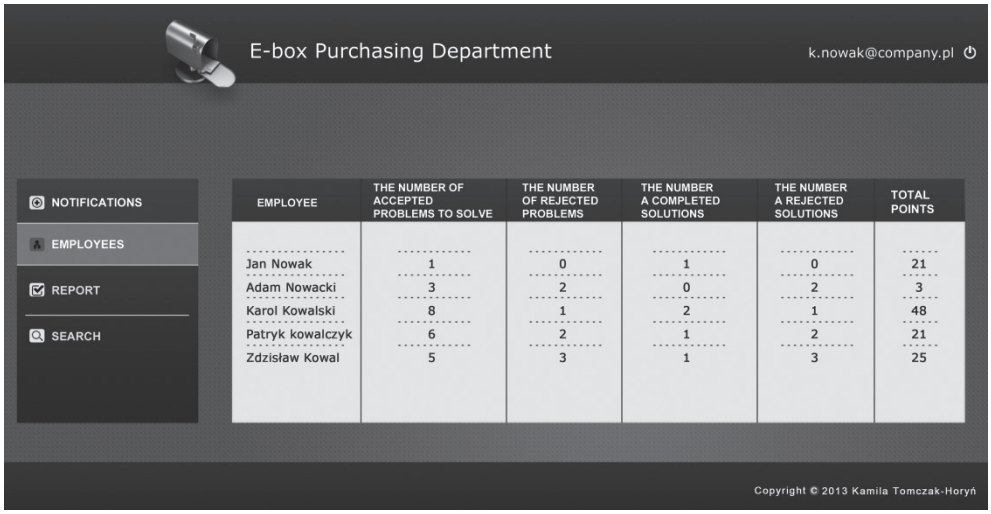

Fig. 6. The graphic design of workers high-level panel – workers management

executed. For example, when the employee received one point he can get the bonus. Total score which an employee obtain for a period of time, will be influenced to the amount of the money premium.

Table 1

Scoring for the activity type

Action	evaluation a notification	Points
Reporting an issue	rejected	0
Reporting an issue	accepted for the solving	1
Application to solve the problem	rejected	0
application to solve the problem	adopted for the solving	20

The proposed system will facilitate the evaluation of employees to monitor and collect information on their creativity.

6. Conclusions

Important thing in the system of a production accounting measurement is element of creativity. When reviewing the literature on this issue, it was concluded that creativity is characterized by perceiving what is invisible to others. An employee who is creative is capable of perceiving problems and to propose innovative improvements. They may involve the whole company or position to work. This approach to creativity allows you to establish

guidelines for its measurement. The proposed tool allows monitoring and evaluation of junior staff and senior management with respect to the criterion of creativity. The online staff appraisal system based on MySQL technology enables anywhere, anytime access to information about the creativity of the employee.

If you want to motivate the employees to application of electronic box you can create additional bonus system. Workers would be rewarded for the problems or their solutions.

References

[1] Brzeziński M., *Organizacja kreatywna*, PWN, Warszawa 2009.

[2] Naramore E., Gerner J., Le Scouarnec Y., Stolz J., Glass M.K., *PHP, Apache I My SQL od podstaw. Tworzenie dynamicznych stron www za pomocą technologii open source*, Helion, Gliwice 2005.

[3] Nęcka E., *Trening twórczości*, GWP, Gdańsk 2005.

[4] Knosala R., Boratyńska-Sala A., Jurczyk-Bunkowska M., Moczała A., *Zarządzanie innowacjami*, PWE, Warszawa 2013.

[5] Knosala R., Tomczak-Horyń K., *System rozliczania pracowników produkcyjnych w przykładowym przedsiębiorstwie*, [in:] Matuszek J., Gregor M., Mičieta B. (red.): *Metody i techniki zarządzania*, Oficyna Wydawnicza ATH, Bielsko-Biała 2013, 53-64.

[6] Król H., Ludwiczyński A., *Zarządzanie Zasobami Ludzkim*, Wyd. Naukowe PWN, Warszawa 2006.

[7] Luecke R., *Managing creativity and innovation*, Harvard Business School Press, Boston 2003.

[8] Proctor T., *Creative Problem Solving for Managers*, Routledge, New York 2005.

[9] Sloane P., *Twórcze myślenie w zarządzaniu*, GWP, Gdańsk 2005.

[10] Strączek M., *Kreatywność. Jak ją rozwijać w sobie i organizacji?*, Edison Team, Warszawa 2012.

[11] Von Oech R., *A Whack on the side of the head. How you can be more creative?*, Warner Books, New York 2008.

[12] Zając Cz., *Zarządzanie Zasobami Ludzkimi*, Wyd. WSB, Poznań 2007.

TECHNICAL TRANSACTIONS | CZASOPISMO TECHNICZNE
MECHANICS | MECHANIKA
2-M/2014

BARBARA WASILEWSKA, RYSZARD KNOSALA*

STIMULATING TECHNICAL SOLUTIONS USING A HEURISTIC METHOD

STYMULOWANIE ROZWIĄZAŃ TECHNICZNYCH Z WYKORZYSTANIEM METOD O CHARAKTERZE HEUTYSTYCZNYM

Abstract

The paper explains selected methods of stimulating innovative solutions as shown by the created model of creative problem solving. Heuristic methods allow for developing creative thinking for the development of an enterprise. Two case studies are presented using the methods typical for the studied enterprise.

Keywords: *creative methods, innovations, production engineering*

Streszczenie

Artykuł ma na celu przybliżenie wybranych metod stymulowania innowacyjnych rozwiązań na przykładzie utworzonego modelu kreatywnego rozwiązywania problemów. Metody o charakterze heurystycznym pozwalają kształcić zdolności myślenia twórczego w rozwoju przedsiębiorstwa. Zostaną przedstawione dwa studia przypadków z wykorzystaniem metod w badanym przedsiębiorstwie.

Słowa kluczowe: *metody twórcze, innowacje, inżynieria produkcji*

* M.Sc. Eng. Barbara Wasilewska, Prof. Ryszard Knosala, Institute of Processes and Products Innovation, Opole University of Technology.

1. Introduction

Creative thinking may be used in many different fields of human activity. Among the factors activating creativity are heuristic methods whose task is to facilitate action course in open situations problem [1, 2]. The appropriate stimulation for creating new ideas and solving tasks is indispensable nowadays. This type of mobilization allows one to independently create conditions for shaping a pro-innovative work environment. The action of solving problems usually starts the mode cycle of the creative process that allows for the obtaining of intellectual success. This usually involves three following phases: discovering the problem, creating new ideas and their verification and assessment. The creative process is usually long, however, it depends on the problem specifics and complexity. Therefore, it can be a discontinuous process that requires strong motivation and work discipline from the solver.

As shown by Kozielecki [3], heuristic methods provide a high probability of solving the problem. They facilitate the overcoming of obstacles such as functional fixedness defined as the attitude that limits a person to perceive an object only in one established, traditional way.

There are many ways to create valuable solutions, but it is necessary to perform a few steps to learn how to create them. The approach to innovation based on reason and current development [4] includes the following steps:

- choosing the best ideas based on their expedience and merchantability – this gives a rise to other important questions: how to manage ideas and which strategy should be adopted for creating reserves of such ideas? At this moment, the idea might be unrealisable, expensive or even superfluous, but the history of scientific research in many fields show that "the time brought practical application for even highly abstract problems and theories" [5, p. 69];
- determining existing company resources and evaluation of their usefulness in new tasks – Will the risky projects obtain support? Will the company require new personnel with creative potential? People need to learn creative thinking, just as they learn any other skills [6] and one of the ways to improve it within the organization is to involve employees in achieving set objectives in an elastic and open way in order to prevent the trend to reduce diversity and to stay on a beaten path [5];
- creating a new business model – employees, process, results.

While the approach to innovation based on imagination and trend anticipating [4] assumes the study of all possible solutions created as a result of a new perspective on company problems. It also suggests an expansion of the scope of the case study. This might involve looking for alternative problem solutions. Such an approach suggests rethinking the innovation context for a given company and the creative combination of the best ideas, using, for example, the variety of employees' knowledge and their insights. Finally, it recommends the creation of new meaningful concepts that can involve people and improve their life quality at the same time.

Stimulating solutions requires a good understanding of the processes accompanying the formation of idea. This allows for the planning of correct procedures. The Nosal presents four types of cognitive situations [5], naming them type A, B, C, D. For the purposes of this paper, type C seems to be the most interesting – is an example of a situation that is innovative

activity. Type C includes: looking for a new environment; DIY principle; converting existing conditions; inexpedient routine. A creative person who plans to pursue an unusual goal in a typical environment can either change the environment or create a new idea on his/her own, step by step. Therefore, the innovative activity might be initiated from forming of creative problem solving skills, especially in stimulating technical solutions that are created in ordered and systematic manner.

2. Model of stimulating technical solutions by means of heuristic methods

The following methods were proposed for use in subsequent stages of problem solving in the creative processes indicated in the study [1]:

1. Perceiving new problems – Analogies.
2. Problem formulation and reformulation – Generative metaphor and Necessary and unnecessary.
3. Constructing the auxiliary problem – Content-rich realistic analogy, Visual realistic analogy and Personal identification.
4. Solving auxiliary problem – Self-solving problem and Unreality.

The tools for creative problem solving used in this article are a part of the model of stimulating technical solutions (Fig. 1). It was used for generating problems that were undertaken during creative sessions in the studied enterprise. This involves two stages of the creative process – defining the problem (defining the objective) and creating ideas. The presented general workflow can also be applied to existing rules and strategies of creative thinking. If they are unfamiliar to the reader, it is worth reading and understanding them before applying the method for creating ideas [see 7].

Analogies were used for problem detection. They are quite general and can be applied at different stages of the process, as well as for predicting and designing solutions. The other method was Fantasy Analogy that is reduced to wishful thinking. This allows creating a variety of ideas. The analogy mechanism was activated by the phrase: 'What if...' There were such questions as: if anything was possible, what would be your ideas?

The stage of problem formulation and reformulation should not be omitted as it enriches the process of looking for solutions by additional preparatory actions. One of the methods – generative metaphor is defined as "(...) object, situation or phenomenon forming a clear, though tacitly accepted, a reference to the problem in its current formulation" [1, p. 146]. The metaphor should determine a possible line for creating improvement ideas. The second method – 'necessary and unnecessary', is designed to determine the requirements for future solutions in order to maintain everything that is necessary and eliminate everything that is seen as unnecessary.

The stage of constructing insert the auxiliary problem also involved analogies. The rich-content realistic analogy assumes the 'departure' from the main task in a controlled manner. The task was compared to similar problems encountered in a completely different field of knowledge or ability. The visual realistic analogy refers to visual imagination and episodic knowledge gained through experience [4]. It can be expressed by words. The third method in this stage – the personal identification (in order to gain a deeper understanding of production

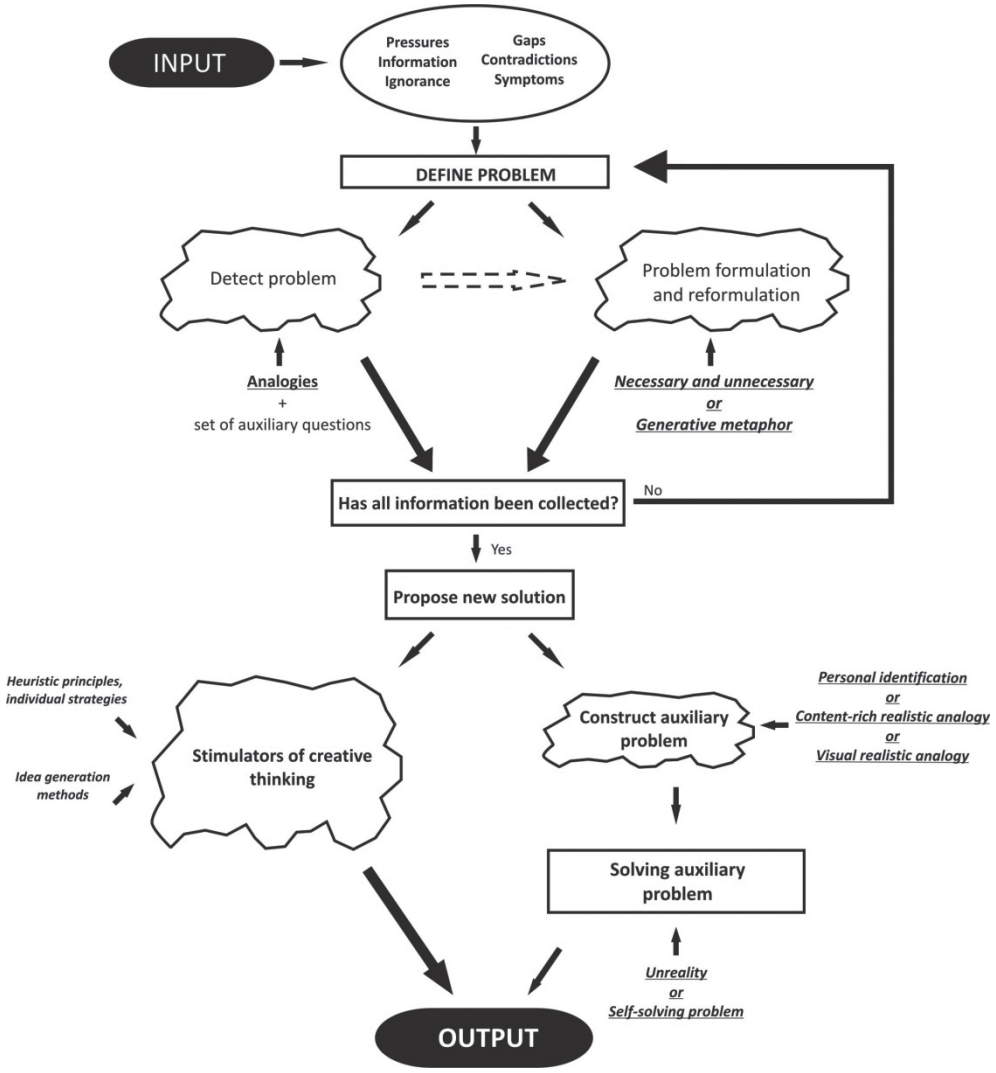

Fig. 1. Model of creative problem solving using heuristic methods

problem) suggests impersonating some machine components and analysing their weakest aspects. The problem that exists objectively is experienced by one's own body [1].

The last stage involves the method of self-solving problem. It is an example of personification, i.e. attributing human characteristics to objects (physical objects, processes, whole tasks) [1]. Therefore, the question is asked: how can my problem find its own solution by itself? Thus, the problem itself is personified. While the method of unreality needs to get some ideas from fairy tales and fables. Their plot and characters may by themselves contain solutions.

3. Case study – improvement of the production system

Nowadays, the ability to perceive the need for changes and improvement, and the ability to initiate new approaches for multi-solution problems becomes more and more useful. The presented methods aim to be a source of inspiration for goals generally defined as improvement of the production system. The goal assessment is very broad and might involve either human element, existing procedures, selected field – position in the system etc.

3.1. Method of analogy for supporting problem perception

For keyword (improvement) can suggest any of the following analogies: golden mean; machine; system's Chinaman; perfect product; air after the storm; hair colouring, latest fashion trend; holy man. Such analogies allow for a more profound analysis of the task, because the improvement requires a new, refreshed perspective (e.g. air after the storm). It also needs a choice of recent solutions (e.g. latest fashion trend) that shall be quick and effective (e.g. machine) and, basically, they should be perfect – optimum for their dedicated function (e.g. holy man). However, this may force some artificiality, when based on assumption that improvement knows no end (e.g. hair colouring).

3.2. Generative metaphor supporting problem formulation and reformulation

Metaphors adequate to this subject are as follows:

1. Military – the proposition of the development of a strategic plan for production manoeuvres.
2. Education – the development of a production system syllabus.
3. Health – creating supplements that improve 'production health' and prevent relapses of production defects.

Did the metaphors facilitate finding a new idea or inspired solution? Certainly, they outlined surprising fields that can be a source for taking and developing new ideas based on personal expectations and research objective. People interested in a selected field (military, education, health) might find it desirable to develop the subject using other methods such as: *Purge* (for military) as the elimination of instant ideas from know issues; *Figure-background* (for education) in order to omit typical educational elements and consider neglected ones. Could it be unusual training methods? (for example collage technique, or forms embody the role of the production system?) The last example (for health) is *Problem as a subproblem*, because preventing a recurrence of production defects is a part of greater structure and formulate the problem should be wider, which will eliminate him.

3.3. Using realistic content-rich analogy and realistic visual analogy for constructing insert the auxiliary problem

The following examples seem to be valuable for constructing an auxiliary problem by means of content-rich analogies:

- how to properly season a dish?
- how to correctly finish a house?
- how to correctly repair a car?

Seasoning a dish is an improvement of an existing object, which however is not excellent at its core. Finishing a house requires many actions that occur in some order, this requires prior reflection. The repair points at elimination or reduction of the problem. The system requires appropriate 'seasoning', serving, a pinch of spice etc. The individual detail, department or part may be seasoned. I repair what is currently inappropriate, or was badly set in the past.

The other model of problem of the output may be too long downtime. The following examples come to mind:

– waiting for a green light,
– waiting in line in a shop,
– waiting for a helpline consultant.

What can be done to avoid waiting too long at a red light or accelerate the green light – avoid inhibition of subsequent stages of goods production? What other actions can be undertaken during waiting, just as when waiting in line? How to react to for delays of start of first production stage, in a similar way how we wait for quick and substantive connection?

The analogies regarding the elimination of time wasted during production were evoked for the issue of improvement of the production system. The following analogies can be distinguished:

– trains arriving late,
– tightening a tap to prevent water from dripping,
– waiting in a line to see a doctor.

For instance, the elimination of resulting delays may be impossible due to weather conditions, unexpected or new situations that could not have been foreseen in a perfect manner. Where in the system is it possible to tighten a dripping tap, which part is ineffective or does not show full effectiveness? As in the queue for the doctor reorganization of the system requires the work of people, willingness to change and introducing procedures of adequate behaviour in such situation.

3.4. Self-solving problem method for the auxiliary problem

If the production system behaves as a doctor then it diagnoses itself on its own – it can determine which part aches, it knows what to treat and it understands the need for regular prophylaxis to prevent relapse or further complications. If the problem could solve itself, it would be done through an operator panel which functions as an operator-machine interface and supports the user in the operating of the system by providing high precision. Through the integration of all devices working in one installation into one cohesive system, it is easier to find the causes of faults and downtimes. Table 1 presents data that could be placed in the panel with a drop-down list of causes, names of devices/line parts and part of automatic areas.

Table 1

Exemplary data for operator panel

1	2	3	4	5	6	7	8
Machine	Component	Cause	Stop	Start	Time	Team	Recipe No.

The improvement of the production system requires a new evaluation of the formed inspirations. Auxiliary stages were supposed to direct to solving the undertaken task. This way it is possible to get closer to the solution using a non-standard approach. The last of the methods used determines the final result a problem, it allows for a further elimination of problems in the way of the assumed solution.

4. Case study – increasing performance of production machines

In this part presents another example of issue in the studied enterprise – increasing machine performance in product manufacturing. It is an inspiration to stimulate creative thinking.

4.1. Method of fantasy analogy for supporting the perception of new problems

Problem detection allows for a better definition of the objective. The desired effect involves increasing the number of manufactured products, smooth operation without downtimes and decreasing failure rate. Table 2 presents five questions starting with the phrase 'What if...' which is aimed at developing the problem of a low number of products produced during one shift – the more questions, the better.

Table 2

Perceiving new problems using the Fantasy analogy

Fantasy analogy
Problem: low number of products produced during one shift
1. *What if each employee would recorder production course at his work station?* Such actions would allow for faster diagnostics of machine failures. 2. *What if machine of defined application produced the same number of products?* The amount of dosed material for extruder would have to be the same – the material would come from one supplier. No possibility of mixing or combining. 3. *What if each machine had a temperature sensor?* The temperature sensor would allow for faster diagnostics of machine failures. 4. *What if each machine had a system for signalling failure that directly informed the repair department?* The system would give data regarding which machine has failed and where it is located in the production hall. 5. *What if each machine had a counter that displayed the number of manufactured components in a given time?* The counter would show the number of produced pieces and whether the worker made his quota during the shift. This would decrease the probability of employee error or fraud.

4.2. 'Necessary and unnecessary' method supporting problem formulation and reformulation

The unnecessary was demonstrated to be installation of temperature sensors in production machines and installation of the computer at the station of injection moulding machine and recording process of the machine. The list of necessary actions was a bit longer. It includes the installation of cooling systems and counters in the machines as well as the replacement of old motors in selected production machines and increasing the size of tables (welder, press). As a consequence, the objective is still the same – to increase machine performance, which would result in an increase in the number of manufactured products. The planned number for one working shift shall amount to 120 pieces.

4.3. Using personal identification for the construction of the auxiliary problem

The chosen example created during a creative session based on this method will be presented. The effectiveness of this method increases with the frequency of its use. It is useful to impersonate a few different components to grasp the differences of the identification.

I am the extruder responsible for tape extrusion

I would install a temperature sensor that would measure my temperature so I could inform my employer in the case of overheating. I would also install the counter that would show how many components I produced and how long it took. Such a solution would allow me to verify which material is more effective. I would certainly replace the motor responsible for tape pitch. I hope this decreases my failure rate. Finally, I would install a cooling system to cool specific machine subsystems and avoid downtimes.

4.3. Unreality problem method for solving the auxiliary problem

The installation of a cooling system in production system evokes the story of the Wavel Dragon and King Krakus. The Wavel Dragon can be compared to high temperature in the machine, while King Krakus is the coolant that fights it. King Krakus, by fighting the dragon, makes the environment safe and restores peace and order, just as in the enterprise that uses a cooling system.

"When he ascended, Poland was wooden, when he left us, it was from stone" suggests the replacement of motors with obsolete designs that can be compared to wooden buildings from that period. The new motors, equipped with state-of-the-art technology, can be compared to stone buildings. This means higher durability and allows long-term operation, just as stone buildings can stand for many years.

5. Conclusions

Heuristic methods can create conditions for the emergence of new ideas. Sometimes the process of thinking grows and expands. The stimulation should not be an imposed scheme which is used in a strict manner. Rather, the scheme shall be built based on the nature of the

problem, but usually multi-solution problems require constant stimulation. As a result of the carried out creative sessions, unrealistic solution ideas can often emerge. The choice of more analytical and common sense methods or methods based on intuition and imagination depends on one's personal abilities. Combining them in harmony is the way to go.

References

[1] Nęcka E., *TROP…Twórcze Rozwiązywanie Problemów*, Oficyna Wydawnicza „Impuls", Kraków 1994.

[2] Płóciennik E. et. all., *Metoda i wyobraźnia. Podręcznik dla nauczyciela*. *Lekcje twórczości w klasie I*, Wydawnictwo Difin, Warszawa 2009.

[3] Kozielecki J., *Myślenie i rozwiązywanie problemów*, [in:] T. Tomaszewski, *Psychologia ogólna*, Wydawnictwo Naukowe PWN, Warszawa 1995.

[4] Fisk P., *Geniusz biznesu. Kreatywne podejście do rozwoju firmy*, Wolters Kluwer Polska, Warsaw 2009.

[5] Nosal Cz., *Umysł menedżera: Problemy – decyzje – strategie*, Wydawnictwo „Przecinek", Wrocław 1993.

[6] Henry J., *Creative Management*, Sage, Great Britain 2001.

[7] Karlińska B., Knosala R., *Sesja twórcza jako sposób kreatywnego rozwiązywania problemów w przedsiębiorstwie*, „Zarządzanie przedsiębiorstwem", 2/2013, 16-22.

TECHNICAL TRANSACTIONS | CZASOPISMO TECHNICZNE
MECHANICS | MECHANIKA
2-M/2014

ANETA SZEWCZYK-NYKIEL*

THE EFFECT OF THE ADDITION OF BORON ON THE DENSIFICATION, MICROSTRUCTURE AND PROPERTIES OF SINTERED 17-4 PH STAINLESS STEEL

WPŁYW DODATKU BORU NA ZAGĘSZCZENIE, MIKROSTRUKTURĘ I WŁAŚCIWOŚCI SPIEKANEJ STALI NIERDZEWNEJ 17-4 PH

Abstract

It is generally known that boron is an effective activator of the sintering process of iron as well as stainless steels. During sintering, boron contributes to the formation of a liquid phase wetting the surfaces of powder particles. As a consequence, a reduction of porosity, the rounding of pores and an increase in density is obtained. It is necessary to improve mechanical properties and corrosion resistance. The aim of this study is to investigate the effect of the addition of boron in the amounts of 0.2, 0.4 and 0.6% wt. on the density, microstructure and selected properties of sintered 17-4 PH stainless steel.

Keywords: *17-4 PH steel, boron, microstructure, sintering, dilatometry*

Streszczenie

Bor jest skutecznym aktywatorem procesu spiekania żelaza, ale także stali nierdzewnych. Podczas spiekania bor aktywuje proces spiekania w wyniku pojawienia się cieczy zwilżającej powierzchnie cząstek proszków. W konsekwencji przyczynia się do zmniejszenia porowatości, zaokrąglenia porów i wzrostu gęstości niezbędnego do poprawy właściwości mechanicznych i odporności na korozję. Celem przeprowadzonych badań było wyjaśnienie wpływu dodatku boru w ilości 0,2, 0,4 i 0,6 % ciężaru w postaci elementarnego proszku na kształtowanie się mikrostruktury i właściwości utwardzanych wydzieleniowo stali nierdzewnych gatunku 17-4 PH.

Słowa kluczowe: *stal 17-4 PH, bor, mikrostruktura, spiekanie, dylatometria.*

* Ph.D. Aneta Szewczyk-Nykiel, Institute of Material Engineering, Cracow University of Technology.

1. Introduction

PM stainless steels were developed in order to improve on the mechanical properties offered by their wrought counterparts. Precipitation hardening (PH) stainless steels are defined by the strengthening mechanism [1]. The strengthening of these alloys is developed by aging. Several elements are commonly used for the precipitation reaction, including aluminum, copper and titanium. Because aluminum and titanium have high affinities for nitrogen and oxygen, it is difficult to sinter without the formation of oxides or nitrides in PM stainless steels. For this reason, it is necessary to strictly control the atmosphere during sintering. Therefore, copper is the most commonly element used in precipitation hardening steels. It is known that excessive amounts of copper can lead to lower densities of sintered steels, this is due to its negative effect on compaction. Consequently, their mechanical properties are inferior due to their limited final density [1–5]. It is known that the combination of a relatively high temperature (usually above 1350°C) and an extended sintering time should be used in order to obtain a high density of sintered 17-4 PH steel [6–8].

It should be pointed out that one of the most common PH stainless steel grades is 17-4 PH [1–7, 9, 10]. This is a martensitic stainless steel containing approximately 3% (by mass) of Cu and is strengthened by the precipitation of highly dispersed copper particles in the martensite matrix. 17-4 PH exhibits high strength, high apparent hardness and superior corrosion resistance compared with martensitic stainless steels [1–3, 8]. The ductility and toughness of this steel are generally higher than in the carbon-containing martensitic grades [3]. 17-4 PH combines high strength and good corrosion resistance at a reasonable cost [6–12]. In addition, the mechanical properties of sintered 17-4 PH steel can be improved by heat treatment [1–3, 5, 11]. Due to these properties, 17-4 PH has widespread applications in the automotive, aerospace, military, chemical and food processing industries [2, 6–7, 9–11]. 17-4 PH stainless steel can also be used in medicine as biomaterial [10–11].

If we compare wrought and powder metallurgy materials, a disadvantage of sintered stainless steels is the deleterious effect of porosity on mechanical properties such as tensile strength, ductility and impact toughness [5]. It is known that a high density of sintered materials is necessary for improved mechanical properties and corrosion resistance. It is not surprising that residual pores decrease the above mentioned properties in sintered stainless steel [6, 7]. It is worth mentioning that the properties of interfaces (for example, the presence of hard and brittle phases) are also important for mechanical properties and the corrosion resistance of sintered stainless steels.

Analysis of the literature leads to the conclusion that the introduction of boron as a sintering additive to iron-based material may lead to a noticeable improvement in the total density and the mechanical properties. Several pieces of research indicate that boron is an excellent activator for the sintering of ferrous alloys [6, 7, 9–11, 13–27].

The analysis of a binary Fe-B diagram phase leads to the conclusion that boron is the ideal sintering additive. Namely the eutectic reaction ($Fe_2B + Fe \rightarrow$ liquid) occurs at 1174°C [11, 18–22]. The solubility of boron in iron is very low, whereas the solubility of iron in the eutectic melt is high. The liquid phase has a very low solubility in iron and provides a continuous network between the solid grains [20]. The eutectic phase has a low melting point, and therefore even small amounts of boron should be sufficient to generate a fast mass transport after the liquid phase formation [22]. It is not surprising that the higher the

boron content, the higher the amount of eutectic [18]. In addition, boron has a high affinity to oxygen. Therefore, during the sintering process, boron reacts with oxygen which is chemically bounded on the surface of powder particles. This simultaneously activates the sintering process [7, 25, 26]. As a consequence, this results in higher densities, rounded pores, and improved mechanical properties [18]. According to [6, 7, 9], the addition of boron increases the hardenability of steels, improves grain boundary and cohesive strength, and enhances corrosion resistance.

The earliest studies were related to the addition of boron to iron, wherein boron was used in various forms – elemental boron powder (crystalline or amorphous) or borides, such as FeB, Fe_2B. These studies focused on the effect of: powder characteristics, form and amount of boron addition, and also sintering atmosphere, sintering temperature, sintering time on microstructure, densification and mechanical properties of sintered. The conclusions of these studies are that the addition of boron to iron resulted in greater densification and a noticeable improvement in the mechanical properties compared to sintered iron [6].

Many investigators were involved in studies concerning the addition of boron to iron-based materials such as: Astaloy Mo [14, 22]; Astaloy CrL [22]; Astaloy CrM [16]; Distaloy AE [20]; Distaloy SA [13, 23]; austenitic stainless steel (mainly 316L) [19, 21, 25, 27, 28]; ferritic stainless steel [18, 23, 24]; martensitic stainless steel [17, 29]; 17-4 PH steel [6, 7 9–11]. Boron was introduced in different forms and different mass percentages. Thus, the following forms of boron were used – an elemental boron powder [10, 11, 22–26] or compounds such as: FeB [17, 18, 20]; h-BN [21, 22]; B_4C [16, 22]; CrB_2 [28]; NiB [7] and boron containing master alloy [16, 19, 27]. Their studies showed that the addition of boron increased density (at a lower sintering temperature), mechanical properties and corrosion resistance. Thus, boron can be successfully applied to enhance the sintering process and obtain high-density sintered iron-based alloys [19].

There are only a few studies regarding the 17-4 PH steel with boron or different borides in the literature [6, 7, 9]. The sintering behaviour and properties of an injection molded 17-4 PH stainless steel with additions of elemental boron [9–11, 22, 24, 29], FeB [6] and nickel boride [7] were studied. The addition of elemental boron as well as FeB and NiB increased the sintered density, the ultimate tensile strength, elongation, impact energy and hardness of 17-4 PH steel. Moreover, it decreased the time and temperature of sintering process [6, 7, 9].

In accordance with the presented results, the full density and the highest mechanical properties were obtained with the addition of 0.5% (by mass) of boron at 1250°C for 30 min [9] and 1% (by mass) of NiB at 1280°C for 45 min [7]. The heat treatment (a solution treatment in argon for 1 hour at 1050°C, and then aging treatment in argon for 4 hours at 480°C) after sintering resulted in a further increase of mechanical properties. For example, the properties of heat treated 17-4 PH steel containing 0.5% (by mass) of B were an ultimate tensile strength of 1520 MPa and a hardness of 55.1 HRC [9]. Whereas in the case of heat treated 17-4 PH steel containing 1% (by mass) of NiB the following properties were obtained: ultimate tensile strength of 1402 MPa; elongation of 4.8%; impact energy of 23 J; hardness of 52.3 HRC [7].

Based on the review of literature, it can be concluded that there is virtually no information about the effect of boron addition on 17-4 PH stainless steel produced by conventional powder metallurgy.

It is known that the combination of a relatively high temperature (usually above 1350°C) and an extended sintering time should be used in order to obtain a high density of sintered 17-4 PH steel [6, 7]. To facilitate the sintering process of 17-4 PH stainless steel, boron was added to create a liquid eutectic phase. Thus, the aim of this investigation was to study the effect of the elemental boron powder on the densification, microstructure and sintering behaviour of 17-4 PH steel.

2. Materials for research

In this research, water atomized 17-4 PH stainless steel powder provided by AMETEK was used. The chemical composition of 17-4 PH powder (corresponding with standards: ASTM-A564 grade 630; UNS S17400) was given in Fig. 1. It should be noted that the studied powder contained Acrawax lubricant at an amount of 0.75% wt. The apparent density of 17-4 PH powder was 2.54 [g/cm^3] while its flow was 31 [s/50 g]. Boron in the form of elemental powder (product of Goodfellow, average particle size of 2 μm, purity of 99.8 %) was used.

The following powder mixtures were prepared:

– 17-4 PH + 0.2% wt. B,
– 17-4 PH + 0.4% wt. B,
– 17-4 PH + 0.6% wt. B.

In order to compare the results, pure 17-4 PH steel powder was also used for the studies.

Table 1

Chemical composition of 17-4 PH stainless steels powder (% wt.)

C	S	Si	Cr	Ni	Cu	Nb	Mn	P	Fe
0.027	0.011	0.73	16.28	4.28	4.04	0.32	0.05	0.015	Bal.

3. Experimental procedure

All investigated mixtures were prepared by mixing in Turbula®mixer. The mixing time was 6 hours. Then mixtures of powders and also powder of 17-4 PH were uniaxial pressed in a rigid matrix at 600 MPa. In this manner, the following samples were obtained: cuboidal samples with dimensions of 4 × 4 × 15 [mm] for dilatometric studies; cylindrical samples of size ∅20 × 5 [mm]. After pressing, the cuboidal samples were sintered in the horizontal NETZSCH 402E dilatometer, while the sintering process of cylindrical samples was carried out in a Nabertherm furnace. All green compacts were sintered in a pure (99.9992%) and dry (dew point below –60°C) hydrogen atmosphere. The flow rate of the gas was 100 ml/min. The temperature of isothermal sintering was 1260°C. The sintering time was 45 minutes. The samples were slowly heated to the isothermal sintering temperature at a rate of 10°C/min. The same rate was applied during the cooling of the samples from sintering temperature to

ambient temperature. In order to remove the lubricant, the samples were held at a temperature of 400°C for 60 minutes during heating.

The density measurements of green compacts were carried out by the geometrical method. The density and porosity of the sintered cylindrical samples were measured by the water-displacement method (according to the demands of the PN-EN ISO 2738:2001 norm).

Before and after sintering, samples were measured to estimate dimensional changes caused by densification. Due to possibility of vaporization of boron and chromium, samples were weighted to estimate mass loss.

The hardness byVickers method was determined with the computer-aided hardness tester INNOVATEST CV-600.

Metallographic cross-sections were prepared. The microstructural study of the sintered steels was done with Nikon Eclipse ME 600P Light Optical Microscopy and Scanning Electron Microscopy (SEM).

Dilatometric investigations were carried out in the horizontal NETZSCH 402E dilatometer.

4. Results and discussion

Figure 1 shows the results of green and sintered density measurements of unalloyed and boron alloyed 17-4 PH steel. Results obtained through the measuring of the open and closed porosity of the studied steels are presented in Figure 2 by the amount of boron added.

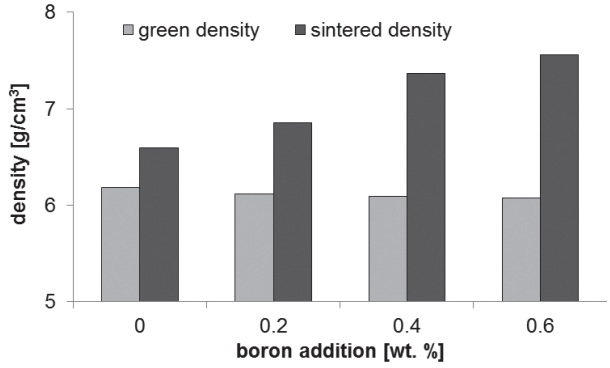

Fig. 1. Green and sintered density of 17-4 PH stainless steel depending on the amount of the addition of boron

The introduction of boron to steel powder caused a slight deterioration of compressibility. The higher the quantity of boron the lower the green density of the studied compacts.

The density of sintered 17-4 PH steel was 6.60 [g/cm^3]. It can be observed that the density of boron alloyed steel was higher than the density of sintered 17-4PH steel. It is clear that boron promotes densification of 17-4 PH steel. The degree of densification depends on the amount of boron introduced to the powder mixture. Specifically, the higher the amount of boron introduced to 17-4 PH steel, the higher the sintered density, while an open and closed

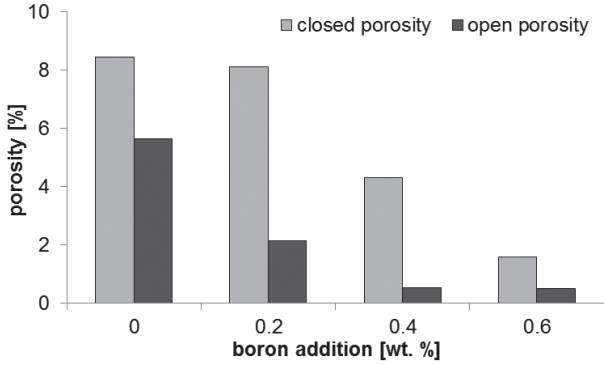

Fig. 2. Open and closed porosity of boron alloyed 17-4 PH stainless steel after sintering in hydrogen at 1260°C

porosity decreases with increasing the amount of boron. It is not surprising that the highest density of boron-alloyed steel was obtained for boron at an amount of 0.6 % wt. This steel had the lowest open and closed porosity.

Measurement of sample heights before and after sintering was carried out in order to designate dimensional changes. The obtained results are presented in Figure 3. The steel samples shrank during sintering. The amount of shrinkage (determined by means of Δh) was primarily dependent upon chemical composition. In the case of pure 17-4 PH steel, dimensional changes of height were approximately 1.5%. It can be observed that the presence of boron contributed to a larger shrinkage of steel samples. Specifically, dimensional changes of samples height increased with increasing of the boron content in powder mixtures. When the boron content was 0.6% wt., Δh reached a level of almost 10%. These results confirm that the addition of boron improves the densification of the 17-4PH stainless steel.

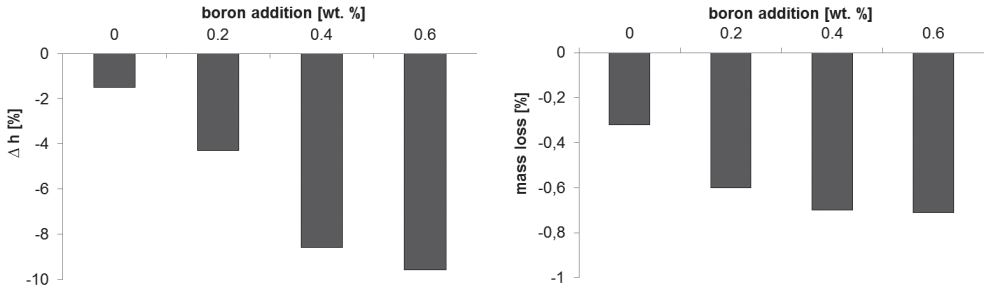

Fig. 3. Dimensional changes of samples height and mass loss of sintered 17-4 PH stainless steel depending on the amount of the addition of boron

The mass loss of samples occurred during sintering for all of the studied steels. The final values obtained after sintering are presented in Figure 3. In the case of sintered 17-4 PH steel, loss of sample mass was associated with the removal of the lubricant. It can be seen that the loss of mass of boron-alloyed steels was much higher in comparison to the value obtained for boron-free 17-4 PH steel and it cannot be exclusively caused by lubricant removal.

The addition of boron improves the densification and also the hardness of the sintered stainless steel 17-4PH. The results of the hardness measurement of studied materials (by the Vickers method) are presented in Figure 4. As can be seen from this figure, the presence of boron effected a significant increase in the hardness of the sintered steel 17-4 PH. The hardness of boron-alloyed steel increases with an increasing proportion of boron. As can be seen in a later section of this article, the introduction of boron changed the microstructure of the investigated steels, and the presence of a hard eutectic phase on the grain boundary has an influence on hardness. The 17-4 PH steel which was modified boron in an amount of 0.6 wt. % obtained two times higher value of hardness in compared with hardness value of boron-free steel.

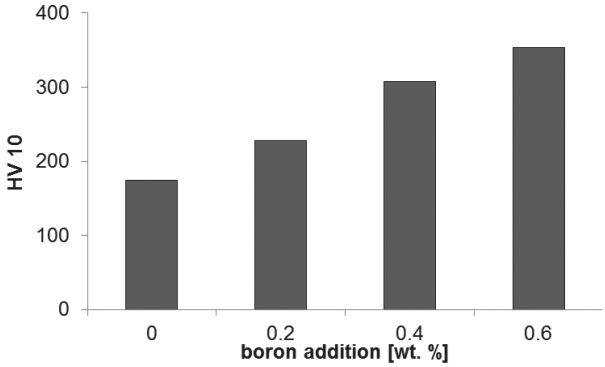

Fig. 4. Hardness of sintered 17-4 PH steel depending on the amount of the addition of boron

The addition of boron to 17-4 PH steel caused a distinct change in the microstructure. It can be observed that the morphology of porosity changed. Specifically, as the boron amount increases, the number of pores reduces. Also the shape of the pore is changed from an irregular shape (existing in the microstructure of sintered stainless 17-4 PH) to a spheroidal shape (for 0.4 and 0.6% wt. of boron added).

The microstructure obtained for stainless steels with boron addition are presented in Fig. 5 and 6. The microstructure of sintered 17-4 PH steel consists of the martensite matrix and δ ferrite. Besides it in the microstructure of boron-alloyed steel appeared the solidified eutectic at the grain boundaries. It is particularly observed for sintered 17-4 PH steel with higher amount of boron.

The SEM microstructure of sintered 17-4 PH steel modified 0.4% wt. of boron is presented in Figure 7. An EDS analysis was performed in order to distinguish the differences in chemical composition of observed constituents: eutectic and matrix. Therefore, the point analyses was performed at points 1, 2 and 3. The results of chemical composition microanalysis are shown in the table below the photograph. Point number 1 was designated in the matrix, which is martensite, while points numbers 2 and 3 were on the grain boundary where the presence of eutectic was previously observed.

Microanalysis of chemical composition indicated that the main elements in point number 1 are Fe, Cr, Ni, Cu – traces of Si also appear. It should be noted that the chromium content in martensite grain is lower than the chromium content in the chemical composition of 17-4 PH

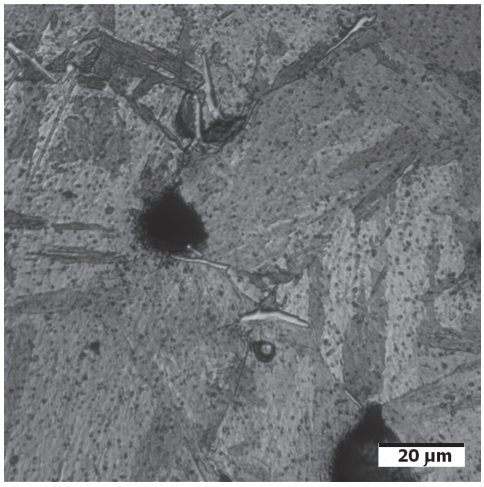

Fig. 5. Microstructure of sintered 17-4 PH steel modified 0.2% wt. of boron

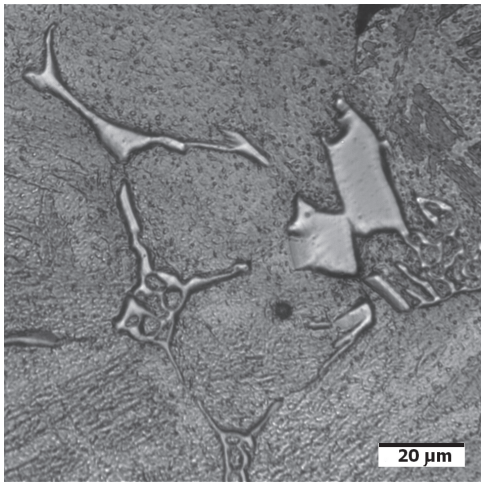

Fig. 6. Microstructure of sintered 17-4 PH steel modified 0.6% wt. of boron

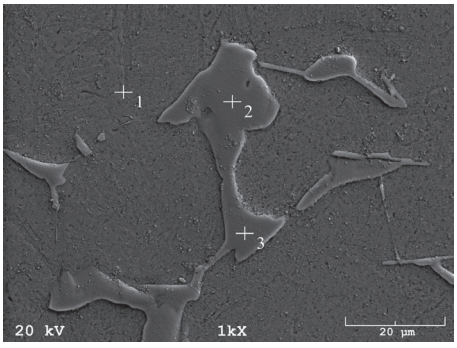

Elt.	Line	Intensity (c/s)	Error 2-sig	Conc.	Units
Point 1					
Si	Ka	7.70	0.292	0.865	wt.%
Cr	Ka	93.00	0.543	14.714	wt.%
Fe	Ka	280.16	1.465	76.040	wt.%
Ni	Ka	10.22	0.619	3.980	wt.%
Cu	Ka	9.23	0.712	4.401	wt.%
Point 2					
Cr	Ka	286.29	1.237	58.865	wt.%
Fe	Ka	129.40	1.315	41.135	wt.%
Point 3					
Cr	Ka	285.71	1.263	58.408	wt.%
Fe	Ka	130.24	1.362	41.592	wt.%

Fig. 7. The SEM microstructure and microanalysis of chemical composition of sintered 17-4 PH – 0.4% wt. of boron

steel (table 1). The main elements in point number 2 and 3 are Fe and Cr. The eutectic occurs on the martensite grain boundaries. This is associated with the Fe – B equilibrium phase diagram. Based on the results of the EDS analysis, it could be concluded that complex iron and chromium borides were formed during heating up to sintering temperature. Subsequently, a liquid phase was formed on grain boundaries as a result of eutectic reaction between the alloy matrix and the borides.

The results of the EDS analysis clearly shows that the boron amount slightly influences the chemical composition of both the matrix and eutectic. Generally, it can be concluded that as boron content increases, the chromium and iron content decrease in the matrix.

Figure 8 presents the sintering behaviour of the investigated steels. The presented dilatometric curves show the dimensional changes which occur during sintering in hydrogen for boron-free as well as boron modified 17-4 PH stainless steels. In the case of boron-free 17-4 PH, three distinct peaks can be distinguished during heating to the temperature of isothermal sintering. The first peak is at a temperature of approximately 800°C. It is associated with the typical for iron-based alloys phase transformation involving tetragonal-to-cubic crystal lattice reconstruction. Water atomized powder of 17-4PH stainless steel has a martensitic microstructure. Thus, martensite (α) – austenite (γ) transformation occurs during heating to the temperature of isothermal sintering. This is accompanied by a reduction in the specific volume and it results in momentary shrinkage. The second peak on the presented curve is at a temperature above 1000°C. This is related to the start of densification. specifically the material transport mechanisms, which lead to shrinkage, start to dominate over the phenomena associated with the thermal expansion. In turn, the third peak is at a temperature above 1200°C. This is associated with the beginning of the δ ferrite formation in the microstructure. δ ferrite specifically enhances the densification process of a sintered sample. The beginning of the δ ferrite formation results in a rapid shrinkage prior to reaching the isothermal sintering temperature.

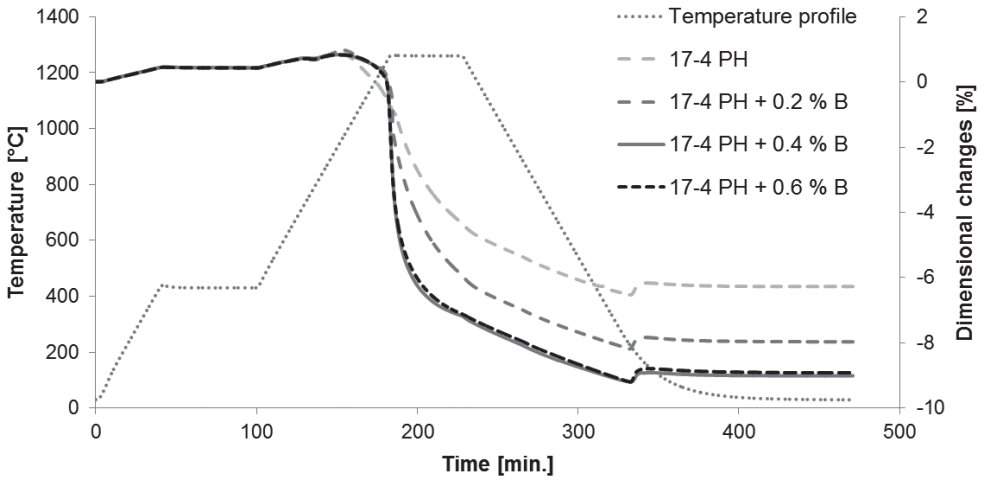

Fig. 8. Dimensional changes during sintering in hydrogen boron modified 17-4 PH steel

The addition of boron to 17-4 PH does not influence dimensional in the range from ambient temperature to about 800°C. However, above this temperature, the presence of boron has an effect on the sintering behaviour of 17-4 PH stainless steel. Specifically, boron slightly raises the transformation temperature, contributes to significant shrinkage during both heating and isothermal sintering compared to boron-free steel. This is directly due to the formation of a boron-rich liquid on the grain boundaries during heating. This liquid improves mass transport phenomena, promotes rearrangement and the fragmentation of particles. The temperature of the creation of a eutectic phase is dependent upon the amount of boron, specifically it ranged of 1160°C up to 1185°C with increasing quantities of boron. The total shrinkage of boron-alloyed 17-4 PH is higher than the total shrinkage of boron-free 17-4 PH. It can be concluded that even a small boron addition (such as 0.2% wt.) is enough to intensify the sintering process of 17-4 PH steel.

Thus, the addition of boron produces a permanent liquid phase that enhances the densification of the compacts during sintering (especially for steel modified by 0.4 and 0.6% wt. addition of boron). This was confirmed in the results of density presented in Fig. 1.

5. Conclusions

17-4 PH stainless steel was modified by boron powder in amounts of 0% wt., 0.2% wt., 0.4% wt. and 0.6% wt. and manufactured using powder metallurgy technology. Boron was added to activate the sintering process.

Experimental results showed that a persistent liquid phase appeared during sintering at 1260°C. There was a formation of borides and an occurrence of eutectic reactions between borides and 17-4 PH stainless steel during sintering. The liquid phase remained as an almost continuous network between solid grains. As a consequence, the classical phenomena of the liquid phase sintering, densification, porosity and microstructure of 17-4 PH steel have been changed. The number of pores reduces with an increasing content of boron. Furthermore, the pore shape is changed from irregular to spherical.

The use of boron has contributed to the successful obtaining of high density sintered stainless steel with improved hardness. However, density and other properties are determined by the amount of boron. It seems that the optimum amount of boron to add to 17-4 PH is 0.6% wt.

It should be underlined that boron has contributed to achieving a reduction of porosity and increase in density, both of which are necessary to improve corrosion resistance of 17-4 PH stainless steel.

References

[1] Samal P.K., Nandivada N., Hauer I., *Properties of 17-4PH Stainless Steel Produced via Press and Sinter Route*, Advances in Powder Metallurgy & Particulate Materials, Part 7, 2008, 109-120.

[2] Szewczyk-Nykiel A., Gądek S., Nykiel M., Kazior J., *Właściwości spiekanych stali nierdzewnych utwardzonych wydzieleniowo*, Rozdział w monografii Ed. Instytut Zaawansowanych Technologii, 2011, 445-458.

[3] Schade Ch., Schaberl J., Lawley A., *Stainless Steel AISI Grades for PM Applications*, International Journal of Powder Metallurgy, 44(3), 2008, 57-67.
[4] Rivolta B., Gerosa R., *On the non-isothermal precipitation of copper-rich phase in 17-4 PH stainless steel using dilatometric techniques*, Journal of Thermal Analysis and Calorimetry, 102, 2010, 857-862.
[5] Schade Ch., *Processing, Microstructures and Properties of a Dual Phase Precipitation-Hardening PM Stainless Steel*, Berlin 2010.
[6] Gülsoy H.Ö., Salman S., Özbek S., *Effect of FeB additions on sintering characteristics of injection moulded 17-4PH stainless steel powder*, Journal of Materials Science, 39, 2004, 4835-4840.
[7] Gülsoy H. Ö., Salman S., *Microstructures and mechanical properties of injection molded 17-4PH stainless steel powder with nickel boride additions*, Journal of Materials Science, 40, 2005, 3415-3421.
[8] Szewczyk-Nykiel A., Gądek S., Hebda M., Nykiel M., Kazior J., *Badania zagęszczania proszku stali nierdzewnej 17-4 PH podczas spiekania w próżni i w wodorze*, Inżynieria Materiałowa, 33(5), 2012, 469-472.
[9] Gülsoy H.Ö., Salman S., Özbek S., Findik F., *Sintering of a boron-doped injection moulded 17-4PH stainless steel*, Journal of Materials Science, 40, 2005, 4101-4104.
[10] Mutlu I., Oktay E., *Processing and properties of highly porous 17-4 PH stainless steel*, Powder Metallurgy and Metal Ceramics, 50(1-2), 2011, 73-82.
[11] Mutlu I., Oktay E., *Production and aging of highly porous 17-4 PH stainless steel*, Journal of Porous Materials, 19, 2012, 433-440.
[12] Murray K., Coleman A.J., Tingskog T.A., Whychell D.T., *Effect of particle size distribution on processing and properties of MIM 17-4PH*, International Journal of Powder Metallurgy 47(4), 2011, 21-28.
[13] Karwan-Baczewska J., *The Properties of Novel Sintered Materials base on Distaloy SA Powder with Carbon and Boron*, Rudy i Metale Nieżelazne, 57(6), 2012, 404-409.
[14] Dudrova E., Selecka M., Bures. S., Kabatova M., *Effect of Boron Addition on Microstructure and Properties of Sintered Fe-1,5Mo*, Powder Materials ISIJ International, 37(1), 1997, 59-64.
[15] Karwan-Baczewska J., *Właściwości nowych spiekanych stali molibdenowych modyfikowanych borem*, Rudy i Metale Nieżelazne, 48(6), 2003, 279-284.
[16] Bagliuk G., *Properties and Structure of Sintered Boron Containing Carbon Steels*, Sintering – Methods and Products, InTech China, 12, 2012, 249-266.
[17] Akhtar F., *Sintering Behavior of Elemental Powders with FeB Addition in the Composition of Martensitic Stainless Steel*, Journal of Materials Engineering and Performance, 16, 2007, 726-729.
[18] Cabral-Miramontes J.A., Barceinas-Sánchez J.D.O., Almeraya-Calderón F., Martinez-Villafañe A., Chacón-Nava J.G., *Effect of Boron Additions on Sintering and Densification of a Ferritic Stainless Steel*, Journal of Materials Engineering and Performance, 19, 2010, 880-884.
[19] Skałoń M., Kazior J., *Enhanced sintering of austenitic stainless steel powder AISI 316L through boron containing master alloy addition*, Archives of Metallurgy and Materials, 57(3), 2012, 789-797.

[20] Yilmaz R., Ekici M.R., *Microstructural and hardness characterization of sintered low alloyed steel*, Journal of Achievements in Materials and Manufacturing Engineering, 31(1), 2008, 23-28.

[21] Mahathanabodee S., Palathai T., Raadnui S., Tongsri R., Sombatsompop N., *Effect of h-BN content on the sintering of SS316L/h-BN composites*, Advanced Materials Research, 410, 2012, 216-219.

[22] Gierl Ch., Mohsin I.U., Danninger H., *Boron Activated Sintering of PM Steels – Alternative Boron Sources*, Powder Metallurgy Progress, 8 (2), 2008, 135-141.

[23] Lozada L., Castro F., *Controlled densification of boron-containing stainless steels*, Advances in Powder Metallurgy & Particulate Materials 2011, May 18–21, San Francisco, California.

[24] Cabral-Miramontes J.A., Barceinas-Sánchez J.D.O., Poblano-Salas C.A., Pedraza-Basulto G.K., Nieves-Mendoza D., Zambrano-Robledo P.C., Almeraya-Calderón F., Chacón-Nava J.G., *Corrosion Behavior of AISI 409Nb Stainless Steel Manufactured by Powder Metallurgy Exposed in H_2SO_4 and NaCl Solutions*, International Journal of Electrochemical Science, 8, 2013, 564-577.

[25] Kazior J., Pieczonka T., *Influence of boron on the surface microstructure of sintered AISI 316L austenitic stainless steel*, Inżynieria Materiałowa, 31(3), 2010, 487-490.

[26] Karwan-Baczewska J., *The Properties of Fe-Ni-Mo-Cu-B Materials Produced Via Liquid Phase Sintering*, Archives of Metallurgy and Materials, 56(3), 2011, 789-796.

[27] Tojal C., Gómez-Acebo T., Castro F., *Development of PM Stainless Steels with Improved Properties through Liquid Phase Sintering*, Materials Science Forum, 534-536, 2007, 661-664.

[28] Becker B.S., Bolton J.D., Eagles A.M., *Sintering of 316L stainless steels to high density via the addition of chromium diboride powders Part 1: Sintering performance and mechanical properties*, Proceedings of the Institution of Mechanical Engineers, Part L: Journal of Materials Design and Applications, 214(3), 2000, 139-152.

[29] Capus J., *Seeking high strength in PM stainless steels*, Metal Powder Report, 65(6), 2010, 30-35.

CONTENTS

TREŚĆ